

The Standard Model in 5D: Theoretical Consistency and Experimental Constraints

Dissertation zur Erlangung des
naturwissenschaftlichen Doktorgrades
der Bayerischen Julius-Maximilians-Universität Würzburg

vorgelegt von

Alexander Mück

aus Fulda

Würzburg 2004

Eingereicht am: 30.07.04

bei der Fakultät für Physik und Astronomie

1. Gutachter: Prof. Dr. R. Rückl
 2. Gutachter: Prof. Dr. M. Böhm
 3. Gutachter: Prof. Dr. A. Buras
- der Dissertation.

1. Prüfer: Prof. Dr. R. Rückl
 2. Prüfer: Prof. Dr. M. Böhm
 3. Prüfer: Prof. Dr. J. Niemeyer
- im Promotionskolloquium.

Tag des Promotionskolloquiums: 25.10.04

Doktorurkunde ausgehändigt am:

Abstract

The four-dimensional Minkowski space is known to be a good description for space-time down to the length scales probed by the latest high-energy experiments. Nevertheless, there is the viable and exciting possibility that additional space-time structure will be observable in the next generation of collider experiments. Hence, we discuss different extensions of the standard model of particle physics with an extra dimension at the TeV-scale. We assume that some of the gauge and Higgs bosons propagate in one additional spatial dimension, while matter fields are confined to a four-dimensional subspace, the usual Minkowski space. After compactification on an S^1/Z_2 orbifold, an effective four-dimensional theory is obtained where towers of Kaluza-Klein (KK) modes, in addition to the standard model fields, reflect the higher-dimensional structure of space-time. The models are elaborated from the 5D Lagrangian to the Feynman rules of the KK modes. Special attention is paid to an appropriate generalization of the R_ξ -gauge and the interplay between spontaneous symmetry breaking and compactification.

Confronting the observables in 5D standard model extensions with combined precision measurements at the Z -boson pole and the latest data from LEP2, we constrain the possible size R of the extra dimension experimentally. A multi-parameter fit of all relevant input parameters leads to bounds for the compactification scale $M = 1/R$ in the range 4-6 TeV at the 2σ confidence level and shows how the mass of the Higgs boson is correlated with the size of an extra dimension. Considering a future linear e^+e^- collider, we outline the discovery potential for an extra dimension using the proposed TESLA specifications as an example.

As a consistency check for the various models, we analyze Ward identities and the gauge boson equivalence theorem in W -pair production and find that gauge symmetry is preserved by a complex interplay of the Kaluza-Klein modes. In this context, we point out the close analogy between the traditional Higgs mechanism and mass generation for gauge bosons via compactification.

Beyond the tree-level, the higher-dimensional models studied extensively in the literature and in the first part of this thesis have to be extended. We modify the models by the inclusion of brane kinetic terms which are required as counter terms. Again, we derive the corresponding 4D theory for the KK towers paying special attention to gauge fixing and spontaneous symmetry breaking. Finally, the phenomenological implications of the new brane kinetic terms are investigated in detail.

Zusammenfassung

Bis hin zu den kleinsten Längenskalen, die bisher in Hochenergieexperimenten getestet werden konnten, lässt sich die Natur auf der Basis des vierdimensionalen Minkowski-Raums beschreiben. Dennoch kann man die aufregende Möglichkeit nicht ausschließen, dass bereits die nächste Generation von Beschleunigerexperimenten eine zusätzliche Struktur der Raumzeit aufdecken wird. Daher betrachten wir verschiedene Erweiterungen des Standardmodells der Teilchenphysik mit einer zusätzlichen Dimension im TeV-Bereich. Wir nehmen an, dass einige oder alle Higgs- und Eichbosonen in einer fünften, raumartigen Dimension propagieren können, während die fermionische Materie auf den gewöhnlichen Minkowski-Raum beschränkt bleibt. Durch Kompaktifizierung auf ein S^1/Z_2 Orbifold wird eine effektive vierdimensionale Theorie abgeleitet, in der sich die zusätzliche Raumzeitstruktur durch ein Spektrum von Kaluza-Klein (KK) Moden widerspiegelt. Dabei werden die untersuchten Modelle, ausgehend von der 5D Lagrangedichte, bis hin zu den Feynmanregeln für die KK Moden ausgearbeitet. Insbesondere zeigen wir die konsistente Verallgemeinerung der R_ξ -Eichung und untersuchen das Wechselspiel von spontaner Symmetriebrechung und Kompaktifizierung.

Um den Radius R der fünften Dimension durch Messungen einzuschränken, benutzen wir sowohl Daten aus Experimenten auf der Z -Boson-Resonanz als auch LEP2 Wirkungsquerschnitte. Bei 2σ Signifikanz finden wir für die verschiedenen Modelle als untere Schranke für die Kompaktifizierungsskala $M = 1/R$ etwa 4-6 TeV. Mit Hilfe eines Multiparameterfits werden auch Korrelationen zwischen der Kompaktifizierungsskala und der Masse des Higgs-Bosons aufgezeigt. Darüber hinaus wird am Beispiel des TESLA-Projektes das Entdeckungspotential eines zukünftigen e^+e^- Linearbeschleunigers für zusätzliche Raumzeitstruktur ausgelotet.

Als Konsistenztest für die verschiedenen Modelle untersuchen wir Ward-Identitäten und das Eichboson-Äquivalenztheorem am Beispiel der W -Boson-Paarproduktion, in der ein komplexes Zusammenspiel der KK Moden die Eichinvarianz sicherstellt. Des Weiteren wird die enge Analogie zwischen dem traditionellen Higgs-Mechanismus und der Massenerzeugung für Eichbosonen durch Kompaktifizierung herausgearbeitet.

Auf Einschleifen-Niveau zeigt sich schließlich, dass die einfachsten, im ersten Teil dieser Arbeit sowie in der Literatur eingehend untersuchten Modelle erweitert werden müssen. Daher beziehen wir lokalisierte kinetische Terme ein, die als Counterterme benötigt werden. Für die so erweiterten Modelle leiten wir wiederum die effektive 4D Theorie für die KK Moden ab und untersuchen insbesondere die Eichfixierung und spontane Symmetriebrechung. Abschließend bestimmen wir den Einfluss der neuen kinetischen Terme auf die Phänomenologie.

Contents

1	Introduction	1
2	5-Dimensional Abelian Models	7
3	5-Dimensional Extensions of the Standard Model	20
3.1	Higher-Dimensional Non-Abelian Theory	20
3.2	$SU(2)_L \otimes U(1)_Y$ -Bulk Model	23
3.3	$SU(2)_L$ -Brane, $U(1)_Y$ -Bulk Model	26
3.4	$SU(2)_L$ -Bulk, $U(1)_Y$ -Brane Model	28
3.5	Fermions on the Brane	29
4	Bounds on the Compactification Scale $M = 1/R$	32
4.1	Framework and Input Parameters	32
4.1.1	$SU(2)_L \otimes U(1)_Y$ -Bulk Model	34
4.1.2	$SU(2)_L$ -Brane, $U(1)_Y$ -Bulk Model	35
4.1.3	$SU(2)_L$ -Bulk, $U(1)_Y$ -Brane Model	36
4.2	Statistics	37
4.3	Bounds from Precision Observables	38
4.4	LEP2 Constraints	42
4.4.1	Fermion-Pair Production	44
4.4.2	W^+W^- Production	46
4.5	Combined Bounds on $M = 1/R$	47

5	Sensitivity at a Linear Collider	50
5.1	GigaZ Option	50
5.2	Tests at $\sqrt{s} = 800$ GeV	51
6	Ward Identities, the Goldstone Boson Equivalence Theorem, and Tree-Level Unitarity in W-Pair Production	56
6.1	The Standard Model	58
6.2	5D Models	60
6.2.1	5D-QED	61
6.2.2	Purely Geometric Symmetry Breaking	61
6.2.3	Bulk-Bulk Model with a Bulk Higgs	64
6.2.4	Bulk-Bulk Model with a Brane Higgs	65
6.3	The Phenomenology of W -Pair Production	69
7	Brane Kinetic Terms	72
7.1	5D-QED with Brane Kinetic Terms	74
7.1.1	The Spectrum	75
7.1.2	Gauge Fixing	79
7.1.3	Brane Kinetic Terms for Both S^1/Z_2 Branes	84
7.2	Spontaneous Symmetry Breaking	85
7.3	Phenomenology	88
7.3.1	Bulk-Bulk Model with a Brane Higgs	89
7.3.2	Other Models with a Brane Higgs	95
7.3.3	Bulk-Bulk Model with a Bulk Higgs	95
8	Conclusions	98
A	Infinite Sums	101
B	KK Masses and Couplings to Fermions on the Brane	104
C	Observables, SM Predictions, and Input Parameters	108

D Multi-Parameter Fits in the 5DSM	111
E The Unified Approach in Statistics	113
F $\Delta_{\mathcal{O}}^{5\text{DSM}}$ for Precision Observables	117
F.1 $SU(2)_L \otimes U(1)_Y$ -Bulk Model	117
F.2 $SU(2)_L$ -Brane, $U(1)_Y$ -Bulk Model	118
F.3 $SU(2)_L$ -Bulk, $U(1)_Y$ -Brane Model	119
G Kaluza-Klein $W_{(0)}W_{(0)}Z_{(n)}$ and $W_{(0)}W_{(0)}\gamma_{(n)}$ Couplings	121
H Kaluza-Klein $H_{(0)}Z_{(0)}Z_{(n)}$ Couplings	123
I Feynman Rules for W Bosons and the Associated Goldstone Modes	125
References	129

List of Figures

2.1	Propagators in 5D-QED	10
2.2	Vertices in 5D-QED	12
2.3	Total cross section for $e^+e^- \rightarrow \mu^+\mu^-$ in 5D-QED	13
3.1	Feynman rules for the triple gauge-boson coupling	22
3.2	Feynman rules for the quartic gauge-boson coupling	22
4.1	Bounds from precision observables	39
4.2	$\Delta\chi^2$ -contours for precision observables	43
4.3	Energy dependence of mixing effects and virtual KK exchange	44
4.4	$\Delta\chi^2$ -contours for combined data	48
5.1	Sensitivity at TESLA for different channels	52
5.2	Combined sensitivity at TESLA	53
5.3	Sensitivity and luminosity at TESLA	54
5.4	Sensitivity at TESLA in angular distributions	55
6.1	Feynman diagrams for W -pair production	59
6.2	Feynman diagrams for Goldstone production	60
6.3	Cross section for W -pair production	70
7.1	Gauge-boson self-energy diagram	72
7.2	Gauge-boson self-energy diagram	73
7.3	KK Masses as a function of r_c/R	77
7.4	KK Couplings as a function of r_c/R	89

B.1	KK gauge- and Goldstone-boson propagators	105
B.2	Gauge-boson-fermion couplings	107
E.1	Comparison of statistical methods	115
G.1	The $W_{(0)}W_{(0)}Z_{(n)}$ and $W_{(0)}W_{(0)}\gamma_{(n)}$ vertices	122
H.1	The $H_{(0)}Z_{(0)}Z_{(n)}$ vertex	124
I.1	Coupling of photon modes to bulk scalars	126
I.2	Coupling of Z -boson modes to bulk scalars	127
I.3	Coupling of photon and Z -boson modes to brane scalars	128

List of Tables

4.1	Bounds from precision observables	40
4.2	Bounds for different significance levels	41
4.3	Effect of correlations on the bounds	42
4.4	Bounds from LEP2	45
4.5	Combined bounds	49
5.1	Sensitivity at GigaZ	51
C.1	SM predictions and measurements for precision observables	110
F.1	Predictions for $\Delta_{\mathcal{O}}^{5\text{DSM}}/X$ in the $SU(2)_L \otimes U(1)_Y$ -bulk model	118
F.2	Predictions for $\Delta_{\mathcal{O}}^{5\text{DSM}}/X$ in the $SU(2)_L$ -brane, $U(1)_Y$ -bulk model	119
F.3	Predictions for $\Delta_{\mathcal{O}}^{5\text{DSM}}/X$ in the $SU(2)_L$ -bulk, $U(1)_Y$ -brane model	120

Chapter 1

Introduction

In how many dimensions do we live? There are at least two possible answers to this fundamental question: So far, all phenomenologically successful physical theories can be formulated within a space-time consisting of one time-like and three space-like dimensions. That is, all our experience starting from our daily life and reaching out to experiments at high-energy colliders or observations on the evolution of the universe is in agreement with the statement that the world is four-dimensional. But on the other hand, will the world still look four-dimensional if we probe nature at higher energy scales or shorter distances, e.g. at CERN's Large Hadron Collider (LHC), at a future e^+e^- linear collider, or in some other ingenious experiment? The answer is simply: We do not know. To clarify this fundamental question one should investigate characteristic features of higher-dimensional theories and their phenomenological signatures as it is done in this thesis for particular model scenarios.

The question about the dimensionality of space-time is actually not new. Already at the beginning of the 20th century Kaluza and Klein speculated [1,2] that the world may consist of an additional, hidden dimension. They tried to utilize the fifth dimension to unify electromagnetism and general relativity. Their specific model is no longer of phenomenological relevance. However, the idea to make use of the specific features of extra dimensions is still present in today's model building [3].

Theoretically, the existence of extra dimensions is most strongly supported by string theory. String theories provide the only known theoretical framework within which gravity can be quantized and so undeniably play a central role in our endeavors of unifying the fundamental forces of nature. Here, extra dimensions are not only a matter of model building. A consistent quantum-mechanical formulation of string theories requires the existence of additional dimensions beyond the four we already know.

These new dimensions must be sufficiently small in some appropriate sense, so as to have escaped our detection so far. As we will see in detail, compactification, where additional

dimensions are considered to be compact manifolds of a characteristic size R (e.g. an n dimensional torus with common radius R), provides a mechanism which can successfully hide them. In the original string-theoretical considerations [4] the inverse length $1/R$ of the extra compact dimensions and the string scale M_s turned out to be closely tied to the 4-dimensional Planck mass $M_P = 1.9 \times 10^{19}$ GeV with the involved mass scales being of the same order. That is why these extra dimensions have not been of immediate phenomenological interest when string theory was born thirty years ago. There is simply no hope to directly probe an extra dimension of Planck size by collider experiments.

More recent studies, however, have shown [5–12] that there could be conceivable scenarios of stringy nature where $1/R$ and M_s may be lowered independently of M_P by several or many orders of magnitude. Taking such a realization to its natural extreme, the radical scenario can be considered in which M_s is of order TeV and represents the only fundamental scale in the universe at which unification of all forces of nature occurs [9–11].

Although we are not concerned with gravity in the main part of this thesis, let us try to understand why n extra, flat dimensions with a large radius R can lower the gravitational scale. After all, this observation [9–11] triggered most of the research on extra dimensions over the past six years. At distances small compared to R the gravitational potential simply changes according to the Gauss law in $n + 4$ dimensions, i.e.

$$V(r) \sim \frac{m_1 m_2}{M_G^{2+n}} \frac{1}{r^{n+1}}, \quad (1.1)$$

where $r \ll R$ and M_G is the true gravitational scale to be distinguished from the Planck scale M_P . At $r \gg R$ the potential again looks effectively four-dimensional, i.e.

$$V(r) \xrightarrow{r \gg R} \frac{m_1 m_2}{M_G^{2+n}} \frac{1}{R^n r} = \frac{m_1 m_2}{M_P^2} \frac{1}{r}. \quad (1.2)$$

Hence, we find the important relation among the parameters M_P , M_G and R [9–11]:

$$M_P^2 = M_G^{2+n} R^n. \quad (1.3)$$

The apparent weakness of gravity is not due to the enormity of the Planck scale M_P but due to the presence of a large volume factor R^n . The above argument can also be more stringently formulated in the language of effective field theory [13]. As a result, the true fundamental gravity scale M_G can be much smaller than M_P . Thus, the so-called gauge hierarchy problem is solved if M_G is of the order of the electroweak scale. For example, extra dimensions of size

$$R \sim \frac{1}{M_G} \left(\frac{M_P}{M_G} \right)^{2/n} \sim \begin{cases} \mathcal{O}(1 \text{ mm}), & n = 2 \\ \mathcal{O}(10 \text{ fm}), & n = 6 \end{cases} \quad (1.4)$$

are needed for a gravitational scale —typically of the order of the string scale M_s — in the TeV range. Therefore, Cavendish-type experiments may potentially test the model by observing deviations from Newton’s law [9–11] at distances smaller than a mm. The most recent bound on the size of two extra dimensions is found to be $130 \mu\text{m}$ [14]. Although the original hierarchy problem disappears in this setup, the question arises why there is another physical scale which is also pretty remote from the electroweak scale and set by the compactification radius around a mm.

A large volume factor is not the only possibility to explain the observed hierarchy between the electroweak and the Planck scale in an extra-dimensional way. A non-trivial background metric in a so-called warped extra dimension can also do the job in a quite distinct way [15, 16]. However, we will not go into details of gravitational physics here. A readable introduction to the subject can be found in [13].

Let us now turn to the Standard Model (SM) of particle physics in the context of extra dimensions. Obviously, a mm size extra dimension for the photon is excluded by experiment. An electromagnetic potential in analogy to (1.1) is clearly falsified by atomic physics. Nevertheless, there is a possibility to embed the SM in such an extra-dimensional setup again provided by string theory. In string theory, there is the concept of branes which allow to locate degrees of freedom in a subspace of the full space-time [7–12, 17]. Hence, it is possible to have gravity propagating in large extra dimensions, while the standard model is confined to a brane and hardly affected until gravity becomes strong in or beyond the TeV region.

On the other hand there is an alternative setup nature could have chosen. As the aforementioned branes may be higher-dimensional as well, in addition to gravitons the SM fields could also propagate within at least a single extra dimension. No matter if the gravitational scale is not around the experimental corner at the TeV-scale nature could reveal an extra dimension populated by SM fields already in the next generation of colliders. This would lead to fascinating signatures for physics beyond the SM. As we will explicitly show in Chapter 2, an extra dimension reflects itself in a tower of heavy copies of any bulk field, i.e. any field propagating in the extra dimension. The masses of these so-called Kaluza-Klein (KK) modes are found to be multiples of the compactification scale $M = 1/R$ in the simplest models. Consequently, the extra dimension becomes visible when the heavy particles can be produced in high-energy experiments or at least leave their fingerprints in observables.

In this thesis, we consider minimal extensions of the SM. We concentrate on a single extra dimension to avoid problems in models with more than five dimensions. In six or more dimensions, already tree-level amplitudes are generally not well-defined because the infinite sums over diagrams, where towers of KK modes are exchanged, diverge. Thus, an explicit

cut-off has to be introduced. Five-dimensional models are less UV sensitive.

As a brief summary of my diploma thesis [18], the simplest possible higher-dimensional theory, QED in five dimensions, is explicitly elaborated in Chapter 2. The basic concepts for a phenomenologically successful model are presented, in particular the notion of an orbifold. We use the simplest orbifold S^1/Z_2 which possesses two branes where parts of the SM spectrum can be localized. After compactifying the extra dimension on S^1/Z_2 , we obtain an effective 4-dimensional theory for the usual SM states and the corresponding infinite towers of massive KK modes. In particular, we consider the question what is an appropriate extension of the R_ξ gauge for the higher-dimensional models. As we will show, the introduced quantization procedure can be successfully applied to theories with spontaneous symmetry breaking, no matter if they include Higgs bosons living in the bulk or on the brane. Most of the technical details are omitted for brevity. A more detailed construction can be found in my diploma thesis [18].

Concerning fermions in the SM, the situation is a little more intricate, because there are no chiral fermions in 5D. However, orbifolds allow for the construction of models with chiral fermions in the low-energy effective 4D theory [19, 20] as pointed out in Chapter 2. For the main part of this thesis, we chose a different setup. The fermionic matter content of the SM is localized on a brane, i.e. fermions live in the usual Minkowski space.

At this point, we can rephrase the introductory question in more physical terms. How large can a possible extra dimension in such a framework be so that it is not in conflict with present experimental data? Localized fermions are shown to couple to each KK mode of gauge fields in the bulk. Hence, KK excitations mediate interactions between light SM fermions already at tree-level. These effective contact interactions imply that the compactification scale M is constrained to lie in the TeV region. In contrast, for so-called universal extra dimensions [5, 12, 20–29] where all SM degrees of freedom propagate in the bulk, the bounds are reduced by almost one order of magnitude. Mainly from the KK loop contributions to the ρ parameter [21] and the decay $Z \rightarrow b\bar{b}$ [28], one finds $M \gtrsim 300$ GeV. Thus, the bounds are not much larger than the energy scale directly probed by the LEP experiments. As introduced in Section 3, this is due to the fact that there is a remnant of momentum conservation with respect to the extra dimension in interactions between bulk fields which survives the orbifold compactification. Corresponding selection rules forbid large tree-level contributions of KK modes to observables below the compactification scale. In particular, there are no effective low-energy contact interactions between SM particles which stem from the exchange of heavy KK modes.

Returning to the class of 5D models with brane fermions, there are different higher-dimensional extensions of the SM [17, 30] because of its gauge group structure. In fact, most of the derived phenomenological bounds in the literature were obtained by assuming

that the SM gauge fields propagate all freely in a common higher-dimensional space [31–41]. In Chapter 3, we lift this limitation and also introduce and discuss models in which either the $SU(2)_L$ or the $U(1)_Y$ gauge bosons are confined to the same brane as the fermions [42]. In Chapter 4, we turn our attention to phenomenological aspects. Model by model we calculate the effects of the fifth dimension on a large number of electroweak observables at the Z peak and LEP2 cross sections and derive bounds on the compactification scale. Hence, we clarify the model dependence of the bounds for non-universal SM extensions. For the first time, we carry out a global multi-parameter fit of the compactification scale M simultaneously with the SM parameters [43]. This allows us to properly include the correlations of the compactification scale with the SM parameters, in particular with the Higgs-boson mass m_H [38, 39]. Thus, we identify those models which favor a larger Higgs mass than the best-fit Higgs mass in the SM.

In Chapter 5, we systematically investigate the sensitivity of future experiments at an 800 GeV linear e^+e^- collider such as TESLA. In this analysis we also study the improvements which can be expected from the so-called GigaZ option of TESLA, where the machine is operated at the Z pole with a luminosity 100 times larger than that of LEP.

Apart from experimental constraints and future discovery potential, the consistency of the higher-dimensional models as quantum theories is investigated. Compactification provides a mechanism for gauge bosons to acquire a mass. In contrast to spontaneous symmetry breaking, the resulting massive gauge theory is non-renormalizable. However, as we will already see in Chapter 2, the two mechanisms for mass generation work in close analogy to each other. In particular, extra components of the gauge fields play the role of the would-be Goldstone modes which are eaten up by the massive gauge bosons to form their longitudinal degrees of freedom. After elaborating the analogy by an appropriate choice for the gauge fixing, in Chapter 6 we proof the Goldstone boson equivalence theorem [44, 45] in the context of the 5D standard model [46] for tree-level W -pair production. In this context, we also consider Ward identities and tree-level unitarity in 5D models [47–50]. Here, we pay special attention to models in which spontaneous symmetry breaking and compactification cooperate to form the mass eigenstates of the gauge bosons.

For consistency beyond the tree-level, the simple setup of 5D models as considered in the first six chapters has to be extended [51]. As we will show in Chapter 7, there are additional counterterms needed to compensate divergences in the self energies of higher-dimensional fields. Their origin can be traced back to the orbifold compactification. As a consequence, these counterterms require so-called brane kinetic terms to be included in the Lagrangian to start with. Their strength is an additional free parameter of the theory. We therefore reconsider the derivation of the effective 4D theory in the presence of these new terms. The spectrum of mass eigenstates and their coupling to brane fermions [52] as well

as the quantization procedure with an appropriate gauge fixing is derived. Furthermore, we analyze the phenomenological implications of the brane kinetic terms. This work is particularly interesting for model building, e.g. for the construction of phenomenologically viable Higgsless SM extensions [53].

Finally, we conclude with a brief summary in Chapter 8. Useful tools for the analysis of higher-dimensional models, some interesting side remarks, tabulated results, and Feynman rules are presented in the appendices.

Chapter 2

5-Dimensional Abelian Models

As a starting point, let us consider the gauge part of the Lagrangian of 5-dimensional Quantum Electrodynamics (5D-QED) given by

$$\mathcal{L}(x, y) = -\frac{1}{4}F_{MN}(x, y)F^{MN}(x, y) + \mathcal{L}_{\text{GF}}(x, y), \quad (2.1)$$

where

$$F_{MN}(x, y) = \partial_M A_N(x, y) - \partial_N A_M(x, y) \quad (2.2)$$

denotes the 5-dimensional field strength tensor, and $\mathcal{L}_{\text{GF}}(x, y)$ is the gauge-fixing term. The Faddeev-Popov ghost terms have been neglected, because the ghosts are non-interacting in the Abelian case. Our notation for the Lorentz indices and space-time coordinates is: $M, N = 0, 1, 2, 3, 5$; $\mu, \nu = 0, 1, 2, 3$; $x = (x^0, \vec{x})$; and $y = x^5$ denotes the coordinate of the additional dimension.

The structure of the conventional QED Lagrangian is simply carried over to the five-dimensional case. The field content of the theory is given by a single gauge boson A_M transforming as a vector under the Lorentz group $\text{SO}(4,1)$. In the absence of the gauge-fixing and ghost terms, the 5D-QED Lagrangian is invariant under a $U(1)$ gauge transformation

$$A_M(x, y) \rightarrow A_M(x, y) + \partial_M \Theta(x, y). \quad (2.3)$$

Hence, the defining features of conventional QED are present in 5D-QED as well. So far, we have treated the spatial dimensions on the same footing. To hide the additional dimension at low energies, we will now compactify the extra dimension, i.e., replace the infinitely extended extra dimension by a compact object.

The simplest compact one dimensional manifold is a circle, denoted by S^1 , with radius R . However, as we will see below, compactification on a circle would introduce a massless scalar to QED. Hence, we require an additional internal reflection symmetry Z_2 with respect to

the origin $y = 0$. So, one is led to the so-called orbifold S^1/Z_2 which turns out to be especially well suited for higher-dimensional physics. The extra dimensional coordinate y runs only from 0 to $2\pi R$ where these two points are identified. Moreover, according to the Z_2 symmetry, y and $-y = 2\pi R - y$ are identified in the following sense: knowing the field content for the segment $y \in [0, \pi R]$ implies the knowledge of the whole system. In other words, each 5D field has a particular Z_2 parity, i.e. it is even or odd with respect to the extra dimension. The fixed points $y = 0$ and $y = \pi R$, which do not transform under Z_2 , are also called boundaries of the orbifold.

Thus, the compactification on S^1/Z_2 is reflected in restrictions for the fields. The above property of gauge symmetry leads to additional constraints. In order to meet all requirements, we demand the fields to satisfy the following equalities:

$$\begin{aligned}
A_M(x, y) &= A_M(x, y + 2\pi R), \\
A_\mu(x, y) &= A_\mu(x, -y), \\
A_5(x, y) &= -A_5(x, -y), \\
\Theta(x, y) &= \Theta(x, y + 2\pi R), \\
\Theta(x, y) &= \Theta(x, -y).
\end{aligned} \tag{2.4}$$

The field $A_\mu(x, y)$ is taken to be even under Z_2 , so as to embed conventional QED with a massless photon into our 5D-QED. Notice that the reflection properties of the field $A_5(x, y)$ and the gauge parameter $\Theta(x, y)$ under Z_2 in (2.4) follow automatically if the theory is to remain gauge invariant after compactification.

Making the periodicity and reflection properties of A_μ and Θ in (2.4) explicit, we can expand these quantities in Fourier series

$$\begin{aligned}
A^\mu(x, y) &= \frac{1}{\sqrt{2\pi R}} A_{(0)}^\mu(x) + \sum_{n=1}^{\infty} \frac{1}{\sqrt{\pi R}} A_{(n)}^\mu(x) \cos\left(\frac{ny}{R}\right), \\
\Theta(x, y) &= \frac{1}{\sqrt{2\pi R}} \Theta_{(0)}(x) + \sum_{n=1}^{\infty} \frac{1}{\sqrt{\pi R}} \Theta_{(n)}(x) \cos\left(\frac{ny}{R}\right).
\end{aligned} \tag{2.5}$$

The Fourier coefficients $A_{(n)}^\mu(x)$ are the so-called Kaluza-Klein (KK) modes. The extra component A^5 of the gauge field is odd under the reflection symmetry and its expansion is given by

$$A^5(x, y) = \sum_{n=1}^{\infty} \frac{1}{\sqrt{\pi R}} A_{(n)}^5(x) \sin\left(\frac{ny}{R}\right). \tag{2.6}$$

Note that there is no zero mode, a phenomenologically important fact, as we will see in a moment.

Using (2.5) and (2.6), we now derive an effective 4D field theory for the four-dimensional fields, the KK modes. The dependence of the Lagrangian density on the extra coordinate y is parameterized by simple Fourier functions so that it can be completely removed by integrating out the extra dimension. From now on, the quantity of interest will be

$$\mathcal{L}(x) = \int_0^{2\pi R} dy \mathcal{L}(x, y). \quad (2.7)$$

In $\mathcal{L}(x)$ the higher-dimensional physics is reflected by the infinite tower of KK modes for each field component. A simple calculation yields

$$\begin{aligned} \mathcal{L}(x) = & -\frac{1}{4} F_{(0)\mu\nu} F_{(0)}^{\mu\nu} + \sum_{n=1}^{\infty} \left[-\frac{1}{4} F_{(n)\mu\nu} F_{(n)}^{\mu\nu} \right. \\ & \left. + \frac{1}{2} \left(\frac{n}{R} A_{(n)\mu} + \partial_\mu A_{(n)5} \right) \left(\frac{n}{R} A_{(n)}^\mu + \partial^\mu A_{(n)5} \right) \right] + \mathcal{L}_{\text{GF}}(x), \end{aligned} \quad (2.8)$$

where $\mathcal{L}_{\text{GF}}(x)$ is defined in analogy to (2.7). The first term in (2.8) represents conventional QED involving the massless field $A_{(0)}^\mu$. Note that the other vector excitations $A_{(n)}^\mu$ from the infinite tower of KK modes come with mass terms, their mass being an integer multiple of the inverse compactification radius. Therefore, a small radius leads to a large mass or compactification scale $M = 1/R$. It is this large scale which is responsible for the fact that an extra dimension, as it may exist, has not yet been discovered. The extra dimension is, so to speak, hidden by its compactness.

Moreover, the absence of $A_{(0)}^5$ due to the odd Z_2 symmetry of $A^5(x, y)$ allows us to recover conventional QED in the low-energy limit of the model. For $n \geq 1$, the KK tower $A_{(n)}^5$ for the additional component of the five-dimensional vector field mixes with the vector modes. The modes $A_{(n)}^5$, being scalars with respect to the four-dimensional Lorentz group, play the role of the would-be Goldstone modes in an Abelian Higgs model in which the corresponding Higgs fields are taken to be infinitely massive. Thus, one is tempted to view the mass generation for the heavy KK modes by compactification as a kind of geometric Higgs mechanism. The Lagrangian (2.8) is still manifestly gauge invariant under the transformation (2.3) which in terms of the KK modes reads

$$\begin{aligned} A_{(n)\mu}(x) & \rightarrow A_{(n)\mu}(x) + \partial_\mu \Theta_{(n)}(x), \\ A_{(n)5}(x) & \rightarrow A_{(n)5}(x) - \frac{n}{R} \Theta_{(n)}(x). \end{aligned} \quad (2.9)$$

The above observations motivate us to seek for a higher-dimensional generalization of 't-Hooft's gauge-fixing condition, for which the mixing terms bilinear in $A_{(n)}^\mu$ and $A_{(n)}^5$ are eliminated from the effective 4-dimensional Lagrangian (2.8). Taking advantage of the fact

that orbifold compactification generally breaks $SO(4,1)$ invariance [51], one can abandon the requirement of covariance of the gauge-fixing condition with respect to the extra dimension and choose the following non-covariant generalized R_ξ gauge [42, 54]:

$$\mathcal{L}_{\text{GF}}(x, y) = -\frac{1}{2\xi}(\partial^\mu A_\mu - \xi \partial_5 A_5)^2. \quad (2.10)$$

The gauge-fixing term (2.10) is still invariant under ordinary 4-dimensional Lorentz transformations. For some calculation, e.g. radiative corrections to KK masses [55], it can be convenient to stick to a covariant gauge fixing with respect to all five dimensions. In this case, Feynman gauge $\xi = 1$ is the obvious choice.

Upon integration over the extra dimension, the mixing terms in (2.8) drop out apart from irrelevant total derivatives. Thus, the gauge-fixed four-dimensional Lagrangian of 5D-QED

$$\begin{aligned} \mathcal{L}(x) = & -\frac{1}{4}F_{(0)\mu\nu}F_{(0)}^{\mu\nu} - \frac{1}{2\xi}(\partial^\mu A_{(0)\mu})^2 \\ & + \sum_{n=1}^{\infty} \left[-\frac{1}{4}F_{(n)\mu\nu}F_{(n)}^{\mu\nu} + \frac{1}{2}\left(\frac{n}{R}\right)^2 A_{(n)}^\mu A_{(n)\mu} - \frac{1}{2\xi}(\partial^\mu A_{(n)\mu})^2 \right] \\ & + \sum_{n=1}^{\infty} \left[\frac{1}{2}(\partial^\mu A_{(n)5})(\partial_\mu A_{(n)5}) - \frac{1}{2}\xi\left(\frac{n}{R}\right)^2 A_{(n)5}^2 \right] \end{aligned} \quad (2.11)$$

explicitly shows the different degrees of freedom in the model. Gauge-fixed QED is accompanied with a tower of its copies for massive gauge bosons. The scalars $A_{(n)5}$ with gauge dependent masses resemble the would-be Goldstone bosons of an ordinary 4-dimensional Abelian Higgs model in the R_ξ gauge. From this Lagrangian, it is obvious that the corresponding propagators take on their usual form given in Figure 2.1. Hereafter, we shall refer to the $A_{(n)5}^5$ fields as Goldstone modes.

In the limit $\xi \rightarrow \infty$ we recover the usual unitary gauge from the R_ξ gauge (2.10) in which the Goldstone modes decouple from the theory [20, 56]. Thus, for the case at hand, we have seen how starting from a non-covariant higher-dimensional gauge-fixing condition, we can arrive at the known covariant 4-dimensional R_ξ gauge after compactification.

$$\begin{aligned} \mu \text{---}\overset{(n)}{\text{~~~~~}}\text{---}\nu &= \frac{i}{k^2 - \left(\frac{n}{R}\right)^2} \left[-g^{\mu\nu} + \frac{(1-\xi)k^\mu k^\nu}{k^2 - \xi\left(\frac{n}{R}\right)^2} \right] \\ \text{---}\overset{(n)}{\text{-----}} &= \frac{i}{k^2 - \xi\left(\frac{n}{R}\right)^2} \end{aligned}$$

Figure 2.1: Propagators for the gauge boson and Goldstone modes in 5D-QED.

Having established the five-dimensional gauge sector, we now introduce fermions. First, let us briefly consider fermions living in the 5D bulk [21, 29]. Since γ_5 is part of the Clifford algebra, there are no Weyl spinors in 5D. In other words, the notion of chirality is not well defined. In analogy to (2.4), transformation properties under the Z_2 orbifold symmetry have to be chosen for the fermion field Ψ , a four component spinor field. In analogy to the gauge field, the naive choice is

$$\Psi(x, y) = \pm \Psi(x, -y). \quad (2.12)$$

However, the Dirac equation for a massless fermion in five dimensions

$$\gamma^M \partial_M \Psi(x, y) = 0 \quad (2.13)$$

is not compatible with (2.12) because $\partial_5 \Psi$ has the opposite Z_2 symmetry with respect to Ψ . A compatible Z_2 transformation for the fermions is given by

$$\Psi(x, y) = \pm \gamma_5 \Psi(x, -y). \quad (2.14)$$

Consequently, $\Psi_{\pm} = (1 \pm \gamma_5) \Psi$ has a well defined Z_2 parity. In particular, only one of the projections Ψ_{\pm} is even and possesses a massless zero mode if expanded in KK modes. Hence, the low-energy spectrum in the 4D effective theory contains only one projection, i.e. it is chiral. This is good news for standard model extensions with fermions in the bulk. Note that a mass term in (2.13) is forbidden if (2.14) is to be compatible with (2.13). To obtain 5D-QED with a massive non-chiral low-energy spectrum, one has to include a second fermion with opposite Z_2 parity.

However, there is an even easier and phenomenologically challenging alternative to this approach. The S^1/Z_2 orbifold, as noted above, has the feature that there are fixed points $y = 0$ and $y = \pi$ not transforming under the Z_2 symmetry. As already mentioned in the introduction, borrowing a concept from string theory, these special points can be considered as branes. The branes can host localized fields which cannot penetrate the extra dimension. Using this idea for the fermions, it can be easily formalized by introducing a δ -function in the Lagrangian density

$$\mathcal{L}_F(x, y) = \delta(y) \bar{\Psi}(x) (i \gamma^\mu D_\mu - m_f) \Psi(x), \quad (2.15)$$

where the covariant derivative

$$D_\mu = \partial_\mu + i e_5 A_\mu(x, y) \quad (2.16)$$

contains the bulk gauge field A_μ and e_5 denotes the coupling constant of 5D-QED. The obvious generalization for the usual gauge-transformation properties of fermion fields reads

$$\Psi(x) \rightarrow \exp(-i e_5 \Theta(x, 0)) \Psi(x). \quad (2.17)$$

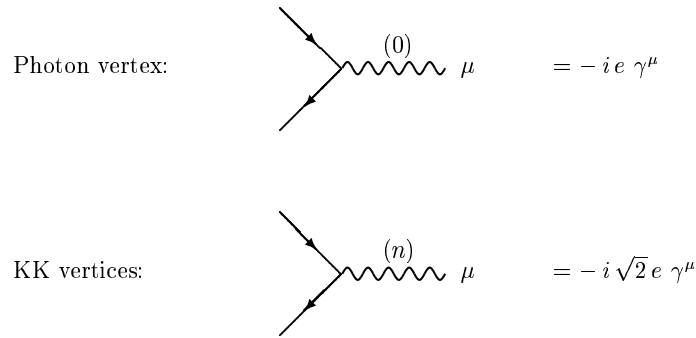


Figure 2.2: Feynman rules for the vertices in 5D-QED

Again integrating out the fifth dimension, we are left with an effective four-dimensional interaction Lagrangian

$$\mathcal{L}_{\text{int}}(x) = -e\bar{\Psi}\gamma^\mu\Psi\left(A_{(0)\mu} + \sqrt{2}\sum_{n=1}^{\infty}A_{(n)\mu}\right), \quad (2.18)$$

which couples all KK modes to the fermion field on the brane. The coupling constant $e = e_5/\sqrt{2\pi R}$ is the QED coupling constant as measured by experiment. The factor $\sqrt{2}$ in (2.18) is a typical enhancement factor for the coupling of brane fields to heavy KK modes ($n \geq 1$) due to their wave-function normalization in (2.5). Note that the scalar modes $A_{(n)}^5$ do not couple to brane fermions even if D_μ is replaced by D_M in (2.15) because their wave functions vanish at $y = 0$ according to the odd Z_2 -symmetry. These interaction terms together with completely standard kinetic terms for the fermion field complete 5D-QED. The corresponding Feynman rules for the electron-photon vertex and the analogous interaction of the heavy KK modes are shown in Fig. 2.2.

An exemplary experimental signature of 5D-QED in future experiments would be a series of s -channel resonances in muon-pair production at an e^+e^- -collider as shown in Fig. 2.3. The generic signatures of extra dimensions in the discussed setup are quite similar to Fig. 2.3 in more realistic theories.

The above quantization procedure can now be applied to more elaborate higher-dimensional models. If we want to extend the standard model by an extra dimension we have to understand spontaneous symmetry breaking in this context in order to explain the fermion and gauge boson masses of the standard model particles. There are numerous attempts to utilize the extra dimension itself for spontaneous symmetry breaking [57, 58]. In contrast to these ideas, we will work in a scheme where the traditional Higgs mechanism is at work. Hence, adding a Higgs scalar in the bulk to 5D-QED, the Lagrangian of the theory reads

$$\mathcal{L}(x, y) = -\frac{1}{4}F^{MN}F_{MN} + (D_M\Phi)^*(D^M\Phi) - V(\Phi) + \mathcal{L}_{\text{GF}}(x, y), \quad (2.19)$$

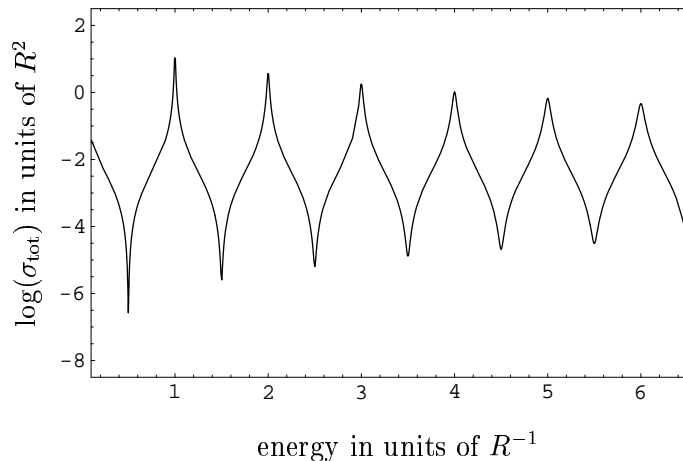


Figure 2.3: Total cross section for $e^+e^- \rightarrow \mu^+\mu^-$ as a function of center-of-mass energy on a logarithmic scale. The width Γ of the KK modes is reasonably approximated by $\Gamma = 0.01n/R$.

where D_M again denotes the covariant derivative (2.16), e_5 the 5-dimensional gauge coupling,

$$\Phi(x, y) = \frac{1}{\sqrt{2}} (h(x, y) + i\chi(x, y)) \quad (2.20)$$

a 5-dimensional complex scalar field, and

$$V(\Phi) = \mu_5^2 |\Phi|^2 + \lambda_5 |\Phi|^4 \quad (2.21)$$

(with $\lambda_5 > 0$) the 5-dimensional Higgs potential. We consider $\Phi(x, y)$ to be even under Z_2 , perform a corresponding Fourier decomposition, and integrate over y to obtain

$$\mathcal{L}_H(x) = \frac{1}{2} \sum_{n=0}^{\infty} \left[(\partial_\mu h_{(n)}) (\partial^\mu h_{(n)}) - \frac{n^2}{R^2} h_{(n)}^2 - \mu^2 h_{(n)}^2 + (h \leftrightarrow \chi) \right] + \dots, \quad (2.22)$$

where the interactions terms are omitted for brevity. For $\mu^2 = \mu_5^2 < 0$, as in the usual 4-dimensional case, the zero KK Higgs mode acquires a non-vanishing vacuum expectation value (VEV) which spontaneously breaks the U(1) symmetry. Moreover, as long as the phenomenologically viable condition $|\mu| < 1/R$ is met, the higher KK modes $h_{(n \geq 1)}$ have positive mass parameters and $h_{(0)}$ will be the only mode to receive a non-zero VEV

$$\langle h_{(0)} \rangle = v = \sqrt{2\pi R |\mu_5|^2 / \lambda_5}. \quad (2.23)$$

The VEV introduces an additional mass term for each KK mode of the gauge field. By construction, the zero mode turns from a massless to a massive degree of freedom. The

masses of the heavy KK modes are slightly shifted. In contrast to the photon-fermion interaction in Fig. 2.2, the gauge and self interactions of the Higgs fields, omitted in (2.22), only involve bulk fields. We postpone the discussion of interactions between bulk fields until Section 3 where we investigate the gauge-boson self-couplings in non-Abelian models. In the context of spontaneous symmetry breaking, it is instructive to introduce the fields $G_{(n)}$ and $a_{(n)}$, where

$$G_{(n)} = \left(\frac{n^2}{R^2} + e^2 v^2 \right)^{-1/2} \left(\frac{n}{R} A_{(n)5} + e v \chi_{(n)} \right), \quad (2.24)$$

and $a_{(n)}$ is the linear combination of $A_{(n)5}$ and $\chi_{(n)}$ which is orthogonal to $G_{(n)}$. In the effective kinetic Lagrangian of the theory for the n^{th} -KK mode ($n \geq 1$)

$$\begin{aligned} \mathcal{L}_{\text{kin}}^{(n)}(x) = & -\frac{1}{4} F_{(n)}^{\mu\nu} F_{(n)\mu\nu} \\ & + \frac{1}{2} (m_{A(n)} A_{(n)\mu} + \partial_\mu G_{(n)}) \left(m_{A(n)} A_{(n)}^\mu + \partial^\mu G_{(n)} \right) \\ & + \frac{1}{2} (\partial_\mu a_{(n)}) (\partial^\mu a_{(n)}) - \frac{1}{2} m_{a(n)}^2 a_{(n)}^2 + \dots \end{aligned} \quad (2.25)$$

$G_{(n)}$ now plays the rôle of a Goldstone mode in an Abelian Higgs model. For $n \geq 1$, both compactification and the traditional Higgs mechanism cooperate to make the KK modes massive. Consequently, the corresponding Goldstone mode (2.24) is a linear combination of $A_{(n)5}$ and $\chi_{(n)}$. Since the mass contribution from spontaneous symmetry breaking is expected to be small compared to the KK masses, the Goldstone modes $G_{(n)}$ are dominated by the extra component of the gauge field for $n \geq 1$. The pseudoscalar field $a_{(n)}$ describes an additional physical KK excitation degenerate in mass with the KK gauge mode $A_{(n)\mu}$, i.e.

$$m_{a(n)}^2 = m_{A(n)}^2 = (n^2/R^2) + e^2 v^2. \quad (2.26)$$

The spectrum of the zero KK modes is simply identical to that of a conventional Abelian Higgs model. This is an essential observation because we want to recover known physics in the low-energy limit when we apply the introduced methods to SM extensions in Chapter 3. From the above discussion, it is evident that the appropriate gauge-fixing Lagrangian in (2.19) for a 5-dimensional generalized R_ξ -gauge should be

$$\mathcal{L}_{\text{GF}}(x, y) = -\frac{1}{2\xi} \left[\partial_\mu A^\mu - \xi \left(\partial_5 A_5 + e_5 \frac{v}{\sqrt{2\pi R}} \chi \right) \right]^2. \quad (2.27)$$

The mixing terms in (2.25) are removed and we again arrive at the standard kinetic La-

grangian for massive gauge bosons and the corresponding would-be Goldstone modes

$$\begin{aligned}
\mathcal{L}_{\text{kin}}^{(n)}(x) = & -\frac{1}{4} F_{(n)}^{\mu\nu} F_{(n)\mu\nu} + \frac{1}{2} m_{A(n)}^2 A_{(n)\mu} A_{(n)}^\mu - \frac{1}{2\xi} (\partial_\mu A_{(n)}^\mu)^2 \\
& + \frac{1}{2} (\partial_\mu G_{(n)}) (\partial^\mu G_{(n)}) - \frac{\xi}{2} m_{A(n)}^2 G_{(n)}^2 \\
& + \frac{1}{2} (\partial_\mu a_{(n)}) (\partial^\mu a_{(n)}) - \frac{1}{2} m_{a(n)}^2 a_{(n)}^2 \\
& + \frac{1}{2} (\partial_\mu h_{(n)}) (\partial^\mu h_{(n)}) - \frac{1}{2} m_{h(n)}^2 h_{(n)}^2 .
\end{aligned} \tag{2.28}$$

The CP-odd scalar modes $a_{(n)}$ and the Higgs KK modes $h_{(n)}$ with mass

$$m_{h(n)} = \sqrt{(n^2/R^2) + \lambda_5 v^2/\pi R} \tag{2.29}$$

are not affected by the gauge-fixing procedure. Finally, we observe that the limit $\xi \rightarrow \infty$ consistently corresponds to the unitary gauge.

As a qualitatively different way of implementing the Higgs sector in a higher-dimensional Abelian model we can localize the Higgs field at the $y = 0$ boundary of the S^1/Z_2 orbifold, following the example of the fermions in 5D-QED. Introducing the appropriate δ -function in the 5-dimensional Lagrangian this amounts to

$$\mathcal{L}(x, y) = -\frac{1}{4} F^{MN} F_{MN} + \delta(y) [(D_\mu \Phi)^* (D^\mu \Phi) - V(\Phi)] + \mathcal{L}_{\text{GF}}(x, y), \tag{2.30}$$

where the covariant derivative is given by (2.16) and the Higgs potential has its familiar 4-dimensional form. Since the Higgs potential is effectively four-dimensional the Higgs field, not having KK excitations as a brane field, acquires the usual VEV. Notice that the bulk scalar field $A_5(x, y)$, as a result of its odd Z_2 -parity, does not couple to the Higgs sector on a brane.

After compactification and integration over the y -dimension spontaneous symmetry breaking again generates masses for the KK gauge modes $A_{(n)}^\mu$. However, the mass matrix for the simple Fourier modes in (2.5) is no longer diagonal because of the δ -function in (2.30). Instead, it is given by

$$M_A^2 = \begin{pmatrix} m^2 & \sqrt{2} m^2 & \sqrt{2} m^2 & \cdots \\ \sqrt{2} m^2 & 2m^2 + (1/R)^2 & 2m^2 & \cdots \\ \sqrt{2} m^2 & 2m^2 & 2m^2 + (2/R)^2 & \cdots \\ \vdots & \vdots & \vdots & \ddots \end{pmatrix}, \tag{2.31}$$

where $m = ev$. Therefore, the Fourier modes are no longer mass eigenstates. In other words, the Fourier modes are mixed by the equations of motion. One can search for the

proper eigenmodes of the system before integrating out the extra dimension. This approach is developed in Section 7.1 for a slightly more complicated model. Here, we will follow an alternative approach using directly the result (2.31) in the Fourier-mode basis.

To find the mass eigenvalues, one has to calculate the zeros of the characteristic polynomial

$$\det(M_A^2 - \lambda I) = \left(\prod_{n=1}^{\infty} (n^2/R^2 - \lambda) \right) \left(m^2 - \lambda - 2\lambda m^2 \sum_{n=1}^{\infty} \frac{1}{(n/R)^2 - \lambda} \right) \quad (2.32)$$

of the the mass matrix (2.31). The infinite sum can be performed analytically using the techniques introduced in Appendix A so that the masses $m_{(n)} = \sqrt{\lambda}$ of the KK mass eigenstates are found to obey the transcendental equation

$$m_{(n)} = \pi m^2 R \cot(\pi m_{(n)} R). \quad (2.33)$$

The zero-mode mass eigenvalues are slightly shifted from what we expect in a 4D model. Expanding the right hand side of 2.33 in powers of $m_{(0)}R$, an approximate calculation to first order in m^2/M^2 yields

$$m_{(0)}^2 \approx m^2 \left(1 - \frac{\pi^2}{3} \frac{m^2}{M^2} \right). \quad (2.34)$$

The respective mass eigenstates can also be calculated analytically from (2.31) using Cramer's rule [59]. They are given by

$$\hat{A}_{(n)}^\mu = \left(1 + \pi^2 m^2 R^2 + \frac{m_{(n)}^2}{m^2} \right)^{-1/2} \sum_{j=0}^{\infty} \frac{2 m_{(n)} m}{m_{(n)}^2 - (j/R)^2} \left(\frac{1}{\sqrt{2}} \right)^{\delta_{j,0}} A_{(j)}^\mu. \quad (2.35)$$

In the following, we will distinguish the Fourier modes $A_{(n)}^\mu$ from the mass eigenstates $\hat{A}_{(n)}^\mu$ by a hat and by calling only the latter ones KK modes. The couplings of the KK modes to fermions will also be slightly shifted with respect to the couplings of the Fourier modes in (2.18). To be specific, the interaction Lagrangian can be parameterized by

$$\mathcal{L}_{\text{int}} = -\bar{\Psi} \gamma_\mu \Psi \sum_{n=0}^{\infty} e_{(n)} \hat{A}_{(n)}^\mu, \quad (2.36)$$

where the couplings $e_{(n)}$ of the different mass eigenstates are found by the basis rotation from the Fourier modes to (2.35). They are given by

$$e_{(n)} = \sqrt{2} e \left(1 + \frac{m^2}{m_{(n)}^2} + \pi^2 \frac{m^2}{M^2} \frac{m^2}{m_{(n)}^2} \right)^{-\frac{1}{2}}. \quad (2.37)$$

For example, the shift in the zero mode coupling is approximately given by

$$e_{(0)} \approx \left(1 - \frac{\pi^2}{3} \frac{m^2}{M^2} \right) e. \quad (2.38)$$

In the Abelian model, the shifts in masses and couplings may seem to be a mere matter of redefinition of the measured masses and couplings in terms of the fundamental constants of the 5D theory. However, they lead to important phenomenological implications in the context of the higher-dimensional standard model, where the various couplings are affected differently as we will see in Chapter 4.

To find the appropriate form of the gauge-fixing term $\mathcal{L}_{\text{GF}}(x, y)$ in (2.30), we follow (2.27), but restrict the scalar field χ to the brane $y = 0$, that is

$$\mathcal{L}_{\text{GF}}(x, y) = -\frac{1}{2\xi} \left[\partial_\mu A^\mu - \xi (\partial_5 A_5 + e_5 v \chi \delta(y)) \right]^2. \quad (2.39)$$

Ignoring the square of the δ -function for a moment, the effective 4-dimensional gauge-fixing Lagrangian $\mathcal{L}_{\text{GF}}(x)$ is given by

$$\begin{aligned} \mathcal{L}_{\text{GF}}(x) = & -\frac{1}{2\xi} (\partial_\mu A_{(0)}^\mu)^2 - \frac{1}{2\xi} \sum_{n=1}^{\infty} \left(\partial_\mu A_{(n)}^\mu - \xi \frac{n}{R} A_{(n)5} \right)^2 \\ & + ev \chi (\partial_\mu A_{(0)}^\mu) + \sqrt{2} ev \chi \sum_{n=1}^{\infty} (\partial_\mu A_{(n)}^\mu) \\ & - \xi \sqrt{2} ev \chi \sum_{n=1}^{\infty} \frac{n}{R} A_{(n)5} - \frac{\xi}{2} e_5^2 v^2 \chi^2 \delta(0). \end{aligned} \quad (2.40)$$

Using this gauge-fixing Lagrangian in (2.30), the mixing terms indeed cancel up to total derivatives. However, one has to understand the meaning of $\delta(0)$ in the last term of (2.40). On the S^1/Z_2 orbifold, the δ -function may be represented by

$$\delta(y) = \frac{1}{2\pi R} + \sum_{n=1}^{\infty} \frac{1}{\pi R} \cos\left(\frac{ny}{R}\right), \quad (2.41)$$

which implies

$$\delta(0) = \frac{1}{2\pi R} + \sum_{n=1}^{\infty} \frac{1}{\pi R}. \quad (2.42)$$

The last identity allows us to regularize $\delta(0)$ by considering only Fourier modes up to a given mode number n and obtain the original model in the limit $n \rightarrow \infty$. Here, in contrast to non-Abelian models (see Section 3.1), this regularization prescription is not in conflict with gauge invariance as can be seen in (2.9). However, it should be used with great care. After integration over the extra dimension, (2.39) leads to the generalized R_ξ gauge

$$\mathcal{L}_{\text{GF}}^{(n)}(x) = -\frac{1}{2\xi} \left[\partial_\mu A_{(n)}^\mu - \xi \left(\frac{n}{R} A_{(n)5} + \sqrt{2}^{(1-\delta_{n,0})} ev \chi \right) \right]^2, \quad (2.43)$$

for each mode, where again $e = e_5/\sqrt{2\pi R}$.

The mass spectrum of the unphysical Goldstone modes may be determined by diagonalizing the mass matrix

$$M_\xi^2 = \begin{pmatrix} e^2 v^2 (1 + \sum_{n=1}^{\infty} 2) & \sqrt{2} (1/R) ev & \sqrt{2} (2/R) ev & \cdots \\ \sqrt{2} (1/R) ev & (1/R)^2 & 0 & \cdots \\ \sqrt{2} (2/R) ev & 0 & (2/R)^2 & \cdots \\ \vdots & \vdots & \vdots & \ddots \end{pmatrix} \quad (2.44)$$

of the fields χ and $A_{(n)5}$ in

$$\mathcal{L}_{\text{mass}}^\xi(x) = -\frac{\xi}{2} (\chi, A_{(1)5}, A_{(2)5}, \dots) M_\xi^2 \begin{pmatrix} \chi \\ A_{(1)5} \\ A_{(2)5} \\ \vdots \end{pmatrix}. \quad (2.45)$$

It can be shown that the characteristic polynomial of M_ξ^2 is formally identical to the one of M_A^2 in (2.31) [18, 42]. Consequently, the mass eigenvalues of M_ξ^2 are given by $m_{(n)}$ in (2.33). Thus, as expected from usual R_ξ gauges in spontaneously broken gauge theories, we find a one-to-one correspondence of each physical vector mode of mass $m_{(n)}$ to an unphysical Goldstone mode with gauge-dependent mass $\sqrt{\xi} m_{(n)}$. Moreover, the Goldstone mass eigenstates are given by

$$\hat{G}_{(n)} = \left(1 + \pi^2 m^2 R^2 + \frac{m_{(n)}^2}{m^2} \right)^{-1/2} \left(\sqrt{2} \chi + \sum_{j=1}^{\infty} \frac{2(j/R) m}{m_{(n)}^2 - (j/R)^2} A_{(j)5} \right). \quad (2.46)$$

In the unitary gauge $\xi \rightarrow \infty$, the fields $\hat{G}_{(n)}$, or equivalently the fields $A_{(n)5}$ and χ , are absent from the theory. Therefore, as opposed to the previously described bulk-Higgs model, the present brane-Higgs model does not predict other massive KK scalars apart from the physical Higgs boson h .

At this point, we cannot decide which of the two possibilities for the Higgs sector, brane or bulk Higgs fields, could be realized in nature. We have to be ready to analyze both of them phenomenologically when we move on to SM extensions. Thus, it is interesting to consider a model with two complex Higgs fields: one Higgs field $\Phi_1(x, y)$ propagating in the bulk and the other field $\Phi_2(x)$ localized on a brane at $y = 0$. The 5-dimensional Lagrangian of this Abelian 2-Higgs model is given by

$$\begin{aligned} \mathcal{L}(x, y) = & -\frac{1}{4} F^{MN} F_{MN} + (D_M \Phi_1)^* (D^M \Phi_1) + \delta(y) (D_\mu \Phi_2)^* (D^\mu \Phi_2) \\ & - V(\Phi_1, \Phi_2) + \mathcal{L}_{\text{GF}}(x, y), \end{aligned} \quad (2.47)$$

where V can be the most general Higgs potential allowed by gauge invariance. The particular features of the Higgs potential will not be of phenomenological relevance in the

following as long as it leads to VEVs for both complex scalar fields. Thus, we may linearly expand Φ_1 and Φ_2 around their VEVs as follows:

$$\Phi_1(x, y) = \frac{1}{\sqrt{2}} \left(\frac{v_1}{\sqrt{2\pi R}} + h_1(x, y) + i \chi_1(x, y) \right), \quad (2.48)$$

$$\Phi_2(x) = \frac{1}{\sqrt{2}} \left(v_2 + h_2(x) + i \chi_2(x) \right). \quad (2.49)$$

Adopting the commonly used notation in 2-Higgs models, we define $v_1 = v \cos \beta$ and $v_2 = v \sin \beta$, i.e. $\tan \beta = v_2/v_1$.

In this 5-dimensional Abelian 2-Higgs model, the effective mass matrix M_A^2 of the Fourier modes $A_{(n)}^\mu$ is given by a sum of two matrices:

$$M_A^2 = M_{\text{brane}}^2 + M_{\text{bulk}}^2. \quad (2.50)$$

The first matrix M_{brane}^2 , which includes the geometric KK masses n^2/R^2 , may be obtained from (2.31) after replacing $m^2 = e^2 v^2$ with $m^2 = e^2 v^2 \sin^2 \beta$. The second matrix M_{bulk}^2 is proportional to unity, $M_{\text{bulk}}^2 = e^2 v^2 \cos^2 \beta \mathbb{1}$. Due to the particular structure of M_A^2 , the mass eigenvalues of the KK gauge modes are given by

$$m_{A(n)}^2 = m_{(n)}^2 + \Delta m_{(n)}^2, \quad (2.51)$$

where $\Delta m_{(n)}^2 = e^2 v^2 \cos^2 \beta$ and $m_{(n)}$ are the roots of the transcendental equation (2.33). The corresponding mass eigenstates $\hat{A}_{(n)}^\mu$ are in turn given by (2.35), after $m_{(n)}^2$ has been replaced with $m_{A(n)}^2 - \Delta m_{(n)}^2$.

Combining our knowledge about gauge fixing, we may eliminate the mixing terms between $A_{(n)}^\mu$ and the fields $A_{(n)5}$, $\chi_{1(n)}$ and χ_2 by choosing

$$\mathcal{L}_{\text{GF}}(x, y) = -\frac{1}{2\xi} \left[\partial_\mu A^\mu - \xi \left(\partial_5 A_5 + e_5 \frac{v}{\sqrt{2\pi R}} \cos \beta \chi_1 + e_5 v \sin \beta \chi_2 \delta(y) \right) \right]^2. \quad (2.52)$$

Performing a quite lengthy calculation, we have shown in [18, 42] that there are also proper Goldstone modes $\hat{G}_{(n)}$ with masses $\sqrt{\xi} m_{A(n)}$ in this model.

We conclude this section by remarking that even for the most general Abelian case, an appropriate higher-dimensional gauge-fixing condition analogous to (2.52) has to be found which leads, after compactification, to the usual R_ξ gauge known from ordinary 4-dimensional theories. In the following, we shall see that the above gauge-fixing quantization procedure can be extended to non-Abelian models (cf. Chapter 3) as well as to models with radiatively induced kinetic terms on a brane (cf. Chapter 7).

Chapter 3

5-Dimensional Extensions of the Standard Model

In this chapter we study minimal 5-dimensional extensions of the SM compactified on an S^1/Z_2 orbifold, in which some or all of the $SU(2)_L$ and $U(1)_Y$ gauge bosons and the Higgs doublets may propagate in the bulk. As before, we assume that the chiral fermions are localized on a brane at the $y = 0$ fixed point of the S^1/Z_2 orbifold. Before we can start our investigation, we have to understand how to formulate non-Abelian gauge theories in five dimensions.

3.1 Higher-Dimensional Non-Abelian Theory

First, we consider a pure non-Abelian theory, such as 5-dimensional Quantum Chromodynamics (5D-QCD), without interactions to matter. The 5D-QCD Lagrangian reads

$$\mathcal{L}(x, y) = -\frac{1}{4} F_{MN}^a F^{aMN} + \mathcal{L}_{\text{GF}} + \mathcal{L}_{\text{FP}}, \quad (3.1)$$

where

$$F_{MN}^a = \partial_M A_N^a - \partial_N A_M^a + g_5 f^{abc} A_M^b A_N^c \quad (3.2)$$

and f^{abc} are the structure constants of the gauge group $SU(N)$, with $N = 3$ for 5D-QCD. The color indices a, b, c are summed over the generators of the gauge group. In (3.1) the gauge-fixing term \mathcal{L}_{GF} and the induced Faddeev-Popov Lagrangian \mathcal{L}_{FP} will be determined later in this section.

We compactify each of the N gauge fields $A_M^a(x, y)$ separately on S^1/Z_2 using the constraints (2.4). Under an $SU(N)$ gauge transformation $A_M^a(x, y)$ transforms as

$$A_M^a(x, y) \rightarrow A_M^a(x, y) + \partial_M \Theta^a(x, y) - g_5 f^{abc} \Theta^b(x, y) A_M^c(x, y). \quad (3.3)$$

After a Fourier expansion of $A_\mu^a(x, y)$, $A_5^a(x, y)$ and $\Theta^a(x, y)$ according to (2.5), one finds that the local $SU(N)$ transformation (3.3) amounts to [12]

$$\begin{aligned}
A_{(0)\mu}^a &\rightarrow A_{(0)\mu}^a + \partial_\mu \Theta_{(0)}^a - \frac{1}{2} \frac{g_5}{\sqrt{2\pi R}} f^{abc} \sum_{m=0}^{\infty} 2^{1-\delta_{m,0}} \Theta_{(m)}^b (1 + \delta_{m,0}) A_{(m)\mu}^c, \\
A_{(n)\mu}^a &\rightarrow A_{(n)\mu}^a + \partial_\mu \Theta_{(n)}^a \\
&\quad - \frac{1}{2} \frac{g_5}{\sqrt{2\pi R}} f^{abc} \sum_{m=0}^{\infty} \sqrt{2^{1-\delta_{m,0}}} \Theta_{(m)}^b \left[\sqrt{2^{-\delta_{m,n}}} (1 + \delta_{m,n}) A_{(|m-n|)\mu}^c + A_{(m+n)\mu}^c \right], \\
A_{(n)5}^a &\rightarrow A_{(n)5}^a - \frac{n}{R} \Theta_{(n)}^a \\
&\quad - \frac{1}{2} \frac{g_5}{\sqrt{2\pi R}} f^{abc} \sum_{m=0}^{\infty} \sqrt{2^{1-\delta_{m,0}}} \Theta_{(m)}^b \left(\text{sgn}(n-m) A_{(|m-n|)5}^c + A_{(m+n)5}^c \right), \quad (3.4)
\end{aligned}$$

where $n \geq 1$. As opposed to the Abelian case, the KK modes mix with each other under a non-Abelian gauge transformation. As a result of this mixing, any attempt to truncate the theory at a given KK mode $n = n_{\text{trunc}}$ will explicitly break gauge invariance. To overcome this difficulty, it has been suggested to “deconstruct” the extra dimension [29, 60, 61], i.e. to put it on a lattice. Although we will not make further use of deconstruction, notice that working on a lattice with a finite number of sites results in a model with only a finite number of degrees of freedom. The lattice model can be formulated manifestly gauge invariant and such that the spectrum and the couplings of the full theory are approximately matched up to some KK number. However, the deconstructed model of course significantly differs if probed at distances close to the lattice spacing. The full theory is recovered in the limit of infinitely many lattice sites.

It is straightforward to generalize the gauge-fixing term of 5D-QED given in (2.10) to the 5D-QCD case. The gauge-fixing term in 5D-QCD is given by

$$\mathcal{L}_{\text{GF}}(x, y) = -\frac{1}{2\xi} (F^a(A^a))^2, \quad (3.5)$$

with

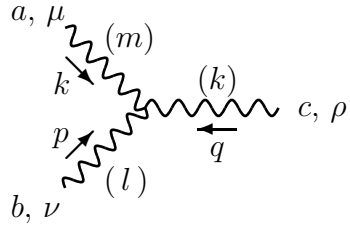
$$F^a(A^a) = \partial^\mu A_\mu^a - \xi \partial_5 A_5^a. \quad (3.6)$$

In this generalized R_ξ gauge the mixing terms $A_{(n)\mu}^a \partial^\mu A_{(n)5}^a$ again disappear, so the Fourier modes represent mass eigenstates. As in the Abelian case, the latter is spoiled by a Higgs mechanism involving brane interactions. The mass eigenstates can then, independently for each color index, be determined in close analogy to the Abelian model.

In non-Abelian theories the R_ξ gauge induces an interacting ghost sector which is described by the Faddeev-Popov Lagrangian

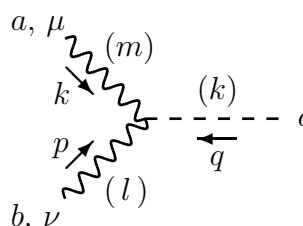
$$\begin{aligned}
\mathcal{L}_{\text{FP}}(x, y) &= \bar{c}^a \frac{\delta F^a(A^a)}{\delta \Theta^b} c^b \\
&= \bar{c}^a \left[\partial^\mu (\partial_\mu \delta^{ab} - g_5 f^{abc} A_\mu^c) - \xi \partial_5 (\partial_5 \delta^{ab} - g_5 f^{abc} A_5^c) \right] c^b. \quad (3.7)
\end{aligned}$$

3-boson vertex:



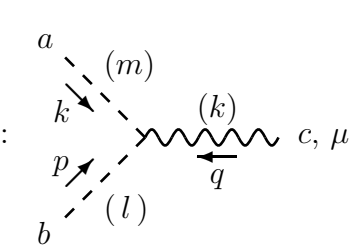
$$g \left(\frac{1}{\sqrt{2}} \right)^{(\delta_{k,0} + \delta_{l,0} + \delta_{m,0} + 1)} \delta_{k,l,m} [g^{\mu\nu} (k-p)^\rho + g^{\nu\rho} (p-q)^\mu + g^{\rho\mu} (q-k)^\nu]$$

vertex with 1 scalar:



$$-i g f^{abc} g^{\mu\nu} \left[\left(\frac{m}{R} \right) \left(\frac{1}{\sqrt{2}} \right)^{(\delta_{l,0} + 1)} \tilde{\delta}_{k,l,m} - \left(\frac{l}{R} \right) \left(\frac{1}{\sqrt{2}} \right)^{(\delta_{m,0} + 1)} \tilde{\delta}_{k,m,l} \right]$$

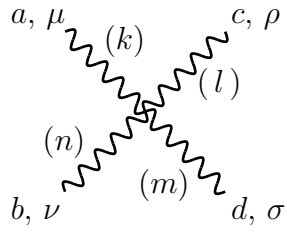
vertex with 2 scalars:



$$g \left(\frac{1}{\sqrt{2}} \right)^{(\delta_{k,0} + 1)} \tilde{\delta}_{l,k,m} f^{abc} (p-k)^\mu$$

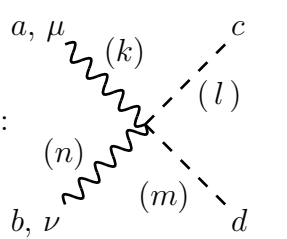
Figure 3.1: Feynman rules for the triple gauge-boson coupling. $\delta_{k,l,m}$ and $\tilde{\delta}_{l,k,m}$ are defined in (3.8).

4-boson vertex:



$$-i g^2 \delta_{k,l,m,n} \left(\frac{1}{\sqrt{2}} \right)^{(\delta_{k,0} + \delta_{l,0} + \delta_{m,0} + \delta_{n,0} + 2)} [f^{ace} f^{bde} (g^{\mu\nu} g^{\rho\sigma} - g^{\mu\sigma} g^{\nu\rho}) + f^{abe} f^{cde} (g^{\mu\rho} g^{\nu\sigma} - g^{\mu\sigma} g^{\nu\rho}) + f^{ade} f^{bce} (g^{\mu\nu} g^{\rho\sigma} - g^{\mu\rho} g^{\nu\sigma})]$$

vertex with 2 scalars:



$$i g^2 \left(\frac{1}{\sqrt{2}} \right)^{(\delta_{k,0} + \delta_{n,0})} \tilde{\delta}_{k,n,l,m} 2 g^{\mu\nu} [f^{ace} f^{bde} + f^{ade} f^{bce}]$$

Figure 3.2: Feynman rules for the quartic gauge-boson coupling. $\delta_{k,l,m,n}$ and $\tilde{\delta}_{k,n,l,m}$ are defined in (3.9).

In the above, $c^a(x, y)$ denote the higher-dimensional ghost fields which are even under Z_2 : $c^a(x, y) = c^a(x, -y)$, i.e. they share the transformation properties with the group parameters $\Theta^a(x, y)$.

Integrating out the extra dimension in the interaction terms we find the Feynman rules for the self-interactions of the KK modes $A_{(n)\mu}^a$ and $A_{(n)5}^a$ in the effective 4-dimensional theory. They are exhibited in Figs. 3.1 and 3.2 for the R_ξ -gauge (3.5). In the unitary gauge, the 5D-QCD Feynman rules reduce to those presented in [56]. The factors

$$\begin{aligned}\delta_{k,l,m} &= \delta_{k+l+m,0} + \delta_{k+l-m,0} + \delta_{k-l+m,0} + \delta_{k-l-m,0}, \\ \tilde{\delta}_{k,l,m} &= -\delta_{k+l+m,0} + \delta_{k+l-m,0} - \delta_{k-l+m,0} + \delta_{k-l-m,0},\end{aligned}\tag{3.8}$$

in the triple gauge boson interaction and

$$\begin{aligned}\delta_{k,l,m,n} &= +\delta_{k+l+m+n,0} + \delta_{k+l+m-n,0} + \delta_{k+l-m+n,0} + \delta_{k+l-m-n,0} \\ &\quad + \delta_{k-l+m+n,0} + \delta_{k-l+m-n,0} + \delta_{k-l-m+n,0} + \delta_{k-l-m-n,0}, \\ \tilde{\delta}_{k,l,m,n} &= -\delta_{k+l+m+n,0} + \delta_{k+l+m-n,0} + \delta_{k+l-m+n,0} - \delta_{k+l-m-n,0} \\ &\quad - \delta_{k-l+m+n,0} + \delta_{k-l+m-n,0} + \delta_{k-l-m+n,0} - \delta_{k-l-m-n,0},\end{aligned}\tag{3.9}$$

in the quartic gauge boson interaction imply selection rules for the KK modes $A_{(n)\mu}^a$ and $A_{(n)5}^a$ being typical for the interactions between bulk fields. They are the analogue of momentum conservation with respect to the extra dimension. On the orbifold, the wave functions for the mass eigenstates are given by trigonometric functions being linear combinations of the momentum eigenfunctions of momenta with opposite sign. The notion of incoming or outgoing KK number in analogy to incoming and outgoing momenta is thus not well defined. As a consequence, we find KK number conservation up to a sign at each vertex.

In particular, the selection rules imply, that no higher KK modes ($n \geq 1$) can be exchanged in tree-level amplitudes in which all external particles are zero modes. The production of a single heavy KK mode is also forbidden at tree-level. Thus, in this respect, the phenomenology of models with universal extra dimensions is similar to R-parity conserving supersymmetry.

3.2 $SU(2)_L \otimes U(1)_Y$ -Bulk Model

Concerning the SM, we first consider the most frequently investigated bulk-bulk model [18, 31–41], where all electroweak gauge fields propagate in the bulk and couple to both a brane

and a bulk Higgs doublet. The Lagrangian of the gauge-Higgs sector is given by

$$\begin{aligned} \mathcal{L}(x, y) = & -\frac{1}{4} B_{MN} B^{MN} - \frac{1}{4} F_{MN}^a F^{aMN} + (D_M \Phi_1)^\dagger (D^M \Phi_1) \\ & + \delta(y) (D_\mu \Phi_2)^\dagger (D^\mu \Phi_2) - V(\Phi_1, \Phi_2) + \mathcal{L}_{\text{GF}}(x, y) + \mathcal{L}_{\text{FP}}(x, y), \end{aligned} \quad (3.10)$$

where B_{MN} and F_{MN}^a ($a = 1, 2, 3$ for $\text{SU}(2)$) are the field strength tensors of the $\text{U}(1)_Y$ and $\text{SU}(2)_L$ gauge fields, respectively. As usual, we define the covariant derivative D_M as

$$D_M = \partial_M - i g_5 A_M^a \tau^a - i \frac{g'_5}{2} B_M, \quad (3.11)$$

where $\tau^a = \sigma^a/2$ are the $\text{SU}(2)$ generators and g_5, g'_5 denote the 5D gauge couplings for $\text{SU}(2), \text{U}(1)$, respectively. Concerning the Higgs potential $V(\Phi_1, \Phi_2)$ of this bulk-bulk model, the only relevant point for phenomenology is that it leads to the correct pattern of spontaneous symmetry breaking. Hence, the bulk Higgs doublet $\Phi_1(x, y)$ and the brane Higgs doublet $\Phi_2(x)$ are linearly expanded around their VEVs, i.e.

$$\Phi_1(x, y) = \begin{pmatrix} -i\chi_1^+ \\ \frac{1}{\sqrt{2}} \left(\frac{v_1}{\sqrt{2\pi R}} + h_1 + i\chi_1 \right) \end{pmatrix}, \quad \Phi_2(x) = \begin{pmatrix} -i\chi_2^+ \\ \frac{1}{\sqrt{2}} (v_2 + h_2 + i\chi_2) \end{pmatrix}, \quad (3.12)$$

where the phase convention in the charged sector is chosen differently from [18, 42] because it will be convenient in Chapter 6. We do not repeat the calculational steps for determining the particle mass spectrum and the KK modes $\hat{A}_{(n)}^\mu, \hat{Z}_{(n)}^\mu$ of the $\text{SU}(2)_L \otimes \text{U}(1)_Y$ -bulk model, as they are analogous to those of the Abelian model discussed in Chapter 2. In fact, the analogy becomes rather explicit if the bulk gauge fields are written in terms of the 5D fields:

$$\begin{aligned} W_M^\pm &= \frac{1}{\sqrt{2}} (A_M^1 \mp i A_M^2), \\ Z_M &= \frac{1}{\sqrt{g_5^2 + g_5'^2}} (g_5 A_M^3 - g_5' B_M), \\ A_M &= \frac{1}{\sqrt{g_5^2 + g_5'^2}} (g_5' A_M^3 + g_5 B_M). \end{aligned} \quad (3.13)$$

In Appendix B the analytic results for the mass eigenvalues are given for the SM model extensions under study. Notice that the photon field is not affected by spontaneous symmetry breaking and, thus, the Fourier modes coincide with the KK modes.

Proceeding as in the Abelian case, we can determine the appropriate R_ξ gauge-fixing func-

tions for the $SU(2)_L$ and $U(1)_Y$ gauge bosons:

$$F^a(A^a) = \partial_\mu A^{a\mu} - \xi_A \left[\partial_5 A_5^a - i \frac{g_5}{\sqrt{2\pi R}} \left(\Phi_1^\dagger \tau^a \Phi_0 - \Phi_0^\dagger \tau^a \Phi_1 \right) \cos \beta - i g_5 \left(\Phi_2^\dagger \tau^a \Phi_0 - \Phi_0^\dagger \tau^a \Phi_2 \right) \sin \beta \delta(y) \right], \quad (3.14)$$

$$F(B) = \partial_\mu B^\mu - \xi_B \left[\partial_5 B_5 - i \frac{g'_5}{2\sqrt{2\pi R}} \left(\Phi_1^\dagger \Phi_0 - \Phi_0^\dagger \Phi_1 \right) \cos \beta - i \frac{g'_5}{2} \left(\Phi_2^\dagger \Phi_0 - \Phi_0^\dagger \Phi_2 \right) \sin \beta \delta(y) \right], \quad (3.15)$$

with

$$\Phi_0 = \frac{1}{\sqrt{2}} \begin{pmatrix} 0 \\ v \end{pmatrix}, \quad v = \sqrt{v_1^2 + v_2^2}, \quad \frac{v_2}{v_1} = \tan \beta. \quad (3.16)$$

To avoid gauge-dependent photon- Z -mixing terms at the tree-level, we assume in the following that $\xi_A = \xi_B = \xi$. Under this assumption, the gauge-fixing Lagrangian $\mathcal{L}_{\text{GF}}(x, y)$ in (3.10) can be expressed in terms of the real gauge-fixing functions $F^a(A^a)$ and $F(B)$ as follows:

$$\mathcal{L}_{\text{GF}}(x, y) = -\frac{1}{2\xi} (F^a(A^a))^2 - \frac{1}{2\xi} (F(B))^2. \quad (3.17)$$

Furthermore, the Faddeev-Popov term $\mathcal{L}_{\text{FP}}(x, y)$ in (3.10) is induced by the variations of $F^a(A^a)$ and $F(B)$ with respect to $SU(2)_L$ and $U(1)_Y$ gauge transformations. More explicitly, $\mathcal{L}_{\text{FP}}(x, y)$ may be computed in the standard way from

$$\mathcal{L}_{\text{FP}}(x, y) = \bar{c}^a \frac{\delta F^a(A^a)}{\delta \Theta^b} c^b + \bar{c} \frac{\delta F(B)}{\delta \Theta} c, \quad (3.18)$$

where $c^a(x, y)$ and $c(x, y)$ are the 5-dimensional ghost fields associated with the $SU(2)_L$ and $U(1)_Y$ gauge groups, respectively. As in 5D-QCD, the ghost fields are even under Z_2 .

In the above R_ξ -gauge-fixing prescription, the complete kinetic Lagrangian of the gauge sector, written in terms of the gauge fields defined in (3.13) and the corresponding scalar modes, is rather analogous to the corresponding one of the Abelian model investigated in Chapter 2. Therefore, we do not repeat the derivation here but give the propagators of the KK gauge and Goldstone modes in the R_ξ gauge in Appendix B, where we also list the exact analytic results for the couplings of the gauge bosons to fermions, to be discussed in Section 3.5.

The self-couplings for the $SU(2)$ gauge-boson Fourier modes are given in Section 3.1. The couplings between the scalar and the gauge Fourier modes can also be computed in a straight forward way. The corresponding Feynman rules being important for the analysis in Chapter 6 are displayed in Appendix I. The Feynman rules for the mass eigenstates are of course harder to calculate if a brane Higgs induces mixing. Some specific, phenomenologically important examples are given in Appendices G and H.

3.3 $SU(2)_L$ -Brane, $U(1)_Y$ -Bulk Model

Let us now consider a different minimal 5-dimensional extension to the SM in which only the $U(1)_Y$ gauge boson propagates in the bulk, while the $SU(2)_L$ gauge field is confined to the $y = 0$ boundary of the S^1/Z_2 orbifold. The Lagrangian of this brane-bulk model reads

$$\begin{aligned} \mathcal{L}(x, y) = & -\frac{1}{4} B_{MN} B^{MN} + \delta(y) \left[-\frac{1}{4} F_{\mu\nu}^a F^{a\mu\nu} + (D_\mu \Phi)^\dagger (D^\mu \Phi) - V(\Phi) \right] \\ & + \mathcal{L}_{\text{GF}}(x, y) + \mathcal{L}_{\text{FP}}(x, y) \end{aligned} \quad (3.19)$$

with $D_\mu = \partial_\mu - i g_5 A_\mu^a(x) \tau^a - i \frac{g'}{2} B_\mu(x, 0)$. Observe that only a brane Higgs doublet

$$\Phi(x) = \begin{pmatrix} -i\chi^+ \\ \frac{1}{\sqrt{2}}(v + h + i\chi) \end{pmatrix} \quad (3.20)$$

can be added in this model because a bulk Higgs doublet would destroy the gauge invariance in the bulk. The gauge fields restricted to the brane $y = 0$ are missing in the bulk to form an appropriate covariant derivative. Generally, if a gauge group is confined to a brane, only matter fields which are not charged with respect to the group (e.g. sterile neutrinos) can propagate in the bulk. As a consequence, the Higgs potential of this model has the known SM form: $V(\Phi) = \mu^2 |\Phi|^2 + \lambda |\Phi|^4$.

In the $SU(2)_L$ -brane, $U(1)_Y$ -bulk model, only the $B^\mu(x, y)$ boson has to be expanded in Fourier modes. While the W -boson sector is completely 4-dimensional, the neutral gauge sector gets complicated by the brane-bulk mixing of $B_\mu(x, y)$ with $A_\mu^3(x)$ through the VEV of the brane Higgs field $\Phi(x)$. To be more precise, considering only the mass terms, we find for the neutral gauge sector

$$\mathcal{L}_{\text{mass}}^N(x) = \frac{1}{2} \left(A^{3\mu}, B_{(0)\mu}^\mu, B_{(1)\mu}^\mu, \dots \right) M_N^2 \begin{pmatrix} A_\mu^3 \\ B_{(0)\mu} \\ B_{(1)\mu} \\ \vdots \end{pmatrix} \quad (3.21)$$

with

$$M_N^2 = \begin{pmatrix} m^2 \frac{g^2}{g'^2} & -m^2 \frac{g}{g'} & -\sqrt{2} m^2 \frac{g}{g'} & \dots \\ -m^2 \frac{g}{g'} & m^2 & \sqrt{2} m^2 & \dots \\ -\sqrt{2} m^2 \frac{g}{g'} & \sqrt{2} m^2 & 2m^2 + (1/R)^2 & \dots \\ \vdots & \vdots & \vdots & \ddots \end{pmatrix} \quad (3.22)$$

and $g' = g'_5 / \sqrt{2\pi R}$, $m^2 = g'^2 v^2 / 4$. The mass matrix M_N^2 contains a single zero eigenvalue which corresponds to a massless photon field

$$\hat{A}_\mu = s_W A_\mu^3 + c_W B_{(0)\mu}, \quad (3.23)$$

where $s_W = \sqrt{1 - c_W^2} = g'/\sqrt{g^2 + g'^2}$ is the sine of the weak mixing angle. The other non-zero mass eigenvalues $m_{Z(n)}$ of M_N^2 are determined as the roots of the transcendental equation

$$m_{Z(n)} = \pi m^2 R \cot(\pi m_{Z(n)} R) + \frac{g^2}{g'^2} \frac{m^2}{m_{Z(n)}}. \quad (3.24)$$

The respective mass eigenstates are given by

$$\hat{Z}_{(n)}^\mu = \frac{1}{N} \left[\frac{m_Z}{m_{Z(n)}} c_W A^{3\mu} - \sum_{j=0}^{\infty} \frac{\sqrt{2} m_{Z(n)} m_Z}{m_{Z(n)}^2 - (j/R)^2} \left(\frac{1}{\sqrt{2}} \right)^{\delta_{j,0}} s_W B_{(j)}^\mu \right], \quad (3.25)$$

where $m_Z = \sqrt{g^2 + g'^2} v/2$ and

$$N^2 = \frac{1}{2} \left[\frac{c_W^2}{s_W^2} \left(\frac{m_Z^2}{m_{Z(n)}^2} - 2 \right) + s_W^2 \pi^2 m_Z^2 R^2 + \frac{m_{Z(n)}^2}{m_Z^2 s_W^2} + 1 \right]. \quad (3.26)$$

Notice that the KK mass eigenmode $\hat{Z}_{(0)}$ has to be identified with the observable Z boson. Although the higher KK modes will be denoted by $\hat{Z}_{(n)}$, one has to keep in mind that they are almost pure $B_{(n)}$ states. There are no KK excitations for the photon in this model.

In analogy to the bulk-bulk model in Section 3.2, the appropriate R_ξ gauge-fixing functions for this brane-bulk model are written

$$F^a(A^a) = \partial_\mu A^{a\mu} + \xi ig \left(\Phi^\dagger \tau^a \Phi_0 - \Phi_0^\dagger \tau^a \Phi \right), \quad (3.27)$$

$$F(B) = \partial_\mu B^\mu - \xi \left[\partial_5 B_5 - i \frac{g'_5}{2} \left(\Phi^\dagger \Phi_0 - \Phi_0^\dagger \Phi \right) \delta(y) \right], \quad (3.28)$$

where Φ_0 is given in 3.16. Due to the specific brane-bulk structure of the higher-dimensional model, the corresponding gauge-fixing Lagrangian has the form

$$\mathcal{L}_{\text{GF}}(x, y) = -\frac{1}{2\xi} (F^a(A^a))^2 \delta(y) - \frac{1}{2\xi} (F(B))^2. \quad (3.29)$$

The charged scalar sector, just as the charged gauge sector, is completely standard in this model. The neutral scalar sector, however, has a structure very similar to the one of the Abelian model discussed in Chapter 2. Again, one can show the existence of a one-to-one correspondence between the KK gauge modes with mass $m_{Z(n)}$ and their associate would-be Goldstone modes with mass $\sqrt{\xi} m_{Z(n)}$. The latter KK modes are given by

$$\hat{G}_{(n)}^0 = \frac{1}{N} \left(\chi - \frac{g'v}{\sqrt{2}} \sum_{j=1}^{\infty} \frac{j/R}{m_{Z(n)}^2 - (j/R)^2} B_{(j)5} \right), \quad (3.30)$$

where the normalization factor N is defined in (3.26).

The Faddeev-Popov Lagrangian \mathcal{L}_{FP} can also be obtained in the standard fashion. Taking the brane-bulk structure of the model into account, we may determine \mathcal{L}_{FP} by

$$\mathcal{L}_{\text{FP}}(x, y) = \bar{c}^a(x) \frac{\delta F^a(A^a(x))}{\delta \Theta^b(x)} c^b(x) \delta(y) + \bar{c}(x, y) \frac{\delta F(B(x, y))}{\delta \Theta(x, y)} c(x, y), \quad (3.31)$$

where the (x, y) -dependence of the different fields is explicitly indicated.

3.4 $SU(2)_L$ -Bulk, $U(1)_Y$ -Brane Model

A third minimal 5-dimensional extension of the SM, complementary to the one discussed in Section 3.3, emerges if the $SU(2)_L$ gauge boson is the only field that feels the presence of the fifth compact dimension. The Lagrangian of this bulk-brane model reads

$$\begin{aligned} \mathcal{L}(x, y) = & -\frac{1}{4} F_{MN}^a F^{aMN} + \delta(y) \left[-\frac{1}{4} B_{\mu\nu} B^{\mu\nu} + (D_\mu \Phi)^\dagger (D^\mu \Phi) - V(\Phi) \right] \\ & + \mathcal{L}_{\text{GF}}(x, y) + \mathcal{L}_{\text{FP}}(x, y), \end{aligned} \quad (3.32)$$

with $D_\mu = \partial_\mu - i g_5 A_\mu^a(x, 0) \tau^a - i \frac{g'}{2} B_\mu(x)$. As in the brane-bulk model there is only one Higgs field on the brane $y = 0$ and the Higgs potential is of the SM form. Since only the $SU(2)_L$ gauge boson lives in the bulk, the charged gauge sector of this higher-dimensional standard model is equivalent to the one in the bulk-bulk model discussed in Section 3.2 with $\sin \beta = 1$. Thus, the bulk-brane model predicts a KK tower of W -boson excitations, while the neutral gauge sector is quite analogous to the one discussed in the previous section. Specifically, instead of (3.21) we find

$$\mathcal{L}_{\text{mass}}^N(x) = \frac{1}{2} \left(B^\mu, A_{(0)\mu}^3, A_{(1)\mu}^3, \dots \right) M_N^2 \begin{pmatrix} B_\mu \\ A_{(0)\mu}^3 \\ A_{(1)\mu}^3 \\ \vdots \end{pmatrix}, \quad (3.33)$$

with

$$M_N^2 = \begin{pmatrix} m^2 \frac{g'^2}{g^2} & -m^2 \frac{g'}{g} & -\sqrt{2} m^2 \frac{g'}{g} & \dots \\ -m^2 \frac{g'}{g} & m^2 & \sqrt{2} m^2 & \dots \\ -\sqrt{2} m^2 \frac{g'}{g} & \sqrt{2} m^2 & 2m^2 + (1/R)^2 & \dots \\ \vdots & \vdots & \vdots & \ddots \end{pmatrix}, \quad (3.34)$$

$g = g_5/\sqrt{2\pi R}$ and $m^2 = g^2 v^2/4$. Again, there is a massless KK mode, the photon, given by the linear combination $\hat{A}_\mu = s_W A_{(0)\mu}^3 + c_W B_\mu$. The other KK modes are massive and their masses may be obtained as the solutions of the transcendental equation

$$m_{Z(n)} = \pi m^2 R \cot(\pi m_{Z(n)} R) + \frac{g'^2}{g^2} \frac{m^2}{m_{Z(n)}}. \quad (3.35)$$

The Z boson, denoted as $Z_{(0)}$, and its heavier KK mass eigenmodes may be conveniently expressed in terms of the gauge eigenstates as

$$\hat{Z}_{(n)}^\mu = \frac{1}{N} \left[\sum_{j=0}^{\infty} \frac{\sqrt{2} m_{Z(n)} m_Z}{m_{Z(n)}^2 - (j/R)^2} \left(\frac{1}{\sqrt{2}} \right)^{\delta_{j,0}} c_W A_{(j)}^{3\mu} - \frac{m_Z}{m_{Z(n)}} s_W B^\mu \right], \quad (3.36)$$

where

$$N^2 = \frac{1}{2} \left[\frac{s_W^2}{c_W^2} \left(\frac{m_Z^2}{m_{Z(n)}^2} - 2 \right) + c_W^2 \pi^2 m_Z^2 R^2 + \frac{m_{Z(n)}^2}{m_Z^2 c_W^2} + 1 \right]. \quad (3.37)$$

Contrary to the model in Section 3.3, here the $\hat{Z}_{(n)}$ are almost pure $A_{(n)}^3$ states.

In close analogy to the previous section, the higher-dimensional gauge-fixing functions leading to the generalized R_ξ -gauge are given by

$$F^a(A^a) = \partial_\mu A^{a\mu} - \xi \left[\partial_5 A_5^a - i g_5 \left(\Phi^\dagger \tau^a \Phi_0 - \Phi_0^\dagger \tau^a \Phi \right) \delta(y) \right], \quad (3.38)$$

$$F(B) = \partial_\mu B^\mu + \xi i \frac{g'}{2} \left(\Phi^\dagger \Phi_0 - \Phi_0^\dagger \Phi \right). \quad (3.39)$$

They give rise to the gauge-fixing Lagrangian

$$\mathcal{L}_{\text{GF}}(x, y) = -\frac{1}{2\xi} (F^a(A^a))^2 - \frac{1}{2\xi} (F(B))^2 \delta(y). \quad (3.40)$$

The charged scalar sector of this model is identical to the one in the bulk-bulk model without the presence of a Higgs field in the bulk. On the other hand, the neutral scalar sector predicts a KK tower of would-be Goldstone modes associated with the longitudinal polarization degrees of the massive KK gauge modes $\hat{Z}_{(n)}$. The would-be Goldstone KK modes are determined by

$$\hat{G}_{(n)}^0 = \frac{1}{N} \left(\chi + \frac{gv}{\sqrt{2}} \sum_{j=1}^{\infty} \frac{j/R}{m_{Z(n)}^2 - (j/R)^2} A_{(j)5}^3 \right), \quad (3.41)$$

with N as defined in (3.37). The Faddeev-Popov Lagrangian can be calculated as in the brane-bulk model (cf. (3.31)) by considering the obvious modifications which account for the complementary bulk-brane structure of the model.

Concerning the self-couplings and the gauge couplings of the scalars, the comments at the end of Section 3.2 apply for both the brane-bulk and the bulk-brane model with only obvious modifications. For example, in the brane-bulk model, the $SU(2)$ self couplings are, of course, completely SM-like.

3.5 Fermions on the Brane

For all introduced SM extensions, we assume that the SM fermions are localized at the $y = 0$ fixed point of the S^1/Z_2 orbifold. Therefore, upon integrating out the y dimension, the kinetic terms of fermions trivially have the usual 4-dimensional SM structure. For a Higgs boson on the brane, the Yukawa sector is also given by its 4D counterpart. Even a Higgs boson in the bulk induces the same mass terms, however, there are additional Yukawa

couplings of the brane fermion to the KK tower of scalars. Clearly, the SM fermions themselves do not have KK modes in this setup. In this thesis we will mostly work in the approximative framework of massless fermions, so the Yukawa sector will not be of special interest for our further investigations of higher-dimensional physics. A more detailed analysis can be found in my diploma thesis [18].

Under a gauge transformation, the left- and right-handed fermions transform according to

$$\begin{aligned}\Psi_L(x) &\rightarrow \exp\left(ig_5\Theta^a(x,0)\tau^a + ig'_5Y^L\Theta(x,0)\right)\Psi_L(x), \\ \Psi_R(x) &\rightarrow \exp\left(ig'_5Y^R\Theta(x,0)\right)\Psi_R(x),\end{aligned}\tag{3.42}$$

where $\Theta^a(x,0)$ or $\Theta(x,0)$ stand for 4D functions if the respective gauge group is restricted to the brane. The corresponding covariant derivatives that couple the chiral fermions to the gauge fields are given by

$$\begin{aligned}D_\mu^L &= \partial_\mu - ig_5A_\mu^a\tau^a - ig'_5Y^LB_\mu, \\ D_\mu^R &= \partial_\mu - ig'_5Y^RB_\mu,\end{aligned}\tag{3.43}$$

where $Y^{L,R}$ denote the $U(1)_Y$ hypercharges.

Hence, after compactification, the couplings of the KK modes of the gauge bosons to the SM brane fermions are determined by their SM quantum numbers. In the Fourier basis, these couplings are generically given by

$$\mathcal{L}_{\text{int}}(x) = g\bar{\Psi}\gamma^\mu(g_V - g_A\gamma^5)\Psi\left(A_{(0)\mu} + \sqrt{2}\sum_{n=1}^{\infty}A_{(n)\mu}\right),\tag{3.44}$$

where g_V and g_A are the usual SM vector and axial vector coupling constants, and $A_{(n)\mu}$ denotes the n^{th} Fourier mode of a given gauge field. To summarize our notation for the SM, the basic couplings g_5 and g'_5 in five dimensions are related to the effective 4D couplings via

$$g = g_5/\sqrt{2\pi R} = e/\sin\theta_W = e/s_W, \quad g' = g'_5/\sqrt{2\pi R} = e/\cos\theta_W = e/c_W,\tag{3.45}$$

where we have define the electromagnetic coupling e . In the presence of a nonzero VEV of a brane Higgs field, the Fourier modes $A_{(n)\mu}$ mix to form KK mass eigenstates $\hat{A}_{(n)\mu}$, as explicitly shown in the preceding sections. The couplings of these physical fields can then be parameterized as follows:

$$\mathcal{L}_{\text{int}}(x) = \sum_{n=0}^{\infty}g_{(n)}\bar{\Psi}\gamma^\mu(g_{V(n)} - g_{A(n)}\gamma^5)\Psi\hat{A}_{(n)\mu}.\tag{3.46}$$

The specific interaction Lagrangian for the higher-dimensional SM is presented in detail in Appendix B. The precise values of the couplings $g_{(n)}$, $g_{V(n)}$, and $g_{A(n)}$ are found by

the corresponding basis rotation and, thus, are specific for each gauge-boson mode. They will be very important for our phenomenological discussion in the next chapter and will be introduced there for the different models. The Feynman rules for the interactions of the mass eigenmodes of the KK gauge bosons to fermions are exhibited in Appendix B. The effective coupling of a fermion to a gauge boson restricted to the same $y = 0$ brane has of course its SM value.

Chapter 4

Bounds on the Compactification

Scale $M = 1/R$

In this chapter, we evaluate the present bounds on the compactification scale $M = 1/R$ of minimal five-dimensional extensions of the standard model (5DSM) by analyzing a large number of high precision electroweak observables both at the Z pole and at LEP2 energies. Observables are affected by the extra dimension in various ways. As we have shown in the previous chapter, electroweak symmetry breaking by a VEV of a Higgs field on the brane leads to mixing between different Fourier modes (cf. (2.35)). This mixing shifts the accurately measured masses and couplings to fermions of the SM zero modes (cf. (2.34) and (2.38)). These shifts are especially important for observables at the Z pole where effects from the exchange of heavier KK modes are negligible. However, even in the absence of a brane Higgs field, the contribution from higher KK modes to the Fermi constant leads to a modification in the definition of the weak mixing angle and, thus, potentially measurable differences between the predictions of the 5DSM as we will see below. At energies well above the Z pole, the virtual exchange of the heavy KK gauge bosons dominates the higher-dimensional corrections.

4.1 Framework and Input Parameters

In our phenomenological analysis, we proceed as follows. The prediction of the 5DSM for a given observable $\mathcal{O}^{5\text{DSM}}$ is related to the SM prediction \mathcal{O}^{SM} by

$$\mathcal{O}^{5\text{DSM}} = \mathcal{O}^{\text{SM}} (1 + \Delta_{\mathcal{O}}^{5\text{DSM}}), \quad (4.1)$$

where $\Delta_{\mathcal{O}}^{5\text{DSM}}$ is the tree-level effect due to the compactified extra dimension. The SM radiative corrections are included in \mathcal{O}^{SM} . However, SM loop effects on $\Delta_{\mathcal{O}}^{5\text{DSM}}$ as well as

KK loop effects are neglected. For compactification scales in the TeV range this is well justified. The tree-level calculation of $\Delta_{\mathcal{O}}^{5\text{DSM}}$ is performed in terms of the compactification scale M and the usual SM input parameters, the electromagnetic fine-structure constant α , the Fermi constant G_F , and the Z -boson mass $m_{Z(0)}$. The index (0) indicates that the observed Z boson is to be identified with the lightest mode of the corresponding KK tower. The remaining relevant SM parameters m_t , m_H , and the strong coupling constant $\alpha_s(m_Z)$ enter in \mathcal{O}^{SM} , but do not influence the calculation of $\Delta_{\mathcal{O}}^{5\text{DSM}}$ in this approximation.

In all 5-dimensional models, spontaneous symmetry breaking by a brane Higgs boson yields deviations of the tree-level Z -boson mass $m_{Z(0)}$ from its SM form $m_Z = \sqrt{g^2 + g'^2} v/2$ (cf. (2.33), (3.24), and (3.35)). Therefore, we write

$$m_{Z(0)}^2 = m_Z^2 (1 + \Delta_Z X), \quad (4.2)$$

where

$$X = \frac{\pi^2}{3} \frac{m_{Z(0)}^2}{M^2} \quad (4.3)$$

represents the typical scale quantifying the higher-dimensional effect and Δ_Z is a model-dependent parameter of order unity to be calculated model by model. The massless photon is not affected by symmetry breaking. Hence, it retains its SM properties through the entire process of compactification as shown for 5D-QED in Chapter 2 and the electromagnetic fine-structure constant is still given by its SM value

$$\alpha = \frac{e^2}{4\pi}. \quad (4.4)$$

In contrast, the Fermi constant G_F as determined by the muon lifetime is sensitive to the extra dimension. On the one hand, in the presence of a Higgs boson on the brane, again shifts of the couplings of the W boson and the masses of the gauge bosons influence the determination of G_F . On the other hand, if there are W boson KK modes the virtual exchange of the heavy KK tower also mediates muon decay. We may account for this modification of G_F by writing

$$G_F = \frac{\pi\alpha}{\sqrt{2}s_W^2 c_W^2 m_{Z(0)}^2} (1 + \Delta_G X). \quad (4.5)$$

In the computation of the electroweak precision observables, it is necessary to express the weak mixing angle θ_W in terms of the input parameters α , $m_{Z(0)}^2$, and G_F by means of (4.5). It is therefore useful to define an effective weak mixing angle $\hat{\theta}_W$ using the tree-level SM relation

$$G_F = \frac{\pi\alpha}{\sqrt{2}\hat{s}_W^2 \hat{c}_W^2 m_{Z(0)}^2}. \quad (4.6)$$

With (4.5) and (4.6), we find

$$\hat{s}_W^2 = s_W^2 (1 + \Delta_\theta X), \quad (4.7)$$

where $\Delta_\theta = c_W^2/(s_W^2 - c_W^2)\Delta_G$. Notice that Δ_θ is a key parameter in the computation of many precision observables, in particular where it enters through the vector coupling of the Z boson (see also Section 5.1).

The parameters of the model like g , g' , e , v , or s_W , being suitable for bookkeeping in the tree-level calculations, can now be easily expressed in terms of the input parameters by using SM relations like (3.45) and inverting (4.2), (4.4), (4.5), and (4.7). Before we can present predictions for the observables under study according to (4.1), we have to be specific about the shifts of the input parameters as well as the couplings and masses which are important for the computation of $\Delta_{\mathcal{O}}^{5\text{DSM}}$.

4.1.1 $\text{SU}(2)_{L\otimes\text{U}(1)_Y}$ -Bulk Model

For the bulk-bulk model, the higher-dimensional modifications of the Z - and W -boson masses read

$$\begin{aligned} \Delta_Z &= -s_\beta^4, \\ \Delta_W &= -s_\beta^4 \hat{c}_W^2, \end{aligned} \quad (4.8)$$

where Δ_W is defined in analogy to (4.2). The dependence on s_β , defined in (3.16), signals that these shifts are exclusively due to the mixing of Fourier modes. The gauge couplings of the physical W and Z bosons to fermions on the brane, as they appear in the Feynman rules (see Figure B.2), are given by

$$\begin{aligned} g_{Z(0)} &= g (1 - s_\beta^2 X), \\ g_{W(0)} &= g (1 - s_\beta^2 \hat{c}_W^2 X) \end{aligned} \quad (4.9)$$

for the SM modes. For the heavy KK modes we have

$$\begin{aligned} g_{Z(n\geq 1)} &= \sqrt{2} g \left(1 - \frac{3}{2\pi^2 n^2} s_\beta^2 X \right), \\ g_{W(n\geq 1)} &= \sqrt{2} g \left(1 - \frac{3}{2\pi^2 n^2} s_\beta^2 \hat{c}_W^2 X \right). \end{aligned} \quad (4.10)$$

These relations are approximate, i.e. they are obtained by expanding the exact analytic results for the masses and couplings, stated in Appendix B, to leading order in the parameter X . The vector and axial vector couplings of the Z boson are not affected in the bulk-bulk model, because each Z boson state possesses the same $\text{U}(1)$ and $\text{SU}(2)$ content as in the

SM (cf. (3.13)). Thus, we have $g_{V(n)} = g_V$ and $g_{A(n)} = g_A$. The photon and its higher KK modes are not affected by mixing and couple to fermions as in 5D-QED (cf. Fig. 2.2).

Finally, from the above, the KK tree-level shift Δ_G of the Fermi constant G_F is

$$\Delta_G = \hat{c}_W^2 \left(1 - 2s_\beta^2 - \frac{\hat{s}_W^2}{\hat{c}_W^2} s_\beta^4 \right), \quad (4.11)$$

which implies

$$\Delta_\theta = -\frac{\hat{c}_W^4}{\hat{c}_{2W}} \left(1 - 2s_\beta^2 - \frac{\hat{s}_W^2}{\hat{c}_W^2} s_\beta^4 \right). \quad (4.12)$$

The terms involving s_β stem again from mixing while the remaining term is due to the afore mentioned virtual exchange of heavy KK modes mediating muon decay.

4.1.2 $SU(2)_L$ -Brane, $U(1)_Y$ -Bulk Model

For the brane-bulk model we have

$$\begin{aligned} \Delta_Z &= -\hat{s}_W^2, \\ \Delta_W &= 0. \end{aligned} \quad (4.13)$$

Obviously, the W -boson mass does not change by KK effects since the W boson is a brane field without KK modes. Also its coupling to fermions is completely SM-like. In contrast, the modification of the Z boson coupling to fermions becomes more involved in this model. Specifically, KK effects induce non-factorizable shifts both in the vector and axial vector part of the $\hat{Z}_{(n)}\bar{f}f$ -coupling for the Z -boson mass eigenstates. Writing

$$g_{V(n)} = T_{3f(n)} - 2Q_{f(n)}s_W^2 \quad \text{and} \quad g_{A(n)} = T_{3f(n)} \quad (4.14)$$

as a generalization of the corresponding SM relations, we can absorb these new non-factorizable modifications by defining the $\hat{Z}_{(n)}\bar{f}f$ -coupling in terms of an effective electric charge $Q_{f(n)}$ and an effective third component of the weak isospin $T_{3(n)}$. For the Z -boson zero-mode, we find

$$\begin{aligned} Q_{f(0)} &= Q_f (1 - X), \\ T_{3f(0)} &= T_{3f} (1 - \hat{s}_W^2 X), \end{aligned} \quad (4.15)$$

where the weak isospin T_{3f} and the electromagnetic charge $Q_f = T_{3f} + Y_f$ denote the usual SM quantum numbers for a given fermion. Notice that (4.15) is a parameterization with $g_{Z(n)} = g$. In principle, it would be more natural to absorb the shifts again in the gauge coupling and the weak mixing angle. By our different choice, we want to avoid the notational mess of too many differently defined mixing angles. Remember that the heavy

KK modes are almost pure U(1) states. However, for simplicity, we will still use the above notation to parameterize their couplings. We find

$$\begin{aligned} Q_{f(n \geq 0)} &= \frac{\sqrt{2}}{s_W} Q_f \left(1 - \hat{s}_W^2 \frac{3}{2\pi^2 n^2} X \right), \\ T_{3f(n \geq 0)} &= \sqrt{2} s_W T_{3f} \left(1 + (\hat{c}_W^2 - \frac{1}{2} \hat{s}_W^2) \frac{3}{\pi^2 n^2} X \right), \end{aligned} \quad (4.16)$$

where the appearance of s_W indicates the U(1) nature of the $\hat{Z}_{(n)}$. The exact relations between $Q_{f(n)}$ and Q_f as well as between $T_{3f(n)}$ and T_{3f} are given in Appendix B. The photon couples completely SM-like and there are no higher photon KK modes, as shown in Section 3.3.

Taking the above results into account, we find

$$\Delta_G = -\hat{s}_W^2 \quad (4.17)$$

and, thereby,

$$\Delta_\theta = \frac{\hat{s}_W^2 \hat{c}_W^2}{\hat{c}_{2W}^2}. \quad (4.18)$$

The above results are so simple because the charged gauge sector lives on the brane and, hence, is not affected by KK effects. Only the shift in the Z mass proliferates into (4.17) and (4.18).

4.1.3 SU(2)_L-Bulk, U(1)_Y-Brane Model

Let us finally consider the complementary scenario. For the bulk-brane model the KK mass shifts for the Z and W^\pm bosons are given by

$$\Delta_Z = \Delta_W = -\hat{c}_W^2. \quad (4.19)$$

The KK effects on the $\hat{Z}_{(0)} \bar{f} f$ -coupling can again be taken into account by introducing an effective third component of the weak isospin

$$T_{3f(0)} = T_{3f} \left(1 - \hat{c}_W^2 X \right). \quad (4.20)$$

In contrast to the brane-bulk model in the previous section, the electric-charge term in the $\hat{Z}_{(0)} \bar{f} f$ -coupling remains unaffected by KK effects, i.e. $Q_{f(0)} = Q_f$. For the heavy KK modes which are almost pure $SU(2)$ fields, we find

$$\begin{aligned} Q_{f(n \geq 0)} &= \sqrt{2} \hat{c}_W Q_f \frac{3}{\pi^2 n^2} X, \\ T_{3f(n \geq 0)} &= \sqrt{2} c_W T_{3f} \left(1 + (\hat{s}_W^2 - \frac{1}{2} \hat{c}_W^2) \frac{3}{\pi^2 n^2} X \right). \end{aligned} \quad (4.21)$$

The couplings of the W boson and its KK modes can be found from the bulk-bulk model results in Section 4.1.1 for $s_\beta = 1$. Thus, from muon decay, we calculate

$$\Delta_G = -\hat{c}_W^2, \quad (4.22)$$

which leads to

$$\Delta_\theta = \frac{\hat{c}_W^4}{\hat{c}_{2W}^2}. \quad (4.23)$$

Here, several contributions from virtual KK exchange and mixing effects compensate to yield the simple result (4.22).

For a moment, let us postpone the explicit determination of the higher-dimensional shifts $\Delta_{\mathcal{O}}^{5\text{DSM}}$ for the observables and turn to the statistics of deriving bounds on the model parameters.

4.2 Statistics

In order to extract bounds on the compactification scale M from the available data, one can proceed in two ways. For a given set of observables, one may fix the SM parameters at their current best fit values and calculate the 5DSM predictions $\mathcal{O}^{5\text{DSM}}$ using (4.1). Here, the SM expectations \mathcal{O}^{SM} can be taken from the literature, e.g. [62] (see also Appendix C). Then, one can perform a one-parameter χ^2 -analysis for M or equivalently for X . The χ^2 -function is given by

$$\chi^2(X) = \sum_{i,j} (\mathcal{O}_i^{\text{exp}} - \mathcal{O}_i^{5\text{DSM}}) V_{ij}^{-1} (\mathcal{O}_j^{\text{exp}} - \mathcal{O}_j^{5\text{DSM}}) \quad (4.24)$$

with the covariance matrix $V_{ij} = \Delta\mathcal{O}_i \rho_{ij} \Delta\mathcal{O}_j$, $\Delta\mathcal{O}_i$ being the measurement error of a given observable $\mathcal{O}_i^{\text{exp}}$ and ρ_{ij} being the matrix of correlation coefficients. This approach is simple and easy to apply. However, possible correlations between the SM parameters and the size of the extra dimension are ignored and, hence, the bounds on M may be overestimated. Therefore, it is interesting to follow a more general approach in which X is fitted simultaneously with the SM parameters $\alpha_{\text{em}}(m_Z)$, G_F , m_Z , $\alpha_s(m_Z)$, m_t , m_H to the data. The radiatively corrected SM predictions $\mathcal{O}_i^{\text{SM}}$ in (4.1) are obtained from ZFITTER [63–66] and in general depend on $\alpha_s(m_Z)$, m_t , and m_H via loop contributions. The 5D corrections $\Delta_{\mathcal{O}}^{5\text{DSM}}$ are still calculated at tree-level. Being able to calculate (4.24) for any given set of input parameters, the multi-parameter minimization of χ^2 for finding the best fit values is performed with the program MINUIT [67]. Appendix D explains in more detail, how the different Fortran programs are combined for the outlined task.

The computation of the bounds is slightly different from the standard analysis [68] because there is an unphysical region in parameter space, that is, there is no physical meaning for $X < 0$. The problem is well known from neutrino mass searches or fits to the Higgs mass, where the direct search result excludes masses up to a given limit. One method to derive bounds on X from (4.24) is Bayesian statistics [68]. For example, in Bayesian statistics with a flat prior in the physical region $X \geq 0$ and a zero prior in the unphysical region, the 95% (1.96 σ) confidence level (CL) bound X_{95} is given by

$$0.95 = \int_0^{X_{95}} dX P(X) / \int_0^\infty dX P(X), \quad (4.25)$$

where $P(X) = \exp[-(\chi^2(X) - \chi_{\min}^2)/2]$. In a widely used and simpler approach, one requires

$$\Delta\chi^2 = \chi^2(X) - \chi_{\min}^2 < n^2 \quad (4.26)$$

for X not to be excluded at the $n\sigma$ confidence level. In the above, $\chi^2(X)$ is the minimum for a given X with respect to the other fit parameters requiring $m_H \geq 114$ GeV, while χ_{\min}^2 is the overall minimum of the χ^2 -function in the physically allowed region $X \geq 0$, $m_H \geq 114$ GeV. If the best fit value of X is not too far in the unphysical region both methods lead to similar results and approximate well the results of the unified approach [69], as is illustrated in Appendix E. In the following sections, we present the bounds as obtained from (4.26).

4.3 Bounds from Precision Observables

Having described the methods, we now discuss the bounds on the compactification scale M resulting from electroweak precision observables. For low-energy observables, we can consistently use $m_{Z(n)} \approx m_{W(n)} \approx n/R$ for $n \geq 1$ in the calculations of $\mathcal{O}^{5\text{DSM}}$ to leading order in X . Furthermore, for the heavy modes it is sufficient to use the couplings without higher-dimensional corrections because their propagators are already of order X . At the Z pole, heavy KK exchange is completely suppressed.

Within this approximative framework we compute the following high precision observables: the W -boson mass m_W , the Z -boson invisible width $\Gamma_Z(\nu\bar{\nu})$, Z -boson leptonic widths $\Gamma_Z(l^+l^-)$, the Z -boson hadronic width $\Gamma_Z(\text{had})$, the weak charge of cesium Q_W measuring atomic parity violation, various ratios R_l and R_q involving partial Z -boson widths and the Z -boson hadronic width, fermionic asymmetries A_f at the Z pole, and various fermionic forward-backward asymmetries $A_{\text{FB}}^{(0,f)}$ at vanishing polarization. A complete list of the considered observables along with the SM predictions and their experimental values is given

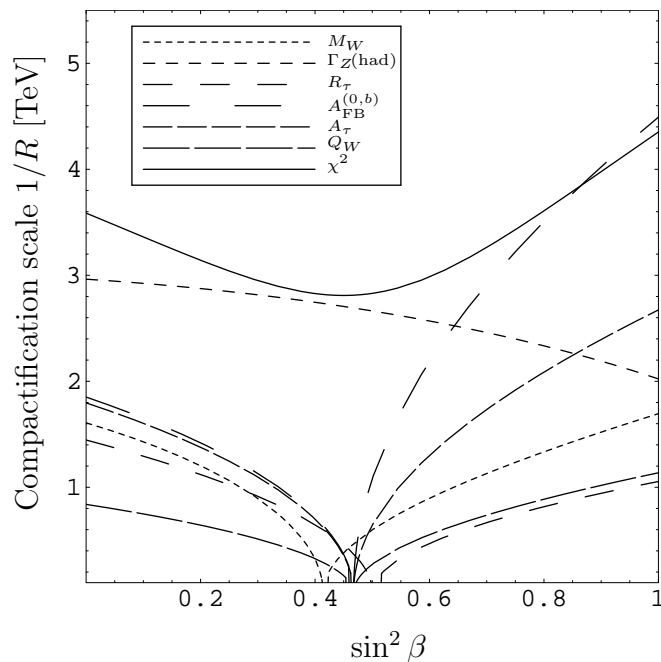


Figure 4.1: Lower bounds on the compactification scale $M = 1/R$ at the 3σ CL from different precision observables and a global χ^2 -analysis in the bulk-bulk model.

in Appendix C. The higher-dimensional corrections $\Delta_{\mathcal{O}}^{5\text{DSM}}$ for the different observables are given model by model in Appendix F.

We also take into account the error correlations between different observables [70]. The error correlations have only a small effect, shifting the resulting bounds by no more than 0.2 TeV. Compared to the bounds [42] which we have obtained from the data published in 2000 [71], the bounds are altered by as much as almost 1 TeV. This is mainly due to the large shift of the experimental value for the forward-backward asymmetry $A_{FB}^{(0,b)}$ which is now found to be more than 3σ below the SM expectation. As can be seen from the results in Appendix F, only the bulk-bulk model with a bulk Higgs predicts a smaller value of $A_{FB}^{(0,b)}$ than the SM. Correspondingly, the bound for this model is lowered while the constraints on the other models become stronger.

Let us first concentrate on the simple one-parameter fit introduced in Section 4.2. For the bulk-bulk model, Figure 4.1 shows lower bounds on the compactification scale M coming from different types of observables as functions of $\sin^2 \beta$, where we take into account only one observable at a time. For a model dominated by a brane Higgs field ($\sin \beta = 1$), the most stringent bound on M is set by the forward-backward asymmetry involving b -quarks. Although $A_{FB}^{(0,b)}$ is not particularly sensitive to an extra dimension, the afore mentioned large deviation from the SM expectation results in a large bound as the deviation increases

Observable	U(1) _Y in bulk	SU(2) _L in bulk
M_W	1.2	1.2
$\Gamma_Z(\text{had})$	0.8	2.3
$Q_W(\text{Cs})$	0.5	0.9
$A_{\text{FB}}^{(0,b)}$	3.9	2.2
A_τ	2.3	1.3
R_τ	1.0	0.5
global analysis	3.8	2.7

Table 4.1: Lower bounds (in TeV) on the compactification scale $1/R$ at the 3σ CL in models where either only the U(1)_Y or only the SU(2)_L gauge boson propagates in the higher-dimensional space.

in 5D for $\sin\beta = 1$.^{*} In contrast, for a model dominated by a bulk-Higgs ($\sin\beta = 0$), the disparity between the experimental result and the SM prediction for $A_{\text{FB}}^{(0,b)}$ is reduced in 5D. Here, M is most severely constrained by the hadronic Z -boson width. In addition, Fig. 4.1 displays the result obtained by the global χ^2 -fit according to (4.26). At the 3σ confidence level, a lower bound on M between 3 and 4 TeV is implied. The smallest bound on M arises for a mixed brane-bulk Higgs scenario with $\sin^2\beta \sim 0.5$ because the different higher-dimensional shifts compensate each other for almost all the observables but the various Z -boson widths.

For the SU(2)_L-brane, U(1)_Y-bulk model, Table 4.1 lists the lower limits on M for each observable separately, together with the limit found by the global analysis. The most restrictive bound is again obtained by the b -quark forward-backward asymmetry giving rise to a lower limit on M of ~ 3.9 TeV at the 3σ CL. However, the best fit value is again far in the unphysical region. Our global-fit analysis leads to the slightly less restrictive lower bound: $M \gtrsim 3.8$ TeV.

In Table 4.1, we also present the lower bounds on M for the SU(2)_L-bulk, U(1)_Y-brane

^{*}Note, that the bound from $A_{\text{FB}}^{(0,b)}$ stated in [42] is even more stringent because, for single observables, χ_{min} has not been restricted to the physical region $X > 0$ there.

model	2σ	3σ	5σ
SU(2) _L -brane, U(1) _Y -bulk	4.9	3.8	2.8
SU(2) _L -bulk, U(1) _Y -brane	3.2	2.7	2.1
SU(2) _L -bulk, U(1) _Y -bulk (brane Higgs)	5.5	4.4	3.3
SU(2) _L -bulk, U(1) _Y -bulk (bulk Higgs)	4.2	3.6	2.9

Table 4.2: Lower bounds (in TeV) on the compactification scale $1/R$ at 2σ , 3σ and 5σ CLs.

model. Here, the hadronic Z width offers the most stringent lower bound $M \gtrsim 2.3$ TeV on the compactification scale at the 3σ CL. Most interestingly, we observe that this lower bound on M is much more relaxed than the one found in the previous models. The same observation applies to the global analysis, where the compactification scale M is constrained to be larger than about 2.7 TeV at the 3σ CL.

In Table 4.2, we summarize the lower bounds on M obtained from our global fits for the four minimal higher-dimensional extensions of the SM. We find that the lower bounds on M at higher confidence levels scale as expected from an approximately quadratic $\chi^2(X)$ -function. The weakest bound on the compactification scale is found for the SU(2)_L-bulk, U(1)_Y-brane model.

In the multi-parameter fit, the correlations between M and the SM parameters reduce the bounds as expected. As can be seen in Table 4.3, the size of the effect varies from model to model. In the brane-bulk model the effect is biggest lowering the bound by almost 40%. Here, the best fit value is relatively far in the unphysical region. Thus, as a cross-check, we also performed a Bayesian analysis which yields the same bound as (4.26) up to 0.1 TeV.

Most interesting is the correlation between the compactification scale and the mass of the Higgs boson. This correlation is illustrated in Fig. 4.2. The data set used for our analysis

	brane-bulk	bulk-brane	bulk-bulk (brane Higgs)	bulk-bulk (bulk Higgs)
one-parameter fit	4.9	3.2	5.5	4.2
multi-parameter fit	3.1	3.1	4.2	3.7

Table 4.3: 2σ bounds on M in TeV derived from electroweak precision measurements [62].

differs from the one used for the familiar blue-band plot [70]. Within the SM ($X = 0$ in Fig. 4.2) it leads to a best fit value of $m_H = 100_{-40}^{+70}$ GeV and to the 2σ upper bound $m_H < 280$ GeV. As can be seen in Fig. 4.2, in the models with the Higgs field localized on the brane, the existence of an extra dimension favors a heavier Higgs boson. This confirms the observation for the bulk-bulk model in [38, 39]. The effect is most pronounced in the bulk-bulk model with a brane Higgs and in the brane-bulk model. Quantitatively, for $M = 5$ TeV, the best fit values increase to $m_H = 170_{-60}^{+105}$ GeV and $m_H = 155_{-60}^{+105}$ GeV, respectively. If the compactification scale is included in the multi-parameter fit, the 2σ upper bound on m_H is relaxed to 330 and 400 GeV, respectively.

4.4 LEP2 Constraints

At energies \sqrt{s} above the Z pole, the virtual exchange of KK excitations ($n \geq 1$) of the SM gauge bosons becomes dominant for the higher-dimensional corrections of observables. As long as $s \ll M^2$, the KK exchange is an effective contact interaction and the main corrections come from the interference of zero with higher KK modes. They scale like s/M^2 in contrast to the energy-independent modifications of masses and couplings. This is illustrated in Fig. 4.3 for an exemplary observable, the total cross section for muon-pair production. The residual energy dependence of the impact of the latter on the cross section (dashed curves in Fig. 4.3) is due to the transition from dominant Z exchange to dominant photon exchange.

Focusing on LEP2, we have investigated the total cross sections for lepton-pair production, hadron production, and Bhabha scattering (see Appendix C). Forward-backward asymmetries for muon and tau production as well as the heavy quark observables $A_{FB}^{(0,b)}$, $A_{FB}^{(0,c)}$, $R_b = \sigma(b\bar{b})/\sigma(\text{had})$, and $R_c = \sigma(c\bar{c})/\sigma(\text{had})$ are included in the fits, although they do not contribute noticeably to the bounds. For completeness, we have also investigated W^+W^-

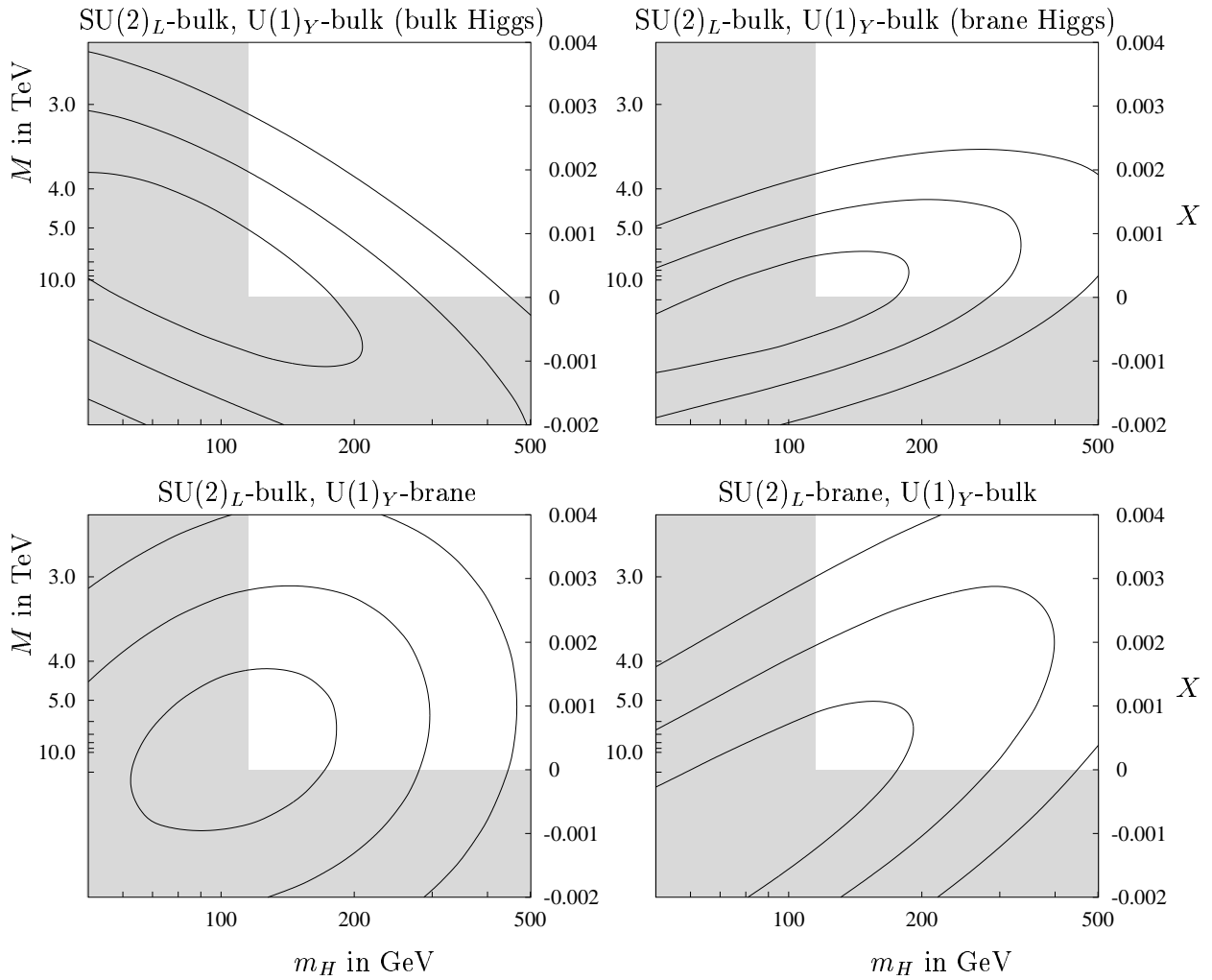


Figure 4.2: Contours of $\Delta\chi^2 = 1, 4, 9$ (cf. (4.26)) derived from multi-parameter fits to electroweak precision data. The shaded regions of the parameter space correspond to $m_H < 114$ GeV and/or $M^2 < 0$.

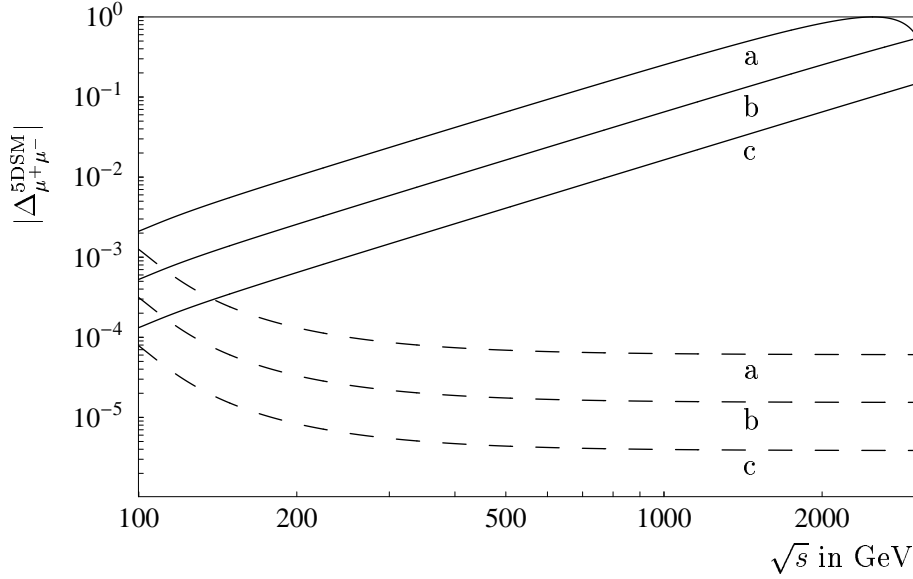


Figure 4.3: The shift $\Delta_{\mu^+\mu^-}^{5\text{DSM}}$ of the total cross section for muon-pair production in the bulk-bulk model with a brane Higgs for $M = 5$ (a), 10 (b), and 20 (c) TeV. The dashed curves show the effects from the mixing of masses and couplings only.

production. In this section, we do not explicitly state $\Delta_{\mathcal{O}}^{5\text{DSM}}$ for the different observables because the expressions are quite messy. Instead, we give the tree-level 5DSM prediction $\mathcal{O}^{5\text{DSM}}$ in terms of the couplings and masses defined in Section 4.1. From the latter, the numerical value of $\Delta_{\mathcal{O}}^{5\text{DSM}}$ can be easily obtained.

4.4.1 Fermion-Pair Production

The differential cross section for fermion-pair production is given by

$$\frac{d\sigma(e^+e^- \rightarrow f\bar{f})}{d\cos\vartheta} = \frac{N_f s}{128\pi} \left[(1 + \cos\vartheta)^2 (|M_{LL}^{ef}(s)|^2 + |M_{RR}^{ef}(s)|^2) + (1 - \cos\vartheta)^2 (|M_{LR}^{ef}(s)|^2 + |M_{RL}^{ef}(s)|^2) \right], \quad (4.27)$$

where ϑ is the scattering angle between the incoming electron and the negatively charged outgoing fermion, and $N_f = 1(3)$ for leptons (quarks) in the final state. For the matrix elements entering (4.27) one finds

$$M_{\alpha\beta}^{ef}(s) = \sum_{n=0}^{\infty} \left(e_{(n)}^2 \frac{Q_e Q_f}{s - m_{\gamma(n)}^2} + \frac{g_{\alpha(n)}^e g_{\beta(n)}^f}{\cos^2\theta_W} \frac{1}{s - m_{Z(n)}^2} \right) \quad (4.28)$$

with the couplings

$$g_{L,R(n)}^f = \frac{g_{Z(n)}}{2} (g_{V(n)} \pm g_{A(n)}) \quad (4.29)$$

	brane-bulk	bulk-brane	bulk-bulk (brane Higgs)	bulk-bulk (bulk Higgs)
$\mu^+\mu^-$	2.0	1.5	2.5	2.5
$\tau^+\tau^-$	2.0	1.5	2.5	2.5
hadrons	2.6	4.7	5.4	5.8
e^+e^-	3.0	2.0	3.6	3.5
W^+W^-	1.1	2.0	2.1	2.2
LEP2 combined	3.5	4.6	5.6	5.9
Electroweak and LEP2 data combined	5.4	4.8	6.9	6.0

Table 4.4: 2σ bounds on M in TeV from a one-parameter fit derived from LEP2 data alone and from LEP2 and electroweak precision data combined.

calculated from Sections 4.1.1-4.1.3. The differential cross section (4.27) has also been used in [41]. There, however, the mixing effects in the couplings and masses included in (4.28) and (4.29) have been neglected as a reasonable approximation (see Figure 4.3).

The data taken by the LEP experiments for muon, tau, and hadron production is properly combined for energies between $\sqrt{s} = 130$ GeV and $\sqrt{s} = 207$ GeV [70]. In the hadronic channel it is very important to take into account the large correlations between the data at different energies. If they are ignored, the bounds on the compactification scale are overestimated by as much as 3 TeV. In contrast, the correlations in the muon and tau channels are extremely small and have little effect.

The bounds from a simple one-parameter analysis are summarized in Table 4.4, where we concentrate on models with only a single Higgs doublet. In the muon and tau channel, the bulk-brane model is least restricted because essentially only left-handed fermions interact with the heavy KK modes. The best fit values turn out to lie always in the physical region

$X \geq 0$. Hadron production puts more stringent bounds on the 5D models because of the larger cross section. In this case, the brane-bulk model is least restricted, since the hadronic cross section is dominated by left-handed quarks whose small hypercharges suppress the interference effects with the heavy $U(1)_Y$ KK modes. In this case, the best fit values lie in the unphysical region $X < 0$.

The differential cross section for Bhabha scattering may conveniently be expressed as

$$\frac{d\sigma(e^+e^- \rightarrow e^+e^-)}{d \cos \vartheta} = \frac{s}{128\pi} \left[(1 + \cos \vartheta)^2 (|M_{LL}^{ee}(s) + M_{LL}^{ee}(t)|^2 + |M_{RR}^{ee}(s) + M_{RR}^{ee}(t)|^2) + (1 - \cos \vartheta)^2 (|M_{LR}^{ee}(s)|^2 + |M_{RL}^{ee}(s)|^2) + 4 (|M_{LR}^{ee}(t)|^2 + |M_{RL}^{ee}(t)|^2) \right], \quad (4.30)$$

where $t = -s(1 - \cos \vartheta)/2$ and $M_{\alpha\beta}^{ee}(s \text{ or } t)$ can be read off from (4.28). The total cross section is calculated by integrating (4.30) over ϑ in the experimental ranges. Since the Bhabha data of the four LEP experiments [72–85] has not yet been combined, possible correlations of the different experiments cannot be accounted for, at least for the time being.

As can be seen from Table 4.4, the bounds on M from Bhabha scattering are approximately 1 TeV stronger than those from the other leptonic channels. This is due to the large Bhabha cross section. On the other hand, the dominance of the t -channel photon exchange, which is not affected by the presence of an extra dimension, reduces the sensitivity of Bhabha scattering compared to hadron production in almost all 5D models.

4.4.2 W^+W^- Production

The differential cross section for W^+W^- production reads [86]

$$\begin{aligned} \frac{d\sigma(e^+e^- \rightarrow W^+W^-)}{d \cos \vartheta} &= \frac{1}{32\pi s} \beta \\ &\times \left\{ \beta^2 [M_L^2(s) + M_R^2(s)] s^2 \left[\frac{s}{m_{W(0)}^2} + \sin^2 \vartheta \left(\frac{3}{4} - \frac{s}{4m_{W(0)}^2} + \frac{s^2}{16m_{W(0)}^4} \right) \right] \right. \\ &+ M_L^2(t) t^2 \left[\frac{s}{4m_{W(0)}^2} + \beta^2 \sin^2 \vartheta \left(\frac{s^2}{16t^2} + \frac{s^2}{64m_{W(0)}^4} \right) \right] \\ &\left. + M_L(t) M_L(s) st \left[2 + 2 \frac{m_{W(0)}^2}{t} + \beta^2 \frac{s}{m_{W(0)}^2} - \beta^2 \sin^2 \vartheta \left(\frac{s}{4t} + \frac{s}{8m_{W(0)}^2} - \frac{s^2}{16m_{W(0)}^4} \right) \right] \right\}, \quad (4.31) \end{aligned}$$

where $\beta = \sqrt{1 - 4m_{W(0)}^2/s}$, $t = m_{W(0)}^2 - s(1 - \sqrt{1 - \beta} \cos \vartheta)/2$ and ϑ is the scattering angle between the electron and the negatively charged W boson. Note that $m_{W(0)} = m_W^{\text{SM}} (1 + \Delta_{m_W}^{\text{5DSM}} X)$ with $\Delta_{m_W}^{\text{5DSM}}$ as given in Appendix F. Furthermore, $M_{L,R}(s)$ and $M_L(t)$ read

$$M_\alpha(s) = \sum_{n=0}^{\infty} \left(\frac{Q_e e_{(n)} g_{3(n)}^\gamma}{s - m_{\gamma(n)}^2} + \frac{g_{\alpha(n)}^e g_{3(n)}^Z}{\cos \theta_W} \frac{1}{s - m_{Z(n)}^2} \right), \quad (4.32)$$

$$M_L(t) = \frac{g_{W(0)}^2}{t},$$

while $M_R(t) = 0$ as in the SM. A novel feature are the triple gauge-boson couplings $g_{3(n)}^\gamma$ and $g_{3(n)}^Z$ of the photon, the Z boson, and their respective heavy KK modes to the W zero modes. They are given in Appendix G along with the corresponding Feynman rules.

As can be seen from Table 4.4, W -pair production at LEP2 provides relatively weak bounds on M . This can be understood by realizing that the effects of heavy KK exchange are almost negligible due to the suppression of the interference of SM and KK exchange by an additional factor X . For the brane-bulk model, this is due to the fact that all KK modes are almost pure $U(1)$ states. For the other models, it is a direct consequence of the selection rules introduced in Section 3.1. The selection rules do not hold exactly due to mixing in models with a brane Higgs but still govern the low-energy cross section (see Section 6.3 for details).

4.5 Combined Bounds on $M = 1/R$

The 2σ bounds on M found from a one-parameter fit to the combined LEP2 data are listed in Table 4.4. The bounds range from 3.5 TeV for the brane-bulk model to 5.9 TeV for the bulk-bulk model with a bulk Higgs. Furthermore, including also the electroweak precision measurements, the bounds range from 4.8 TeV for the bulk-brane model to 6.9 TeV for the bulk-bulk model with a brane Higgs. Our results are in good agreement with the results of [41] for the bulk-bulk models which have been already discussed there. The best fit values always lie in the unphysical region $X < 0$.

For muon-pair, tau-pair and hadron production (including asymmetries and heavy-quark data), where ZFITTER can be used to calculate the SM predictions, we have also performed a multi-parameter fit. Here, it is inescapable to concentrate on the models with a single Higgs field to reduce the computational effort. The resulting $\Delta\chi^2$ -contours are shown in Fig. 4.4. The slight distortions from smooth contours are due to a bug in ZFITTER not being noticed before (see Appendix D). The corresponding 2σ bounds on M are listed in

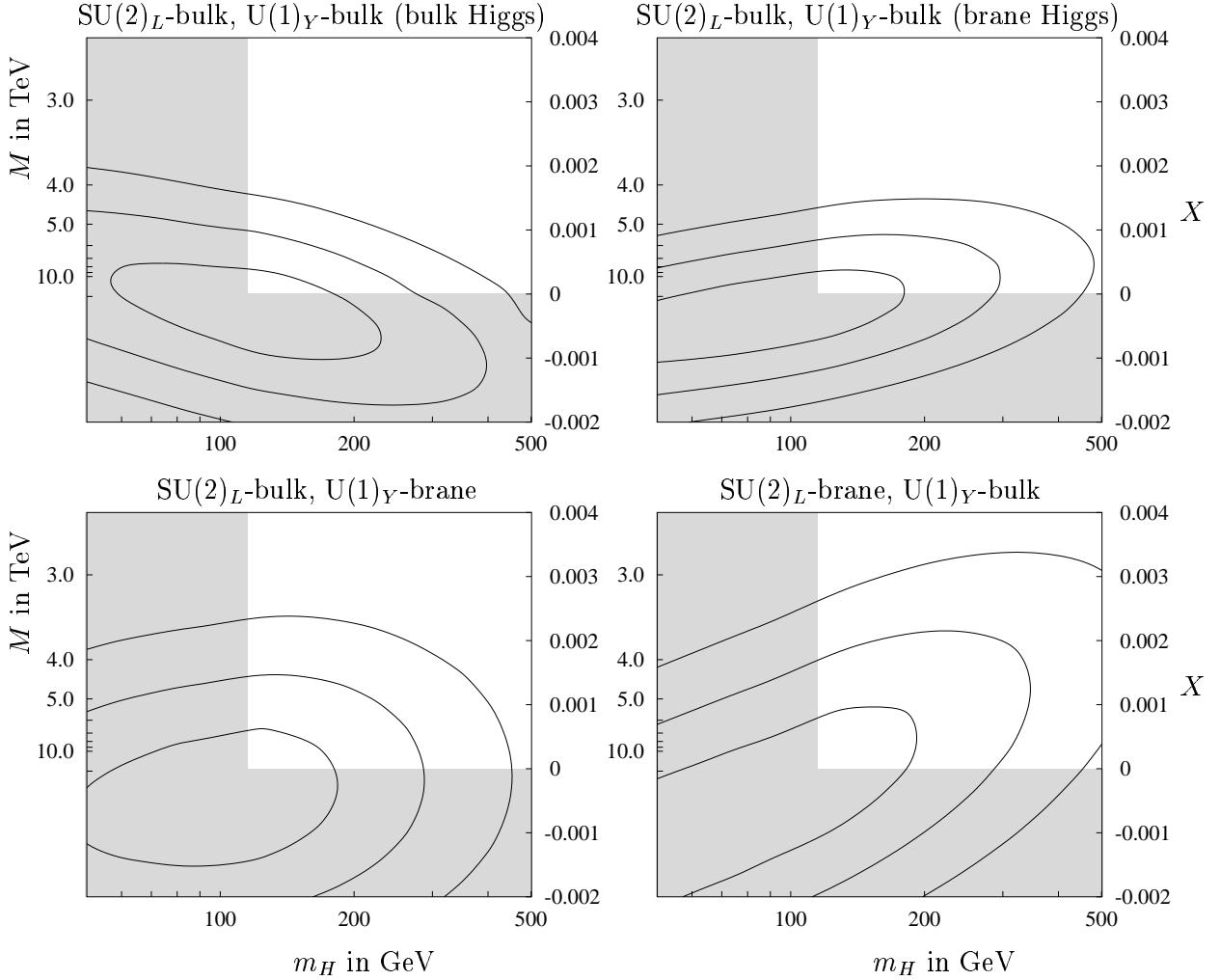


Figure 4.4: Contours of $\Delta\chi^2 = 1, 4, 9$ (cf. (4.26)) derived from the combined analysis of LEP2 data and electroweak precision measurements. The shaded regions of the parameter space correspond to $m_H < 114$ GeV and/or $M^2 < 0$.

	brane-bulk	bulk-brane	bulk-bulk (brane Higgs)	bulk-bulk (bulk Higgs)
one-parameter fit	5.0	4.5	6.4	5.5
multi-parameter fit	3.6	4.3	5.4	5.2

Table 4.5: 2σ bounds on M in TeV derived from the muon, tau, and hadron production at LEP2 combined with electroweak precision measurements.

Table 4.5 along with the bounds from the corresponding one-parameter fit. The correlations between m_H , m_t , and M are similar to what has been found from the precision observables alone in Section 4.3. They are weak in the bulk-brane model and most sizable in the brane-bulk model.

A comparison of Table 4.4 and 4.5 shows that in the one-parameter fit Bhabha scattering and W^+W^- production increase the combined bounds by about 0.5 TeV. Thus, the bounds from a multi-parameter fit to all data including Bhabha scattering and W^+W^- production can be estimated to lie between 4 TeV for the brane-bulk model and 6 TeV for the bulk-bulk model with a brane Higgs.

Chapter 5

Sensitivity at a Linear Collider

Having extracted the bounds on the compactification scale M from available data, we now estimate the reach at a future linear collider such as TESLA [87]. For illustration, we investigate both the potential of the GigaZ option as well as the sensitivity at high energy and luminosity.

5.1 GigaZ Option

At the Z pole, the luminosity goal at TESLA is $\mathcal{L} = 5 \times 10^{33} \text{ cm}^{-2} \text{ s}^{-1}$ which is sufficient to produce 10^9 Z bosons in only 50-100 days of running [87]. This will increase the LEP statistics by more than one order of magnitude. The most relevant improvement in testing the compactification scale will come from the precise measurement of the left-right (LR) asymmetry A_{LR} with polarized e^+e^- beams. Since photon exchange and the exchange of higher KK modes can be neglected at the Z peak, the LR asymmetry at tree level can be approximated by

$$A_{\text{LR}} = \frac{2 g_{V(0)} g_{A(0)}}{g_{V(0)}^2 + g_{A(0)}^2}, \quad (5.1)$$

where $g_{V(0)}$ and $g_{A(0)}$ are the vector and axial vector couplings of the electron to the Z boson given in (4.14). This asymmetry is very sensitive to shifts of the weak mixing angle with respect to the SM value because of the small ratio $g_V/g_A = (1 - 4 \sin^2 \theta_W)$. Using (4.7), (4.9), (4.15), and (4.20) in order to express (5.1) in terms of the input parameters, one obtains the 5DSM corrections $\Delta_{A_{\text{LR}}} = \Delta_{A_e}$ given in Appendix F. With the GigaZ option it will be possible to measure A_{LR} with an absolute error of about 10^{-4} [87]. However, the uncertainties in the fine-structure constant and the Z mass will each induce an additional error of about 10^{-4} which has to be added in quadrature. Coincidence of the measured value of A_{LR} with the SM expectation would then imply the bounds on M shown in Table 5.1.

	brane-bulk	bulk-brane	bulk-bulk (brane Higgs)	bulk-bulk (bulk Higgs)
A_{LR}	12.4	6.8	14.2	12.4
m_W	5.6	5.6	7.8	5.6

Table 5.1: 2σ bound on the compactification scale M in TeV which can be obtained with the GigaZ option at TESLA if the measured values of A_{LR} , m_W coincide with the SM expectation.

Another low-energy observable at TESLA is the mass of the W boson m_W . In contrast to the usual kinematical methods for the mass determination, a threshold scan around 160 GeV using 100 fb^{-1} is proposed leading to a reduction of the experimental error down to 6 MeV [87]. Close to the threshold, a relative shift in m_W leads to a relative shift in the cross section which is enhanced by more than an order of magnitude. Hence, as a first approximation, we consider only the higher-dimensional shifts in m_W and neglect possible further corrections of the cross sections due to shifts in couplings, etc. Otherwise, a full four-fermion calculation is necessary which lies beyond our current analysis. The theoretical error in m_W is expected to be smaller than the experimental one if the top-mass error is reduced to less than a GeV by then [87]. The bounds on the compactification scale from the W mass are also shown in Table 5.1. Since the sensitivity of m_W to higher-dimensional extensions of the standard model, as given in Appendix F, is not large ($\Delta_{m_W} < 0.5$ for all models) the bounds are not as tight as those from A_{LR} .

With excellent b -tagging it will also be possible to considerably improve the measurement of the final state coupling A_b and the cross-section ratio R_b . However, the sensitivity of these observables to M is small and will not allow to explore compactification scales beyond the bounds already known from available data. As can be seen from Table 5.1, except for the bulk-brane model, the GigaZ option should improve the existing bounds by at least a factor of two, mainly driven by the measurement of A_{LR} .

5.2 Tests at $\sqrt{s} = 800$ GeV

At high energies, the interference effects from the exchange of SM and heavy KK modes completely dominate the mixing effects as already illustrated in Fig. 4.3. We consider the same processes as in Section 4.4, except for W -pair production which is not very sensitive

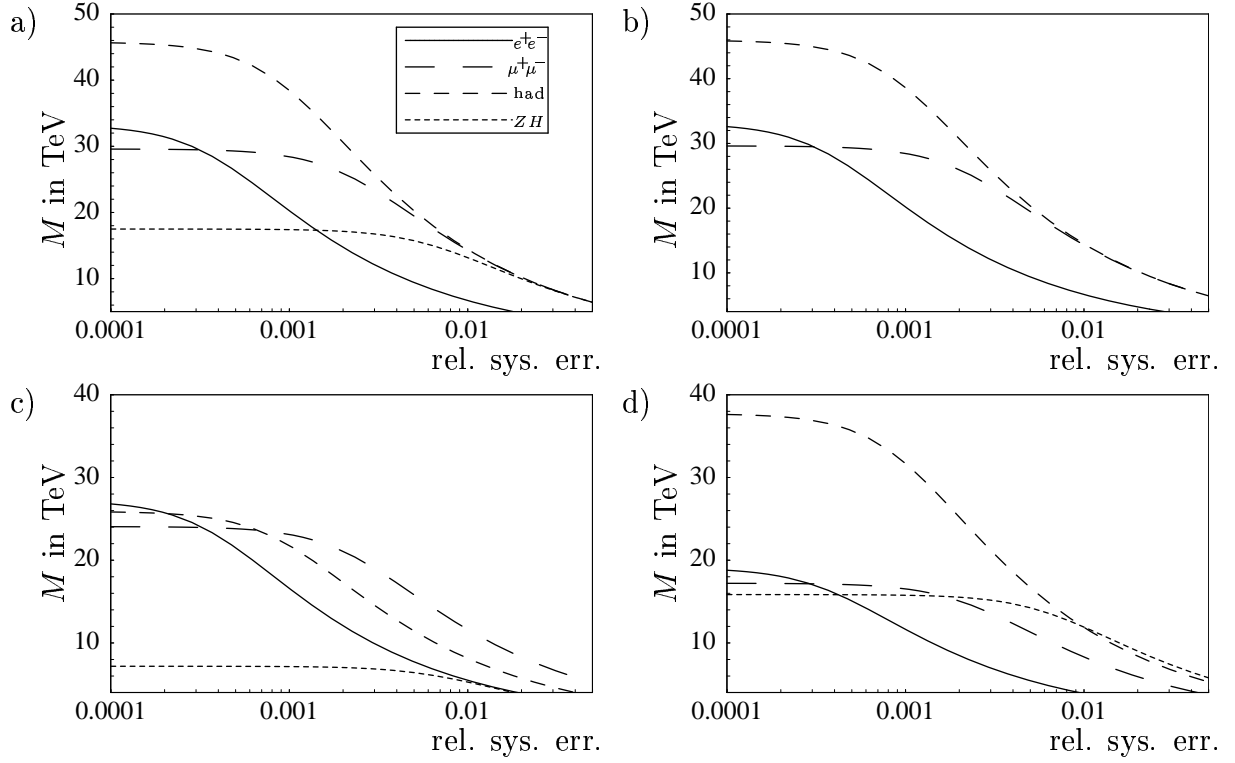


Figure 5.1: Expected sensitivity limit for M as a function of relative systematic error at $\sqrt{s} = 800$ GeV and for an integrated luminosity of 1000 fb^{-1} : (a) bulk-bulk model with brane Higgs, (b) bulk-bulk model with bulk Higgs, (c) brane-bulk model, and (d) bulk-brane model.

to an extra dimension since the couplings of the W bosons to higher KK modes in the s -channel are either forbidden or suppressed. For Bhabha scattering, an acceptance cut, $|\cos \vartheta| < 0.9$, is included. Furthermore, we assume an integrated luminosity of 1000 fb^{-1} .

In addition, we also study Higgsstrahlung, the differential cross section of which is given by

$$\frac{d\sigma(e^+e^- \rightarrow ZH)}{d\cos\vartheta} = \frac{s}{512\pi} \lambda^{1/2}(s) \left[8 \frac{m_{Z(0)}^2}{s} + \lambda(s)(1 - \cos^2\vartheta) \right] [M_L^2(s) + M_R^2(s)]. \quad (5.2)$$

Here, $\lambda(s) = \left(1 - (m_H + m_{Z(0)})^2/s\right) \left(1 - (m_H - m_{Z(0)})^2/s\right)$ is the familiar two-particle phase-space function, ϑ is the scattering angle between the electron and the outgoing Z , and

$$M_\alpha(s) = \sum_{n=0}^{\infty} \left(\frac{g_{\alpha(n)}^e g_{(n)}^{ZH}}{\cos^2\theta_W} \frac{1}{s - m_{Z(n)}^2} \right). \quad (5.3)$$

The couplings $g_{\alpha(n)}^e$ are defined in (4.29) and $g_{(n)}^{ZH}$ is the effective coupling of the Z modes

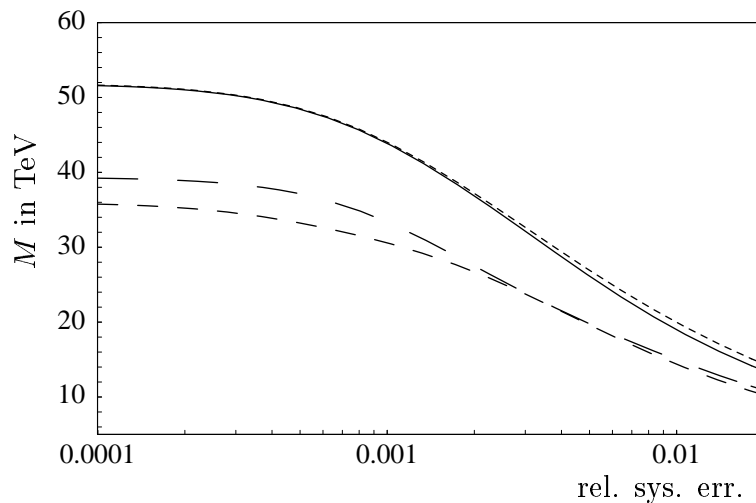


Figure 5.2: Combined sensitivity limit for the compactification scale M as a function of relative systematic error at $\sqrt{s} = 800$ GeV and for an integrated luminosity of 1000 fb^{-1} in the models bulk-bulk with brane Higgs (short dashed), bulk-bulk with bulk Higgs (solid), brane-bulk (dashed), and bulk-brane (long dashed).

to the Higgs boson given in Appendix H. The integrated cross section following from (5.2) in the SM limit can be found, for example, in [88].

The Higgsstrahlung process is certainly not a primary search channel for an extra dimension because of the limited experimental accuracy. For $\int \mathcal{L} dt = 10^3 \text{ fb}^{-1}$ and at $\sqrt{s} = 800$ GeV, the error of the total cross section is expected to be 5% for $m_H \simeq 115$ GeV [87]. Nevertheless, this channel is interesting for distinguishing between a brane and a bulk Higgs in the bulk-bulk model. If the produced Higgs boson is the zero mode of a bulk field, the KK selection rules forbid the coupling $H_{(0)}Z_{(0)}Z_{(n)}$ for $n \geq 1$. Thus, the absence of heavy KK modes in the s -channel is a clear signal for a bulk Higgs. In this case, the process is rather SM-like in contrast to a Higgs boson localized on the brane. The phenomenology of 2-Higgs-doublet models with one bulk and one brane Higgs has been investigated in [89].

In the following, the sensitivity to the presence of an extra dimension is estimated by requiring

$$\chi^2 = \sum_i \frac{(\mathcal{O}_i^{\text{SM}} - \mathcal{O}_i^{\text{5DSM}})^2}{(\Delta\mathcal{O}_i)^2} \leq 4. \quad (5.4)$$

The statistical errors will be so small that the systematic errors become decisive [90, 91]. Since the latter are not known reliably at the present time, we show, in Fig. 5.1, the sensitivity limit of the compactification scale M as a function of the relative systematic error. At $\Delta\mathcal{O}_{\text{sys}} \lesssim 0.001$ the statistical uncertainty begins to dominate and the sensitivity

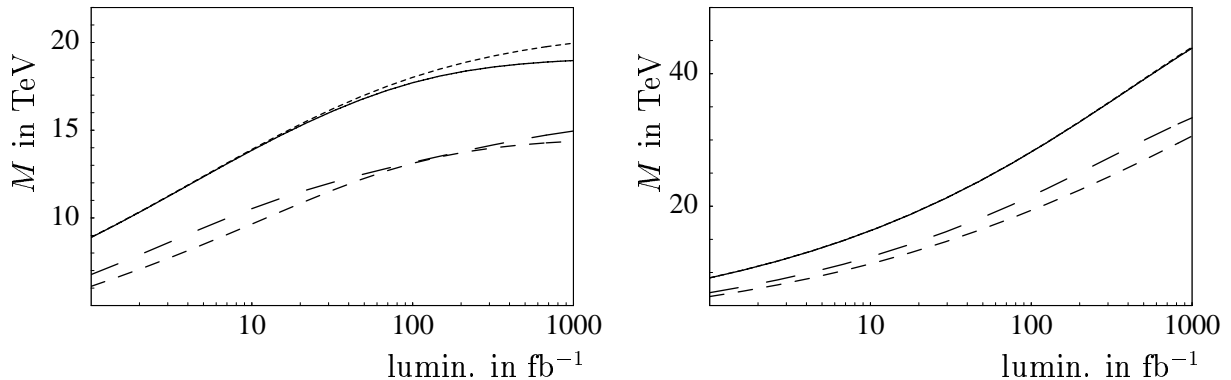


Figure 5.3: Sensitivity limit for M as a function of the integrated luminosity at $\sqrt{s} = 800$ GeV assuming a systematic error of 1.0% (left) and 0.1% (right). Combination of channels and models as in Fig. 5.2.

to the compactification scale saturates.

The combined sensitivity of the search channels of Fig. 5.1 is presented in Fig. 5.2. For bulk/brane (bulk/bulk) models, the sensitivity limit increases from 15 (20) TeV for systematic errors at the 1% level to 35 (50) TeV for negligible systematic errors. The role played by the statistics is illustrated in Fig. 5.3, where the combined sensitivity is plotted as a function of integrated luminosity.

In addition to integrated cross sections, it is also interesting to study the effects of an extra dimension on angular distributions. This may provide further handles to discriminate between different models. For the muon and tau channel, the angular distribution in the bulk-bulk model is almost completely SM-like. However, the brane-bulk and the bulk-brane models lead to significant distortions of the angular distribution because of the almost pure $U(1)_Y$ and $SU(2)_L$ nature of the heavy KK modes. In Bhabha scattering, the s - and the t -channel are affected differently such that the angular distribution is also affected in the bulk-bulk models. For illustration, Fig. 5.4 shows the shift $\Delta_{\vartheta}^{5\text{DSM}}$ of $(d\sigma/d\cos\vartheta)/\sigma_{\text{tot}}$ from the SM prediction as defined in (4.1). If the angular distributions in the muon channel can be measured with a precision better than 1% per bin (using ten bins), one can probe the compactification scale M beyond 10 TeV for the brane-bulk and the bulk-brane model. In Bhabha scattering, one can reach a similar scale also for the bulk-bulk models, while the bulk-brane model is difficult to probe in this channel.

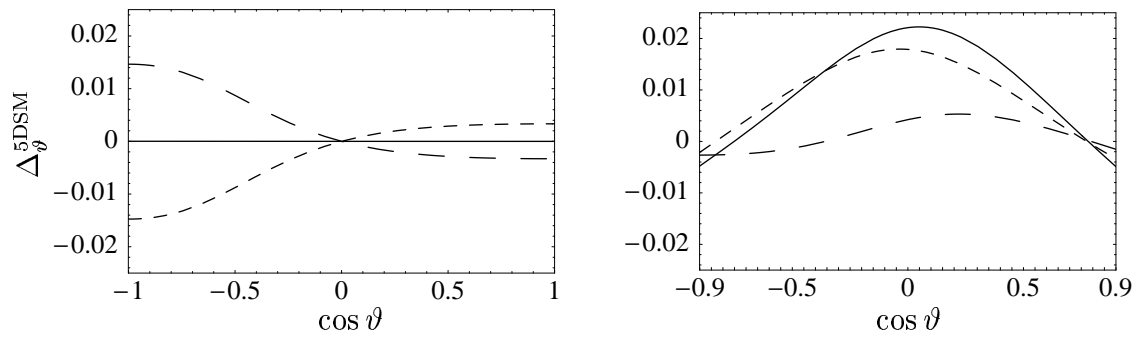


Figure 5.4: Deviation of the angular distribution $(d\sigma/d\cos\vartheta)/\sigma_{\text{tot}}$ in muon-pair production (left) and Bhabha scattering (right) from the SM predictions for $M = 10$ TeV in the bulk-bulk (solid), brane-bulk (dashed), and bulk-brane (long dashed) models.

Chapter 6

Ward Identities, the Goldstone Boson Equivalence Theorem, and Tree-Level Unitarity in W -Pair Production

In Chapter 2, we have noted that the mass generation for the massive KK gauge bosons by compactification works in close analogy to the well known Higgs mechanism in the SM. There are scalar modes $A_{5(n)}$ being eaten by the gauge modes $A_{(n)}^\mu$ to provide the longitudinal degrees of freedom for the massive gauge bosons. Hence, we have identified the scalar modes of the gauge field as the would-be Goldstone modes of the model.

The concept that a scalar disappears from the theory as a physical degree of freedom to become the longitudinal polarization states of a massive vector boson is formalized in the famous gauge boson equivalence theorem (ET) [44, 45]: In the high-energy limit of a spontaneously broken gauge theory, the tree-level amplitude for emission or absorption of longitudinal massive vector bosons equals, up to a phase, the amplitude for emission or absorption of the associated unphysical would-be Goldstone modes, i.e.

$$\begin{aligned} \mathcal{M}(V_L(i_1), \dots, V_L(i_n), A \rightarrow V_L(f_1), \dots, V_L(f_m), B) = \\ i^n (-i)^m \mathcal{M}(\phi(i_1), \dots, \phi(i_n), A \rightarrow \phi(f_1), \dots, \phi(f_m), B) \times (1 + \mathcal{O}(m_V/E)), \end{aligned} \quad (6.1)$$

where V_L are the longitudinal vector bosons, ϕ the corresponding would-be Goldstone modes, A and B denote any set of initial and final state particles other than longitudinal bosons, m_V is the mass of the boson, and E the energy of the process. Note that the phases depend on the conventions used to parameterize the fields. Here, the theorem (6.1) corresponds to the Higgs doublet as introduced in (3.12). Concerning radiative corrections, the theorem (6.1) still holds if, due to renormalization effects, an energy-independent constant on the right hand side is included.

In this chapter, we check if the ET also holds for the Goldstone modes in higher-dimensional, compactified models. In this context, the equivalence theorem has already been concerned on a rather formal level in [46], where the Goldstone modes of various models have been determined following the calculations in Chapters 2 and 3 [42]. In contrast, we show that the equivalence theorem, even in its generalized form introduced below, holds for a specific non-trivial process, W -pair production.

For some of the higher-dimensional models this is highly astonishing at first sight: The amplitude for emission of longitudinal vector bosons potentially includes terms which grow with the energy of the process because, in contrast to transverse polarization, the longitudinal polarization vector

$$\epsilon_L^\mu(p) = \frac{p^\mu}{m_V} + \mathcal{O}\left(\frac{m_V}{E}\right) \quad (6.2)$$

is enhanced for energies above the gauge boson mass. If the amplitude for emission of longitudinal gauge bosons indeed grew with energy the ET could not be satisfied. The right hand side of (6.1) simply does not include energy enhanced terms. Moreover, an amplitude growing with energy would necessarily violate tree-level unitarity. In the SM, governed by Ward identities, the dangerous terms cancel and tree-level unitarity violation is avoided as long as the Higgs-boson mass is less than roughly one TeV [92]. In some of the higher-dimensional extensions of the standard model, introduced in Chapter 3, these cancellations are far from obvious. Whenever a Higgs field on a brane is present the self-couplings of the gauge bosons and their couplings to fermions are subject to the shifts discussed in Chapter 4. It is no longer the same gauge coupling appearing in the different vertices. The simple gauge structure of the SM is lost. Hence, calculating the SM Feynman graphs with the shifted 5DSM vertices, it is no surprise that the ET and tree-level unitarity do not hold. Only the intricate interplay of the zero-mode exchange with the exchange of the complete tower of additional heavy KK modes can restore Ward identities, the ET and (at least at energy scales close to the compactification scale) tree-level unitarity. In particular, it is interesting to study what happens if a bulk gauge field eats up a Goldstone mode on the brane as we will see in Section 6.2.4.

The ET can be proven using Ward identities arising from the BRST invariance of the gauge-fixed Lagrangian. The review [93] gives a readable and instructive introduction to the subject in the context of the SM. For one massive vector boson in the final state, the relevant SM Ward identity reads

$$\langle \text{out} | F(V) | \text{in} \rangle = 0 \quad (6.3)$$

where $F(V) = \partial_\mu V^\mu - \xi m_V \phi$ is the gauge-fixing function and $|\text{in}, \text{out}\rangle$ denote any physical state. To proof the ET at tree-level, it is crucial to realize that (6.3) implies the tree-level

identity

$$i \frac{p^\mu}{m_V} \mathcal{M}_\mu(A \rightarrow B, V(p)) = \mathcal{M}(A \rightarrow B, \phi(p)), \quad (6.4)$$

where $\mathcal{M}(A \rightarrow B, V(p)) = \mathcal{M}_\mu(A \rightarrow B, V(p)) \epsilon^{*\mu}$ and ϵ is the polarization of the vector boson. For W -pair production, we need the corresponding identities for two vector bosons in the final state:

$$(-ip_1^\mu \mathcal{M}_{\mu\nu} + m_{V_1} \mathcal{M}_{4\nu}) \epsilon^\nu(p_2) = 0, \quad (6.5)$$

$$(-ip_2^\nu \mathcal{M}_{\mu\nu} + m_{V_2} \mathcal{M}_{\mu 4}) \epsilon^\mu(p_1) = 0, \quad (6.6)$$

$$-p_1^\mu p_2^\nu \mathcal{M}_{\mu\nu} - ip_1^\mu m_{V_2} \mathcal{M}_{\mu 4} - ip_2^\nu m_{V_1} \mathcal{M}_{4\nu} + m_{V_1} m_{V_2} \mathcal{M}_{44} = 0, \quad (6.7)$$

where the truncated amplitudes $\mathcal{M}_{\mu\nu}$, $\mathcal{M}_{\mu 4}$, $\mathcal{M}_{4\nu}$, and \mathcal{M}_{44} being used in the rest of this chapter are defined by

$$\begin{aligned} \mathcal{M}(A \rightarrow B, V_1(p_1), V_2(p_2)) &= \mathcal{M}_{\mu\nu} \epsilon^{*\mu}(p_1) \epsilon^{*\nu}(p_2), \\ \mathcal{M}(A \rightarrow B, V_1(p_1), \phi_2(p_2)) &= \mathcal{M}_{\mu 4} \epsilon^{*\mu}(p_1), \\ \mathcal{M}(A \rightarrow B, \phi_1(p_1), V_2(p_2)) &= \mathcal{M}_{4\nu} \epsilon^{*\nu}(p_2), \\ \mathcal{M}(A \rightarrow B, \phi_1(p_1), \phi_2(p_2)) &= \mathcal{M}_{44}. \end{aligned} \quad (6.8)$$

Equations (6.5), (6.6), and (6.7) are equivalent to the generalized equivalence theorem (GET) [94] for two external gauge bosons. Given the GET holds, the equivalence theorem (6.1) can be easily proven using (6.2) for the longitudinal polarization vector [93].

Coming back to the different higher-dimensional models, we show in the following sections, that the GET (6.5)-(6.7) holds for the specific example of W -pair production. Hence, the consistency of the gauge-fixing procedure in Chapter 3 is tested successfully. For simple higher-dimensional models without additional symmetry breaking by Higgs fields, the underlying BRST symmetry has been already demonstrated [47]. The exemplary calculations in the following sections are a strong indication that such a proof is indeed possible even in the more complicated models.

6.1 The Standard Model

As an introduction to the explicit calculations, let us first investigate the W -pair production amplitude $\mathcal{M}(e^+, e^- \rightarrow W^+(k^+), W^-(k^-))$ in the SM. For simplicity, we work with a massless fermion anti-fermion pair in the initial state. Hence, the Higgs decouples from the calculation. The relevant Feynman rules can be derived from Appendix I by taking the SM limit of the 5DSM rules presented there. The Feynman diagrams are generically displayed

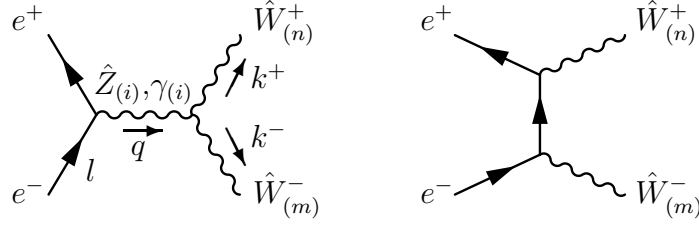


Figure 6.1: Generic Feynman diagrams for W -pair production. The KK modes which are exchanged depend on the specific model.

in Figure 6.1. For left-handed electrons in the initial state, we have

$$\begin{aligned} \mathcal{M}_{\mu\nu} = & -e^2 \bar{v}_L \gamma^\lambda u_L \left[\frac{1}{q^2} + \frac{\frac{1}{2} - s_W^2}{s_W^2} \frac{1}{q^2 - m_Z^2} \right] \\ & \times [g_{\mu\nu}(k^- - k^+)_\lambda + g_{\nu\lambda}(-q - k_-)_\mu + g_{\lambda\mu}(k_+ + q)_\nu] \\ & - \frac{e^2}{2s_W^2} \bar{v}_L \gamma_\mu \frac{(l - k^-)^\rho \gamma_\rho}{(l - k^-)^2} \gamma_\nu u_L, \end{aligned} \quad (6.9)$$

where u and \bar{v} denote the spinors of the incoming electron and positron, k^+ and k^- are the momenta of the W^+ and W^- boson, respectively, $q = k^+ + k^-$, and l is the momentum of the electron. The first two lines stem from the s -channel exchange, while the third line describes the t -channel contribution. To contract $\mathcal{M}_{\mu\nu}$ with momenta, we need the identity

$$\begin{aligned} [g_{\mu\nu}(k^- - k^+)_\lambda + g_{\nu\lambda}(-q - k_-)_\mu + g_{\lambda\mu}(k_+ + q)_\nu] k^{+\mu} k^{-\nu} = \\ \frac{q^2}{2} (k^+ - k^-)_\lambda + \frac{m_-^2 - m_+^2}{2} (k^+ + k^-)_\lambda. \end{aligned} \quad (6.10)$$

For polarization vectors fulfilling $\epsilon^{\pm\mu} k_\mu^\pm = 0$, we furthermore have

$$\begin{aligned} [g_{\mu\nu}(k^- - k^+)_\lambda + g_{\nu\lambda}(-q - k_-)_\mu + g_{\lambda\mu}(k_+ + q)_\nu] \epsilon^{+\mu} k^{-\nu} = \epsilon^{+\lambda} (q^2 - m_+^2), \\ [g_{\mu\nu}(k^- - k^+)_\lambda + g_{\nu\lambda}(-q - k_-)_\mu + g_{\lambda\mu}(k_+ + q)_\nu] k^{+\mu} \epsilon^{-\nu} = \epsilon^{-\lambda} (-q^2 + m_-^2). \end{aligned} \quad (6.11)$$

Using in addition overall momentum conservation and the Dirac equation for a massless fermion in momentum space, one finds

$$\epsilon^{+\mu} k^{-\nu} \mathcal{M}_{\mu\nu} = -e^2 \bar{v}_L \gamma^\lambda u_L \epsilon_\lambda^+ \left[\frac{1}{2s_W^2} - \frac{m_W^2}{q^2} + \frac{\frac{1}{2} - s_W^2}{s_W^2} \frac{m_Z^2 - m_W^2}{q^2 - m_Z^2} - \frac{1}{2s_W^2} \right]. \quad (6.12)$$

Hence, the potentially unitarity violating terms which grow with energy, one coming from the s -channel and the other one from the t -channel, cancel. To extract these terms, we have used $q^2/(q^2 - m^2) = 1 + m^2/(q^2 - m^2)$. The cancellation also takes place for the two

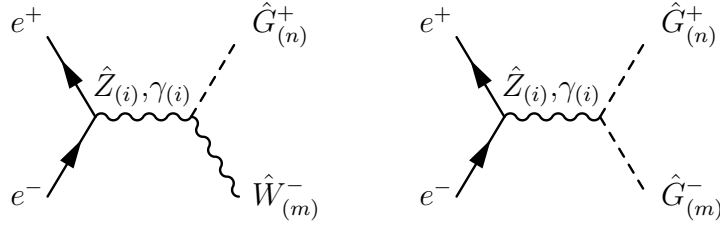


Figure 6.2: Generic Feynman diagrams for the production of one or two Goldstone modes. The KK modes which are exchanged in the s -channel depend on the specific model.

remaining relevant expressions

$$k^{+\mu}\epsilon^{-\nu}\mathcal{M}_{\mu\nu} = e^2\bar{v}_L\gamma^\lambda u_L\epsilon_\lambda^- \left[-\frac{m_W^2}{q^2} + \frac{\frac{1}{2} - s_W^2}{s_W^2} \frac{m_Z^2 - m_W^2}{q^2 - m_Z^2} \right], \quad (6.13)$$

$$k^{+\mu}k^{-\nu}\mathcal{M}_{\mu\nu} = -e^2\bar{v}_L\gamma^\lambda u_L \frac{1}{2}(k^+ - k^-)_\lambda \left[\frac{\frac{1}{2} - s_W^2}{s_W^2} \frac{m_Z^2}{q^2 - m_Z^2} \right]. \quad (6.14)$$

To relate (6.12)-(6.14) to the amplitudes in which one or both W bosons are replaced by the corresponding would-be Goldstone modes (see Figure 6.2 for the generic Feynman diagrams), a straightforward calculation yields

$$\mathcal{M}_{\mu 4} = ie^2\bar{v}_L\gamma_\mu u_L m_W \left[\frac{1}{q^2} - \frac{\frac{1}{2} - s_W^2}{c_W^2} \frac{1}{q^2 - m_Z^2} \right], \quad (6.15)$$

$$\mathcal{M}_{4\nu} = -ie^2\bar{v}_L\gamma_\nu u_L m_W \left[\frac{1}{q^2} - \frac{\frac{1}{2} - s_W^2}{c_W^2} \frac{1}{q^2 - m_Z^2} \right], \quad (6.16)$$

$$\mathcal{M}_{44} = -e^2\bar{v}_L\gamma_\lambda u_L (k^+ - k^-)_\lambda \left[\frac{1}{q^2} + \frac{\left(\frac{1}{2} - s_W^2\right)^2}{s_W^2 c_W^2} \frac{1}{q^2 - m_Z^2} \right]. \quad (6.17)$$

Using the tree-level relation $m_W^2 = m_Z^2 c_W^2$, one finds that (6.5) and (6.6) hold. With $\bar{v}_L\gamma_\mu u_L k^{+\mu} = -\bar{v}_L\gamma_\mu u_L k^{-\mu}$, one can also prove (6.7).

For right-handed electrons as initial state particles, the analogous calculation is even easier because the t -channel is absent. The GET holds as for left-handed e^- .

6.2 5D Models

Before we start to analyze the questionable models with shifted couplings, let us investigate the GET for gauge bosons with masses from geometric symmetry breaking only.

6.2.1 5D-QED

In 4D-QED, there is no massive vector boson. Thus, the GET does not apply. There is neither a longitudinal photon polarization nor a Goldstone mode. However, in 5D, the geometric symmetry breaking leads to massive KK modes $A_{(n)}^\mu$ for $n \geq 1$. Investigating the process $e^+e^- \rightarrow A_{(n)}^\mu A_{(m)}^\nu$, we add the t - and u -channel to find

$$\mathcal{M} = -e^2 \bar{v} \left[\gamma_\mu \frac{(l - k_{(n)})^\rho \gamma_\rho}{(l - k_{(n)})^2} \gamma_\nu + \gamma_\nu \frac{(l - k_{(m)})^\rho \gamma_\rho}{(l - k_{(m)})^2} \gamma_\mu \right] u \epsilon_{(n)}^{*\mu} \epsilon_{(m)}^{*\nu}, \quad (6.18)$$

where l is again the momentum of the electron and $k_{(n,m)}$ the momentum of $A_{(n,m)}^\mu$. With momentum conservation and the Dirac equation for massless fermions, a simple calculation yields

$$k_{(n)}^\mu \mathcal{M}_{\mu\nu} = 0 \quad \text{and} \quad k_{(m)}^\nu \mathcal{M}_{\mu\nu} = 0. \quad (6.19)$$

No terms with bad high-energy behavior are present. Concerning the corresponding would-be Goldstone modes, $A_{5(n)}$ and $A_{5(m)}$ do not couple to fermions because of their odd Z_2 parity, i.e. $\mathcal{M}_{\mu 4} = \mathcal{M}_{4\nu} = \mathcal{M}_{44} = 0$. Thus, the GET holds. In contrast, the ET as stated in (6.1) breaks down because the right hand side is zero while the amplitude for gauge-boson production (6.18) does not identically vanish. However, the real meaning of the equivalence theorem is still valid because (6.18) tends to zero for large energies, i.e. it becomes equal to the vanishing amplitude for the corresponding Goldstone-boson production \mathcal{M}_{44} .

6.2.2 Purely Geometric Symmetry Breaking

We consider another model with geometric symmetry breaking only, the 5DSM with all gauge fields in the bulk in the limit of vanishing VEV of the Higgs field. As we will see, the interplay of the KK gauge-boson self-couplings ensures the GET for heavy W -pair production. The relevant Feynman rules follow from the general considerations for self-couplings in non-Abelian models. They are displayed in Figures I.1 and I.2 of Appendix I. For simplicity, let us investigate $e^+e^- \rightarrow W_{(n)}^{+\mu} W_{(m)}^{-\nu}$ for $n, m \geq 1, n > m$. Concentrating on heavy KK modes with different KK number in the final state removes additional factors in the Feynman rules being present otherwise. We comment on the general case at the end of the section. As a direct generalization of the SM, the truncated amplitude $\mathcal{M}_{\mu\nu}$ is given

by

$$\begin{aligned}
\mathcal{M}_{\mu\nu} = & -e^2 \bar{v}_L \gamma^\lambda u_L \left[\frac{1}{q^2 - m_{(n-m)\gamma}^2} + \frac{\frac{1}{2} - s_W^2}{s_W^2} \frac{1}{q^2 - m_{(n-m)Z}^2} + (n-m) \rightarrow (n+m) \right] \\
& \times [g_{\mu\nu}(k^- - k^+)_\lambda + g_{\nu\lambda}(-q - k_-)_\mu + g_{\lambda\mu}(k_+ + q)_\nu] \\
& - 2 \frac{e^2}{2s_W^2} \bar{v}_L \gamma_\mu \frac{(l - k^-)^\rho \gamma_\rho}{(l - k^-)^2} \gamma_\nu u_L,
\end{aligned} \tag{6.20}$$

where $m_{\gamma,Z(k)}$ are the masses for the photon and Z -boson KK modes. As dictated by the selection rules introduced in Section 3.1, there are only two KK modes of the photon and two KK modes of the Z boson in the s -channel. Compared to the SM result (6.9), the additional factor of two in the t -channel of (6.20) is due to the enhanced coupling of fermions to heavy KK modes (cf. Fig. 2.2). This factor of two is essential for the cancellation of the terms growing with energy. The enhancement factor of $\sqrt{2}$ in the s -channel is canceled by a factor of $1/\sqrt{2}$ in the Feynman rule for the three gauge-boson vertex. A simple calculation, using again (6.11), results in

$$\begin{aligned}
\epsilon^{+\mu} k^{-\nu} \mathcal{M}_{\mu\nu} = & -e^2 \bar{v}_L \gamma^\lambda u_L \epsilon_\lambda^+ \left[\frac{m_{\gamma(n-m)}^2 - m_{W(n)}^2}{q^2 - m_{\gamma(n-m)}^2} \right. \\
& \left. + \frac{\frac{1}{2} - s_W^2}{s_W^2} \frac{m_{Z(n-m)}^2 - m_{W(n)}^2}{q^2 - m_{Z(n-m)}^2} + (n-m) \rightarrow (n+m) \right].
\end{aligned} \tag{6.21}$$

On the other hand, we find

$$\begin{aligned}
k^{+\mu} \epsilon^{-\nu} \mathcal{M}_{\mu\nu} = & e^2 \bar{v}_L \gamma^\lambda u_L \epsilon_\lambda^- \left[\frac{m_{\gamma(n-m)}^2 - m_{W(m)}^2}{q^2 - m_{\gamma(n-m)}^2} \right. \\
& \left. + \frac{\frac{1}{2} - s_W^2}{s_W^2} \frac{m_{Z(n-m)}^2 - m_{W(m)}^2}{q^2 - m_{Z(n-m)}^2} + (n-m) \rightarrow (n+m) \right],
\end{aligned} \tag{6.22}$$

$$\begin{aligned}
k^{+\mu} k^{-\nu} \mathcal{M}_{\mu\nu} = & -e^2 \bar{v}_L \gamma^\lambda u_L \frac{1}{2} (k^+ - k^-)_\lambda \left[\frac{m_{\gamma(n-m)}^2}{q^2 - m_{\gamma(n-m)}^2} \right. \\
& \left. + \frac{\frac{1}{2} - s_W^2}{s_W^2} \frac{m_{Z(n-m)}^2}{q^2 - m_{Z(n-m)}^2} + (n-m) \rightarrow (n+m) \right].
\end{aligned} \tag{6.23}$$

These results have to be compared with the amplitudes for the production of one or two would-be Goldstone modes, i.e. the scalar KK modes $W_{5(m,n)}$. From the diagrams in

Fig. 6.2 and the corresponding Feynman rules in Appendix I, we find

$$\begin{aligned} \mathcal{M}_{\mu 4} = & i e^2 \bar{v}_L \gamma_\mu u_L \left[\left(\frac{1}{q^2 - m_{\gamma(n-m)}^2} + \frac{\frac{1}{2} - s_W^2}{s_W^2} \frac{1}{q^2 - m_{Z(n-m)}^2} \right) \right. \\ & \left. \times \left(\left(\frac{n}{R} \right) \tilde{\delta}_{m,n-m,n} - \left(\frac{n-m}{R} \right) \tilde{\delta}_{m,n,n-m} \right) + (n-m) \rightarrow (n+m) \right]. \end{aligned} \quad (6.24)$$

The definition of $\tilde{\delta}_{k,l,m}$ in (3.8) implies that $\tilde{\delta}_{k,l,m} = 1$ if l is not the largest of the KK numbers (k, l, m) involved in the amplitude. Otherwise, one has $\tilde{\delta}_{k,l,m} = -1$. Thus, (6.24) simplifies to

$$\begin{aligned} \mathcal{M}_{\mu 4} = & i e^2 \bar{v}_L \gamma_\mu u_L \left[\left(\frac{1}{q^2 - m_{\gamma(n-m)}^2} + \frac{\frac{1}{2} - s_W^2}{s_W^2} \frac{1}{q^2 - m_{Z(n-m)}^2} \right) \frac{2n-m}{R} \right. \\ & \left. + \left(\frac{1}{q^2 - m_{\gamma(n+m)}^2} + \frac{\frac{1}{2} - s_W^2}{s_W^2} \frac{1}{q^2 - m_{Z(n+m)}^2} \right) \frac{-2n-m}{R} \right]. \end{aligned} \quad (6.25)$$

An analogous calculation yields

$$\begin{aligned} \mathcal{M}_{4\nu} = & -i e^2 \bar{v}_L \gamma_\nu u_L \left[\left(\frac{1}{q^2 - m_{\gamma(n-m)}^2} + \frac{\frac{1}{2} - s_W^2}{s_W^2} \frac{1}{q^2 - m_{Z(n-m)}^2} \right) \frac{2m-n}{R} \right. \\ & \left. + \left(\frac{1}{q^2 - m_{\gamma(n+m)}^2} + \frac{\frac{1}{2} - s_W^2}{s_W^2} \frac{1}{q^2 - m_{Z(n+m)}^2} \right) \frac{-2m-n}{R} \right]. \end{aligned} \quad (6.26)$$

Using the relation $m_{\gamma,Z,W(n)} = n/R$ between KK number and mass in this simple 5D model, one calculates according to (6.6)

$$\begin{aligned} (-i k^{-\nu} \mathcal{M}_{\mu\nu} + m_{W(m)} \mathcal{M}_{\mu 4}) \epsilon^{+\mu} = \\ i e^2 \bar{v}_L \gamma_\nu u_L \epsilon^{+\mu} \left[\frac{1}{R^2} \frac{(n-m)^2 - n^2 + 2mn - m^2}{q^2 - m_{\gamma(n-m)}^2} + \dots \right] = 0, \end{aligned} \quad (6.27)$$

where the dots represent terms adding up to zero in the same way as the given term. Equation (6.5) holds in analogy. Finally, one has to calculate

$$\begin{aligned} \mathcal{M}_{44} = & -e^2 \bar{v}_L \gamma_\lambda u_L (k^+ - k^-)^\lambda \\ & \times \left[\frac{1}{q^2 - m_{\gamma(n-m)}^2} + \frac{\frac{1}{2} - s_W^2}{s_W^2} \frac{1}{q^2 - m_{Z(n-m)}^2} - (n-m) \rightarrow (n+m) \right], \end{aligned} \quad (6.28)$$

where the extra minus sign in the amplitude for the $(n+m)$ KK exchange is again due to the definition of $\tilde{\delta}_{k,l,m}$. Using (6.23), (6.25), and (6.26) one can show that (6.7) also holds. That is, the GET is valid.

For $n = m$, there are diagrams with zero-mode exchange in the s -channel. Thus, the enhancement factor $\sqrt{2}$ from the fermion coupling is missing. However, the Feynman rules for the self couplings in these diagrams do not carry a factor of $1/\sqrt{2}$ either such that the above results are recovered. Another special case arises for $m = 0$. Since one of the final-state gauge bosons is massless, the GET is even easier to check because the corresponding Goldstone mode is absent. There is only one Z boson and one photon KK mode being exchanged in the s -channel. Here, the t -channel for gauge-boson production is only enhanced by a factor of $\sqrt{2}$. The s -channel of the relevant amplitudes is also enhanced by $\sqrt{2}$ to ensure the cancellation of terms growing with energy and (6.5)-(6.7). Testing the GET does not provide any hint for the inconsistency of this simple model. Moreover, as a byproduct, it provides a non-trivial test for the Feynman rules describing the self-interaction of gauge bosons and their associated would-be Goldstone modes presented in Section 3.1.

6.2.3 Bulk-Bulk Model with a Bulk Higgs

Following the phase convention of (3.12), the Goldstone modes of this model are given by

$$G_{(n)}^{\pm} = m_{W(n)}^{-1} \left(\frac{n}{R} W_{(n)5}^{\pm} + \frac{gv}{2} \chi_{(n)}^{\pm} \right), \quad (6.29)$$

where $m_{W(n)}^2 = n^2/R^2 + g^2v^2/4$. Geometrical symmetry breaking and symmetry breaking by a VEV play together as reflected in the structure of the Goldstone modes.

In order to prove (6.5) to (6.7), we can make use of the results from the preceding sections. The Feynman rules for the truncated amplitudes $\mathcal{M}_{\mu\nu}$ do not change. Thus, the results in Section 6.2.2 are correct for the bulk-bulk model with a bulk Higgs if one inserts the correct masses $m_{W(n)}^2$ and $m_{Z(n)}^2 = n^2/R^2 + (g^2 + g'^2)v^2/4$. Consequently, there are two classes of numerators, one being proportional to the geometric masses n^2/R^2 and the other one to the VEV of the Higgs field.

According to this observation, the other amplitudes are most easily calculated using the Feynman rules (cf. Appendix I) for the two scalar fields which are combined in (6.29) to form the Goldstone mode. This is particularly easy, because there is no diagram for the production of a $\chi_{(n)}^{\pm}$ mode together with a $W_{(n)}^{\pm}$ mode contributing to \mathcal{M}_{44} . Moreover, in (6.5) to (6.7), any amplitude with a Goldstone mode in the final state is multiplied by the corresponding vector boson mass. Hence, the factor $m_{W(n)}^{-1}$ from (6.29) is canceled everywhere. Amplitudes with $W_{5(n)}^{\pm}$ in the final state have to be multiplied by n/R according to (6.29). They combine with the terms in $\mathcal{M}_{\mu\nu}$ being proportional to geometric masses, exactly as in Section (6.2.2). The terms being proportional to the Higgs VEV combine with the amplitudes for $\chi_{(n)}^{\pm}$ production as in the SM calculation of Section 6.1, such that

the GET is satisfied. Here, there is no cross-talk between the two mechanisms for symmetry breaking. For production of two equal higher KK modes ($n = m$) or one zero mode ($m = 0$), the same considerations as in Section (6.2.2) apply.

6.2.4 Bulk-Bulk Model with a Brane Higgs

We now concentrate on pair production of the W -boson zero modes $\hat{W}_{(0)}^\pm$. In the preceding sections, this case has been of no particular interest, because zero-mode production was completely standard model like. This is no longer true in the bulk-bulk model with a brane Higgs. Also the interplay between geometrical symmetry breaking and the VEV of the brane Higgs field is more involved. First, mixing between Fourier modes induces the exchange of all heavy KK modes of the photon and the Z boson in the s -channel, originally forbidden by selection rules. However, the couplings of the final state W bosons to heavy KK modes are suppressed by a factor X . The Goldstone modes of the model are given by

$$\hat{G}_{(n)}^\pm = \left(1 + \pi^2 (gv/2)^2 R^2 + \frac{m_{W(n)}^2}{(gv/2)^2} \right)^{-1/2} \left(\sqrt{2} \chi^\pm + \sum_{j=1}^{\infty} \frac{2(j/R)(gv/2)}{m_{W(n)}^2 - (j/R)^2} W_{(j)}^\pm \right), \quad (6.30)$$

in analogy to (2.46). Thus, the would-be Goldstone that corresponds to the zero mode of the W boson is, up to small admixtures, a brane field. Consequently, it couples to the heavy KK modes without suppression. Nevertheless, as dictated by the ET (6.1), the amplitudes for the production of the zero-mode Goldstone and gauge boson should become equal at large energies. Moreover, the couplings in the different Feynman rules are subject to shifts of different size. Thus, the cancellation between the s - and t -channel is questionable. Having indicated possible problems, we now outline the calculation.

The truncated amplitude $\mathcal{M}_{\mu\nu}$ for $\hat{W}_{(0)}^+ \hat{W}_{(0)}^-$ production is given by

$$\begin{aligned} \mathcal{M}_{\mu\nu} = & -\bar{v}_L \gamma^\lambda u_L \sum_{n=0}^{\infty} \left[\frac{e_{(n)} g_{3(n)}^\gamma}{q^2 - m_{\gamma(n)}^2} + \frac{\frac{1}{2} - s_W^2}{c_W} \frac{g_{Z(n)} g_{3(n)}^Z}{q^2 - m_{Z(n)}^2} \right] \\ & \times [g_{\mu\nu}(k^- - k^+)_\lambda + g_{\nu\lambda}(-q - k_-)_\mu + g_{\lambda\mu}(k_+ + q)_\nu] \\ & - \frac{g_{W(0)}^2}{2} \bar{v}_L \gamma_\mu \frac{(l - k^-)^\rho \gamma_\rho}{(l - k^-)^2} \gamma_\nu u_L, \end{aligned} \quad (6.31)$$

where the couplings are defined in Appendices B and G. Contracting with external mo-

menta, the truncated s - and t -channel amplitudes combine to

$$\begin{aligned}
k^{+\mu}k^{-\mu}\mathcal{M}_{\mu\nu} &= -\bar{v}_L\gamma^\lambda u_L\frac{1}{2}(k^+ - k^-)_\lambda \\
&\times \sum_{n=0}^{\infty} \left[e_{(n)}g_{3(n)}^\gamma + \frac{\frac{1}{2} - s_W^2}{c_W}g_{Z(n)}g_{3(n)}^Z - \frac{g_{W(0)}^2}{2}\delta_{n,0} \right. \\
&\quad \left. + m_{\gamma(n)}^2\frac{e_{(n)}g_{3(n)}^\gamma}{q^2 - m_{\gamma(n)}^2} + m_{Z(n)}^2\frac{\frac{1}{2} - s_W^2}{c_W}\frac{g_{Z(n)}g_{3(n)}^Z}{q^2 - m_{Z(n)}^2} \right]. \tag{6.32}
\end{aligned}$$

The terms in the second line of (6.32) grow with energy and cannot be present in the Goldstone channels. Hence, they better should cancel. It is hard to exactly calculate the couplings, but it is already very instructive to work to first order in X as in Chapter 4. The relevant couplings are then given by the following list:

$$\begin{aligned}
e_{(0)} &= e \\
g_{Z(0)} &= g(1 - X) \\
g_{W(0)} &= g(1 - c_W^2 X) \\
g_{3(0)}^\gamma &= e \\
g_{3(0)}^Z &= g c_W \\
g_{3(n\geq 1)}^\gamma &= -\sqrt{2} e c_W^2 \frac{6}{n^2\pi^2} X \\
g_{3(n\geq 1)}^Z &= \sqrt{2} g c_W (s_W^2 - c_W^2) \frac{3}{n^2\pi^2} X
\end{aligned} \tag{6.33}$$

Furthermore, we can use $e_{(n)} = \sqrt{2}e$ and $g_{Z(n)} = \sqrt{2}g$ for $n \geq 1$ because these couplings appear only in terms being already of order X . The crucial cancellation in (6.32) indeed takes place using $\sum_1^\infty 1/n^2 = \pi^2/6$. The complete KK tower is involved in this intricate cancellation which is expected from the gauge structure of the untruncated 5DSM. Truncating the model at a given KK number destroys the cancellation, as it destroys gauge invariance.

For $n \geq 1$ the terms in the third line of (6.32) can be manipulated according to

$$\begin{aligned}
m_{\gamma(n)}^2\frac{e_{(n)}g_{3(n)}^\gamma}{q^2 - m_{\gamma(n)}^2} &= -n^2 M^2 \frac{2e^2}{q^2 - m_{\gamma(n)}^2} c_W^2 \frac{6}{n^2\pi^2} X + \mathcal{O}(X^2) \\
&= -m_{Z(0)}^2 \frac{4e^2}{q^2 - m_{\gamma(n)}^2} c_W^2 + \mathcal{O}(X^2).
\end{aligned} \tag{6.34}$$

Hence, despite the order X suppression in the couplings, the terms from the exchange of higher KK modes are enhanced to $\mathcal{O}(1)$. The appearance of the factor $m_{\gamma(n)}^2$ in (6.34)

can be traced back to the additional q^2 term in the numerator of the amplitude due to the longitudinal polarization vectors. There is no such enhancement for transverse polarization. The light longitudinal W bosons mainly originate from eating up the Goldstone mode χ in (6.30) which is restricted to the brane $y = 0$. As suggested by the equivalence theorem, we find that they indeed behave like a brane field and couple with full gauge strength to the heavy KK modes, in spite of the selection rules for bulk fields. At high energies, the longitudinal $\hat{W}_{(0)}^{\pm\mu}$ cannot conceal their origin. To further quantify this observation, we return to the GET. Since the amplitude includes terms of order X which are enhanced to $\mathcal{O}(1)$, we can only reliably calculate the leading order of $\mathcal{M}_{\mu\nu}$, given by

$$k^{+\mu}k^{-\mu}\mathcal{M}_{\mu\nu} = -e^2\bar{v}_L\gamma^\lambda u_L\frac{1}{2}(k^+ - k^-)_\lambda \left[\frac{\frac{1}{2} - s_W^2}{s_W^2} \frac{m_{Z(0)}^2}{q^2 - m_{Z(0)}^2} - 4c_W^2 \sum_{n=1}^{\infty} \left(\frac{m_{Z(0)}^2}{q^2 - m_{\gamma(n)}^2} + \frac{(\frac{1}{2} - s_W^2)^2}{c_W^2 s_W^2} \frac{m_{Z(0)}^2}{q^2 - m_{Z(n)}^2} \right) \right]. \quad (6.35)$$

For the other two important amplitudes, we find

$$\epsilon^{+\mu}k^{-\mu}\mathcal{M}_{\mu\nu} = -e^2\bar{v}_L\gamma^\lambda u_L\epsilon_\lambda^+ \left[\frac{-m_{W(0)}^2}{q^2} + \frac{\frac{1}{2} - s_W^2}{s_W^2} \frac{m_{Z(0)}^2 - m_{W(0)}^2}{q^2 - m_{Z(0)}^2} - 4c_W^2 \sum_{n=1}^{\infty} \left(\frac{m_{Z(0)}^2}{q^2 - m_{\gamma(n)}^2} + \frac{(\frac{1}{2} - s_W^2)^2}{c_W^2 s_W^2} \frac{m_{Z(0)}^2}{q^2 - m_{Z(n)}^2} \right) \right], \quad (6.36)$$

$$\epsilon^{-\mu}k^{+\mu}\mathcal{M}_{\mu\nu} = e^2\bar{v}_L\gamma^\lambda u_L\epsilon_\lambda^- \left[\frac{-m_{W(0)}^2}{q^2} + \frac{\frac{1}{2} - s_W^2}{s_W^2} \frac{m_{Z(0)}^2 - m_{W(0)}^2}{q^2 - m_{Z(0)}^2} - 4c_W^2 \sum_{n=1}^{\infty} \left(\frac{m_{Z(0)}^2}{q^2 - m_{\gamma(n)}^2} + \frac{(\frac{1}{2} - s_W^2)^2}{c_W^2 s_W^2} \frac{m_{Z(0)}^2}{q^2 - m_{Z(n)}^2} \right) \right]. \quad (6.37)$$

The contributions from the exchange of heavy modes are unchanged at leading order compared to (6.35).

For the modes χ^\pm , the Feynman rules to leading order can be calculated as for any field restricted to a brane: For the coupling to the zero modes, there is the SM vertex. For the higher modes, apart from the enhancement factor $\sqrt{2}$, the vertex function is identical (see Fig. I.3 in Appendix I). Besides the χ^\pm field, the Goldstone mode $G_{(0)}^\pm$ consists only of small admixtures of $W_{5(n)}^\pm$ modes being of order R/n . Nevertheless, even in a leading order calculation these admixtures cannot be ignored because the relevant $W_{(n)5}^+ \hat{W}_{(0)}^- \hat{Z}_{(n)}$ vertex is enhanced by a KK mass n/R as shown in Fig. I.1 and I.2. The other $W_{(m)5}^+ \hat{W}_{(0)}^- \hat{Z}_{(n)}$ vertices for $m \neq n$, being originally forbidden by selection rules, can be ignored at leading order

because of an additional suppression factor X . Thus, we find for the truncated amplitude $\mathcal{M}_{\mu 4}$

$$\begin{aligned} \mathcal{M}_{\mu 4} = ie^2 \bar{v}_L \gamma_\mu u_L \frac{gv}{2} & \left[\frac{1}{q^2} - \frac{\frac{1}{2} - s_W^2}{c_W^2} \frac{1}{q^2 - m_{Z(0)}^2} \right. \\ & + 2 \sum_{n=1}^{\infty} \left(\frac{1}{q^2 - m_{\gamma(n)}^2} - \frac{\frac{1}{2} - s_W^2}{c_W^2} \frac{1}{q^2 - m_{Z(n)}^2} \right) \\ & \left. + 2 \sum_{n=1}^{\infty} \left(\frac{1}{q^2 + m_{\gamma(n)}^2} + \frac{\frac{1}{2} - s_W^2}{s_W^2} \frac{1}{q^2 - m_{Z(n)}^2} \right) \right], \end{aligned} \quad (6.38)$$

leading to

$$\begin{aligned} \mathcal{M}_{\mu 4} = ie^2 \bar{v}_L \gamma_\mu u_L \frac{gv}{2} & \left[\frac{1}{q^2} - \frac{\frac{1}{2} - s_W^2}{c_W^2} \frac{1}{q^2 - m_{Z(0)}^2} \right. \\ & \left. + 4 \sum_{n=1}^{\infty} \left(\frac{1}{q^2 - m_{\gamma(n)}^2} + \frac{(\frac{1}{2} - s_W^2)^2}{s_W^2 c_W^2} \frac{1}{q^2 - m_{Z(n)}^2} \right) \right] \end{aligned} \quad (6.39)$$

and $M_{4\nu} = -g_\nu^\mu M_{\mu 4}$. For the amplitude \mathcal{M}_{44} , no contribution from the heavy scalar KK modes $W_{5(n)}^\pm$ in (6.30) arises at leading order. One obtains

$$\begin{aligned} \mathcal{M}_{44} = -e^2 \bar{v}_L \gamma_\lambda u_L (k^+ - k^-)^\lambda & \left[\frac{1}{q^2} + \frac{(\frac{1}{2} - s_W^2)^2}{s_W^2 c_W^2} \frac{1}{q^2 - m_{Z(0)}^2} \right. \\ & \left. + 2 \sum_{n=1}^{\infty} \frac{1}{q^2 - m_{\gamma(n)}^2} + \frac{(\frac{1}{2} - s_W^2)^2}{s_W^2 c_W^2} \frac{1}{q^2 - m_{Z(n)}^2} \right]. \end{aligned} \quad (6.40)$$

Combining the final results for the different amplitudes and using the SM relations $m_{W(0)} = gv/2$, $m_{Z(0)}^2 = m_Z^2 c_W^2$, being valid at zeroth order in X , it is easy to show that the GET does hold. Considering right-handed electrons in the initial state, a similar calculation leads to the same conclusion. The terms growing with energy arise as a different combination of coupling shifts which also vanishes. The GET and the equivalence theorem in its original formulation (6.1) also hold. There is no indication that Ward identities and in turn gauge invariance are violated.

Moreover, the cancellation of the terms growing with energy provides a highly non-trivial test for a large number of Feynman rules, in particular for the size of the couplings in (6.33). This test can also be successfully performed for the other two models with brane Higgs fields and, hence, shifted couplings.

6.3 The Phenomenology of W -Pair Production

The analysis in the preceding section can also help us to understand the cross section for W -pair production as a function of energy, displayed in Figure 6.3 for the bulk-bulk model with a brane Higgs. For illustration, we have chosen $X = 0.01$. As a rough estimate for the width of the heavy modes, we take $\Gamma = 0.01m_{W(n)}$, where $m_{W(n)} \sim n/R$. Let us now try to understand the resonances. Naively, on resonance, one could expect that the cross section is enhanced by a factor $\Gamma^2 \sim 10^4$ compared to the SM cross section due to the exchange of the on-shell KK mode. However, if both W bosons in the final state are transversely polarized the coupling to the on-shell KK mode is suppressed by a factor X diminishing the squared amplitude by a factor of $X^2 \sim 10^{-4}$. As a result, the resonant contribution from the transversely polarized W bosons in the final state is only of the order of the SM cross section and does not lead to a pronounced resonance peak. From (6.34) we know that the longitudinal W bosons couple to the heavy KK modes in the s -channel like a brane field, i.e. in an unsuppressed way. Thus, on resonance the cross section is indeed enhanced as can be seen in Fig. 6.3 and completely dominated by W pairs containing at least one longitudinal W boson.

At energies smaller than the compactification scale, the production of longitudinal W bosons only contributes a small fraction to the unpolarized cross section [95]. Thus, the 5DSM shift in the cross section is almost negligible because the sizable negative interference for the production of longitudinally polarized W bosons from heavy KK exchange is only a small effect on top of a large background of transverse W bosons. For this reason, the bounds from W -pair production in Section 4.4.2 are found to be weak.

Finally, let us briefly comment on the issue of unitarity in the context of W^+W^- production in the 5D models. Fig. 6.3 also shows the cross section for W -pair production for the bulk-bulk model with a brane Higgs in which the amplitudes from virtual heavy KK exchange are set to zero by hand. As we have seen in Section 6.2.4, the terms growing with energy do not cancel without KK contributions and the amplitude violates unitarity at some energy scale. As expected, the cross section does no longer decrease with energy above the compactification scale.

In the full higher-dimensional model, disregarding the resonances, the cross section is better behaved because of the intricate interplay of the KK modes. Nevertheless, at higher center-of-mass energies, the cross section also does not decrease as $1/s$ signaling that the amplitude rises with energy. This may be surprising at first sight because we have shown in the last section that there is no single term in amplitudes like (6.35) which is growing with energy. However, due to the infinite tower of KK modes, each amplitude consists of an infinite

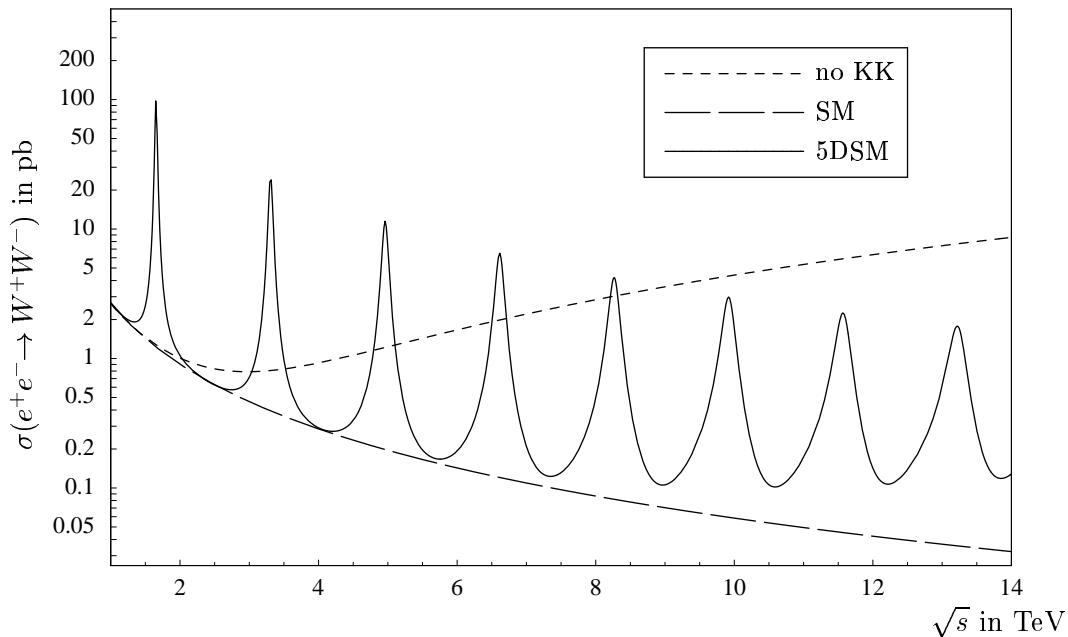


Figure 6.3: Cross section for W -pair production in the SM and the 5DSM in a bulk-bulk model with a brane Higgs. The cross section for the 5DSM where the contributions from the heavy KK modes are ignored is also shown (no KK).

number of terms $\mathcal{M}_{(n)}$. For each of these terms, one finds

$$\mathcal{M}_{(n)} \propto \frac{s}{s - m_{\gamma, Z(n)}^2} \rightarrow 1 \quad (6.41)$$

as soon as $\sqrt{s} \gg m_{\gamma, Z(n)}$. With growing \sqrt{s} , this condition is fulfilled for more and more modes. Thus, at center-of-mass energies much larger than the compactification scale, the amplitude is roughly proportional to \sqrt{s} . As a consequence, unitarity is violated at some high energy scale.

This kind of unitarity violation is a generic feature of any model in which the couplings to an infinite number of exchange modes is not suppressed at least linearly with the mode number. In particular, it is not tied to the production of longitudinal vector bosons. Moreover, let us stress that unitarity violation does not follow from a breakdown of the equivalence theorem (6.1).

There is another source of unitarity violation in 5D models. With growing energy, the production of more and more heavy KK modes becomes kinematically allowed. In a coupled channel analysis, the increase in possible final states can also be shown to violate unitarity. In the electroweak sector of the SM, one finds a breakdown of tree-level unitarity at roughly $\sqrt{s} \sim 10 M$ [48–50]. Here, unitarity violation arises even in models in which selection rules

forbid all but a finite set of Feynman diagrams. At any rate, the 5D models have to be considered as effective field theories valid only up to a certain energy scale.

Chapter 7

Brane Kinetic Terms

In the preceding chapter, we have performed a consistency check for the 5D extensions of the SM at the tree-level. Here, we question if the models under study are consistent effective field theories concerning radiative correction. Indeed, it has been shown that there are certain gauge invariant operators, missing in naive higher-dimensional extension of 4D models like (2.1), which are induced by loops [51].

It is again instructive to work in 5D-QED as introduced in Chapter 2. We consider the one-loop self-energy diagrams of the photon KK modes $\Pi_{(m,n)}^{\mu\nu}$ displayed in Fig. 7.1. For $m = n = 0$, the diagram leads to the well known photon self-energy $\Pi_{(0,0)}^{\mu\nu}(q^2) = \Pi^{\mu\nu}(q^2)$ in QED. As we have seen in Chapter 2, a fermion living on the brane $y = 0$ completely destroys momentum conservation in the direction of the extra compact dimension. Thus, as expressed by the Feynman rules in Fig. 2.2, the fermion loop in Fig. 7.1 couples photon KK modes of any KK number, i.e.

$$\Pi_{(m,n)}^{\mu\nu}(q^2) = \sqrt{2}^{2-\delta_{m,0}-\delta_{n,0}} \Pi^{\mu\nu}(q^2), \quad (7.1)$$

where the factor $\sqrt{2}$ is again the typical enhancement for the coupling of a brane field to higher KK modes. The self-energies $\Pi_{(m,n)}^{\mu\nu}$ are UV-divergent quantities and have to

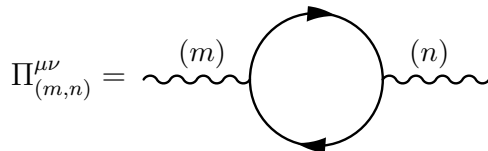


Figure 7.1: Self-energy diagram for the photon KK modes in 5D-QED.

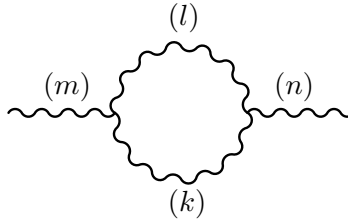


Figure 7.2: Self-energy diagram for the gauge boson KK modes in a non-Abelian 5D model.

be renormalized. Due to the mixing between different KK modes, bulk terms as in (2.1) cannot provide suitable counter terms. However, a gauge-boson kinetic term

$$\mathcal{L}(x, y) \supset -r_c \delta(y) \frac{1}{4} F_{MN}(x, y) F^{MN}(x, y), \quad (7.2)$$

being confined to the $y = 0$ brane where the fermion lives, can remove all one-loop divergences implied by Figure 7.1. As before, $F_{MN}(x, y)$ denotes the usual field strength tensor (2.2) in five dimensions. The parameter r_c is a natural extension of the wave-function renormalization constant in 4D-QED. The resulting mixing between Fourier modes is obvious from the δ -function in (7.2). The factors $\sqrt{2}$ in (7.1) are also correctly provided. As a counter term, the constant r_c can be chosen such that the self-energy contribution from Fig. 7.1 and the corresponding mixing of Fourier modes is compensated at one energy scale. At this energy scale, one could forget about the one-loop correction in Fig. 7.1 as well as about the additional brane kinetic terms (7.2). However, the renormalization group running of r_c reintroduces the mixing at other energy scales. Hence, from the point of view of an effective field theory, a constant like r_c has to be considered as a free parameter of the theory. Note that (7.2) is a perfectly gauge invariant dimension five operator where r_c has mass dimension -1 . In 4D theories, such terms never arise because a δ -function in the Lagrangian density violates translational invariance.

Let us now investigate the self-energy contribution from a bulk field in the loop. As a natural setup, we can work in a non-Abelian model as introduced in Section 3.1, where the gauge-boson self-interactions provide bulk-modes in self-energy loops as exemplified in Fig. 7.2. As we have seen in Section 3.1, the modes k and l propagating in the gauge-boson loop are subject to selection rules. In particular, if m is even k and l have to be either both even or both odd. In consequence, n will also be even if the loop is not to vanish by selection rules. In analogy, n has to be odd if m is odd. Apart from this restriction, a combination of k and l can be found for any pair of even or odd m and n such that the two modes mix. The same considerations apply for the exchanged Goldstone and ghost modes. The corresponding counter terms, again identified as brane kinetic terms, have to

reproduce this structure. Here, it is important to remember that the S^1/Z_2 orbifold has a second fixed point at $y = \pi R$. At $y = \pi R$ the wave functions of the odd Fourier modes come with a minus sign compared to their value at $y = 0$. Hence, the brane kinetic terms

$$\mathcal{L}(x, y) \supset -r_c [\delta(y) + \delta(y - \pi R)] \frac{1}{4} F_{MN}^a(x, y) F^{aMN}(x, y), \quad (7.3)$$

only mix even with even and odd with odd modes. It turns out [51], that (7.3) exactly provides the correct factors to serve as a counter term for the self-energy from bulk fields. As before, the constant r_c has to be considered as a free parameter. The brane kinetic terms (7.3) also contain the self-interactions of the gauge bosons as enforced by gauge invariance. Concerning vertex corrections to gauge-boson self-interactions, these terms are also needed as counter terms as has been shown in specific models [55].

Combining the above results, in a model containing bulk and brane couplings, we are forced to add the terms

$$\mathcal{L}(x, y) \supset - [r_0 \delta(y) + r_\pi \delta(y - \pi R)] \frac{1}{4} F_{MN}^a(x, y) F^{aMN}(x, y) \quad (7.4)$$

to the original Lagrangian for any gauge group in the bulk. Thus, there is a new free parameter for each of the two branes of the orbifold which ultimately has to be measured by experiment if large extra dimensions are realized in nature. In this chapter, we investigate the phenomenological effects of brane kinetic terms after we have analyzed the KK mass spectrum, the eigenmodes and gauge fixing.

7.1 5D-QED with Brane Kinetic Terms

For simplicity, we demonstrate the generic consequences of the brane kinetic terms (BKT) again in the simplest setup. Concentrating on a brane kinetic term for the brane at $y = 0$ only, the Lagrangian of 5D-QED is now given by

$$\mathcal{L}(x, y) = -\frac{1}{4} F_{MN}(x, y) F^{MN}(x, y) - r_c \delta(y) \frac{1}{4} F_{MN}(x, y) F^{MN}(x, y). \quad (7.5)$$

The gauge-fixing and ghost terms are omitted for brevity. The former are considered in Section 7.1.2, the latter elsewhere [96]. Making the scalar components of the gauge fields explicit, one finds

$$\mathcal{L}(x, y) = \left[-\frac{1}{4} F_{\mu\nu} F^{\mu\nu} + \frac{1}{2} (\partial_5 A_\mu)(\partial_5 A^\mu) + \frac{1}{2} (\partial_\mu A_5)(\partial^\mu A_5) - (\partial_\mu A_5)(\partial_5 A^\mu) \right] [1 + r_c \delta(y)], \quad (7.6)$$

where the dependence of the fields on the space-time coordinates is suppressed. Using the usual transformation properties (2.4) for the gauge fields under the Z_2 symmetry of the orbifold, the Lagrangian (7.7) can be equally well expressed by

$$\mathcal{L}(x, y) = -\frac{1}{4}F_{\mu\nu}F^{\mu\nu}[1+r_c\delta(y)] + \frac{1}{2}(\partial_5 A_\mu)(\partial_5 A^\mu) + \frac{1}{2}(\partial_\mu A_5)(\partial^\mu A_5) - (\partial_\mu A_5)(\partial_5 A^\mu). \quad (7.7)$$

The terms being odd with respect to Z_2 do not feel the presence of the brane term. To derive the effective 4D Lagrangian the gauge fields have to be expanded in modes. Obviously, the Fourier modes do not form an orthonormal set of functions when 7.7 is integrated over the extra dimension because of the δ -function. Hence, they are not proper KK wave functions.

7.1.1 The Spectrum

In contrast to Chapter 2, we do not stick to the Fourier modes before integrating out the extra dimension. Instead, we now parameterize the vector field $A^\mu(x, y)$ by

$$A^\mu(x, y) = \sum_{n=0}^{\infty} \hat{A}_{(n)}^\mu(x) f_{(n)}(y) \quad (7.8)$$

and show how to derive the proper KK wave functions $f_{(n)}(y)$ for the KK mass eigenstates $\hat{A}_{(n)}^\mu(x)$ by solving a differential equation following directly from the 5D Lagrangian. Inserting (7.8) into the first two terms of (7.7) and integrating over the compact extra dimension, one obtains

$$\begin{aligned} \mathcal{L}(x, y) \supset & \sum_{n,m=0}^{\infty} -\frac{1}{4}\hat{F}_{(n)\mu\nu}(x)\hat{F}_{(m)}^{\mu\nu}(x)\int_0^{2\pi R} dy f_{(n)}(y)f_{(m)}(y)[1+r_c\delta(y)] \\ & + \sum_{n,m=0}^{\infty} \frac{1}{2}\hat{A}_{(n)\mu}(x)\hat{A}_{(m)}^\mu(x)\int_0^{2\pi R} dy (\partial_5 f_{(n)}(y))(\partial_5 f_{(m)}(y)). \end{aligned} \quad (7.9)$$

Partial integration in the second term yields

$$\int_0^{2\pi R} dy (\partial_5 f_{(n)})(\partial_5 f_{(m)}) = [f_{(n)}\partial_5 f_{(m)}]_0^{2\pi R} - \int_0^{2\pi R} dy f_{(n)}\partial_5^2 f_{(m)}. \quad (7.10)$$

Assuming that the surface term vanishes by means of (2.4), one obtains

$$\begin{aligned} \mathcal{L}(x, y) \supset & \sum_{n,m=0}^{\infty} -\frac{1}{4}\hat{F}_{(n)\mu\nu}(x)\hat{F}_{(m)}^{\mu\nu}(x)\int_0^{2\pi R} dy f_{(n)}(y)f_{(m)}(y)[1+r_c\delta(y)] \\ & - \sum_{n,m=0}^{\infty} \frac{1}{2}\hat{A}_{(n)\mu}(x)\hat{A}_{(m)}^\mu(x)\int_0^{2\pi R} dy f_{(n)}(y)\partial_5^2 f_{(m)}(y). \end{aligned} \quad (7.11)$$

Hence, the wave functions of the physical mass eigenstates of the effective 4D theory with mass $m_{(n)}$ are the normalized mode functions $f_{(n)}(y)$ solving the differential equation

$$\partial_5^2 f_{(n)}(y) = -m_{(n)}^2 f_{(n)}(y) [1 + r_c \delta(y)] \quad (7.12)$$

with periodic boundary conditions

$$\begin{aligned} f_{(n)}(y) &= f_{(n)}(y + 2\pi R), \\ \partial_5 f_{(n)}(y) &= \partial_5 f_{(n)}(y + 2\pi R). \end{aligned} \quad (7.13)$$

To proof this, note that (7.12) and (7.13) form a Sturm-Liouville problem [97] such that the solutions are guaranteed to be orthogonal with respect to the weight function $[1 + r_c \delta(y)]$, i.e.

$$\int_0^{2\pi R} dy f_{(n)}(y) f_{(m)}(y) [1 + r_c \delta(y)] = \delta_{n,m}. \quad (7.14)$$

The above differential equation can equivalently be derived by investigating the equations of motions of the gauge field $A^\mu(x, y)$ in the free theory and demanding that the KK modes $\hat{A}_{(n)}^\mu(x)$ obey the usual equation of motion for massive vector fields.

Solving (7.12) in the interval $[-\pi R, \pi R]$, we find for $y \lesssim 0$,

$$f_{(n)\lesssim}(y) = A_{\lesssim} \sin m_{(n)} y + B_{\lesssim} \cos m_{(n)} y. \quad (7.15)$$

The eigenvalues $m_{(n)}^2$ and the four constants can be determined by the Z_2 symmetry of the wave function, i.e. $f_{(n)}(y) = f_{(n)}(-y)$, $\lim_{\epsilon \rightarrow 0} [\partial_y f_{(n)}(y)]_{-\epsilon}^{\epsilon} = -m_{(n)}^2 r_c f_{(n)}(0)$, the boundary conditions (7.13), and normalization. The KK masses $m_{(n)}$ are given by the transcendental equation

$$\frac{m_{(n)} r_c}{2} = -\tan(m_{(n)} \pi R). \quad (7.16)$$

Hence, $m_{(0)} = 0$ is a solution and the corresponding KK mode is to be identified with the photon. The masses of the heavy KK modes are reduced with growing r_c and approach half integer multiples of $1/R$ as shown in Fig. 7.3. For $y \lesssim 0$, the corresponding wave functions are given by

$$f_{(n)}(y) = N_{(n)} \left[\cos(m_{(n)} y) \pm \frac{m_{(n)} r_c}{2} \sin(m_{(n)} y) \right] \quad (7.17)$$

with the normalization constant

$$N_{(n)} = \left[2^{\delta_{n,0}} \pi R \left(1 + \frac{r_c^2 m_{(n)}^2}{4} + \frac{r_c}{2\pi R} \right) \right]^{-1/2}. \quad (7.18)$$

Note that the derivative of the wave functions at $y = 0$ is not well defined. Only if the δ -function is replaced by the limit of a suitable series of functions, one finds that the derivative vanishes. In this sense, the steps from (7.6) to (7.7) and the omission of the surface term in (7.10) can be justified.

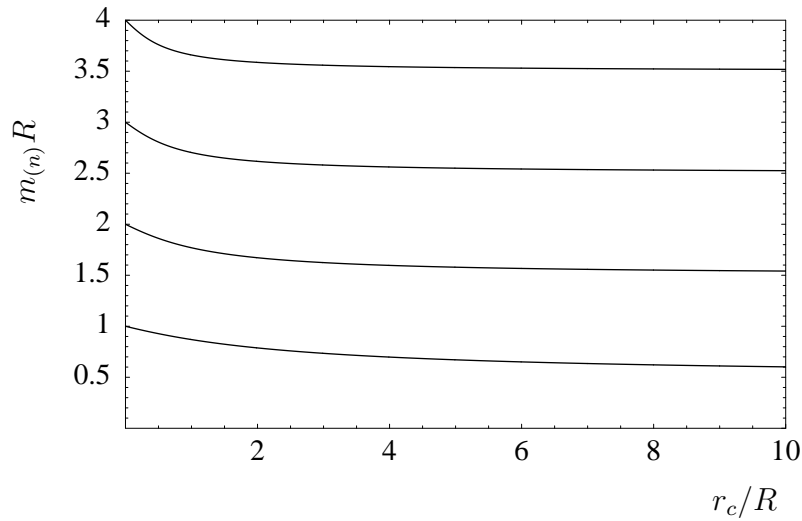


Figure 7.3: Masses $m_{(n)}$ for the first 4 heavy KK modes as a function of r_c/R .

This kind of problems does not appear using Fourier modes. Hence, as a consistency check of the above analysis, we return to the alternative method for calculating the effective 4D theory already introduced in Chapter 2. Using the usual Fourier expansion for the fields in (7.6) according to (2.4), integration over the fifth dimension yields

$$\begin{aligned} \mathcal{L}(x) = & -\frac{1}{4} \sum_{n=0}^{\infty} F_{(n)\mu\nu} F_{(n)}^{\mu\nu} - \frac{\tilde{r}_c}{4} \sum_{n,m=0}^{\infty} \sqrt{2}^{(2-\delta_{n,0}-\delta_{m,0})} F_{(n)\mu\nu} F_{(m)}^{\mu\nu} + \frac{1}{2} \sum_{n=0}^{\infty} \frac{n^2}{R^2} A_{(n)\mu} A_{(n)}^{\mu} \\ & + \frac{1}{2} \sum_{n=1}^{\infty} (\partial_{\mu} A_{(n)5})^2 + \sum_{n=1}^{\infty} \frac{n}{R} A_{(n)}^{\mu} \partial_{\mu} A_{(n)5}, \end{aligned} \quad (7.19)$$

where $\tilde{r}_c = r_c/2\pi R$. Focusing on the vector modes in the first line, this can be recast into

$$\mathcal{L}(x) \supset -\frac{1}{4} \sum_{m,n=0}^{\infty} F_{(n)\mu\nu} K_{nm} F_{(m)}^{\mu\nu} + \frac{1}{2} \sum_{m,n=0}^{\infty} A_{(n)\mu} (M_A^2)_{nm} A_{(m)}^{\mu}, \quad (7.20)$$

where the vector-boson mass matrix M_A^2 is diagonal with $(M_A^2)_{nn} = n^2/R^2$. In contrast to the mixing introduced by a Higgs boson VEV on the brane, the mixing between Fourier modes is found in the kinetic matrix

$$K = \begin{pmatrix} 1 + \tilde{r}_c & \sqrt{2}\tilde{r}_c & \sqrt{2}\tilde{r}_c & \cdots \\ \sqrt{2}\tilde{r}_c & 1 + 2\tilde{r}_c & 2\tilde{r}_c & \cdots \\ \sqrt{2}\tilde{r}_c & 2\tilde{r}_c & 1 + 2\tilde{r}_c & \cdots \\ \vdots & \vdots & \vdots & \ddots \end{pmatrix}. \quad (7.21)$$

To diagonalize the complete Lagrangian, it is extremely useful to define the rescaled fields $\tilde{A}_{(n)}^{\mu} = n A_{(n)}^{\mu}$ for $(n \geq 1)$. For the zero mode we introduce an infinitesimal mass ϵ^2/R^2

and take the limit $\epsilon \rightarrow 0$ in the end. Thus, we can define $\tilde{A}_{(0)}^\mu = \epsilon A_{(0)}^\mu$ and obtain a mass matrix $\tilde{M}_A^2 = \mathbb{1}/R^2$ being proportional to the unit matrix $\mathbb{1}$. Hence, any basis rotation is trivial for the mass terms. Furthermore, the rescaling allows for diagonalizing the kinetic part because the zeros of the characteristic polynomial of the rescaled kinetic matrix

$$\tilde{K} = \begin{pmatrix} (1 + \tilde{r}_c)/\epsilon^2 & \sqrt{2}\tilde{r}_c/\epsilon & \sqrt{2}\tilde{r}_c/(2\epsilon) & \cdots \\ \sqrt{2}\tilde{r}_c/\epsilon & (1 + 2\tilde{r}_c) & 2\tilde{r}_c/2 & \cdots \\ \sqrt{2}\tilde{r}_c/(2\epsilon) & 2\tilde{r}_c/2 & (1 + 2\tilde{r}_c)/4 & \cdots \\ \vdots & \vdots & \vdots & \ddots \end{pmatrix} \quad (7.22)$$

become calculable. Hence, we find the eigenvalue equation

$$\det(K - \lambda\mathbb{1}) = \prod_{n=1}^{\infty} \left(\frac{1}{n^2} - \lambda \right) \frac{1}{\epsilon^2} \left[\tilde{r}_c + \left(1 + 2\tilde{r}_c \sum_{n=1}^{\infty} \frac{1/n^2}{1/n^2 - \lambda} \right) (1 - \epsilon^2\lambda) \right] = 0. \quad (7.23)$$

In the limit $\epsilon \rightarrow 0$, the eigenvalues are given by

$$\frac{\tilde{r}_c}{\sqrt{\lambda}}\pi = -\tan\left(\frac{\pi}{\sqrt{\lambda}}\right), \quad (7.24)$$

where we have again analytically performed the infinite sum (cf. Appendix A). Working in the basis where the rescaled kinetic matrix is diagonal, the masses of the KK modes are found by rescaling the fields such that $K = \mathbb{1}$. Note that the mass matrix will still be diagonal. Hence, the masses are given by $m_{(n)} = 1/(\sqrt{\lambda}R)$. Expressing (7.24) in terms of $m_{(n)}$ and r_c , one indeed recovers (7.16).

The eigenvectors E^λ can be found from an ansatz $E^\lambda = (1, E_j^\lambda)$ for each eigenvalue λ . Using (7.23) and Cramer's rule to solve the system of equations for the components of E^λ , one finds

$$\tilde{E}_j^\lambda = -\frac{\sqrt{2}}{\epsilon} \frac{\tilde{r}_c/j}{1/j^2 - \lambda} \quad \text{and} \quad \tilde{E}_j^\lambda = \frac{\sqrt{2}}{\epsilon} \frac{1/j}{1/j^2 - \lambda}, \quad (7.25)$$

for the zero and higher mass eigenstates, respectively. Note that for the zero mass eigenstate the terms quadratic in ϵ in (7.23) are important because $\lambda \propto 1/\epsilon^2$. Thus, the mass eigenstates $\hat{A}_{(n)}^\mu$ are given by

$$\begin{aligned} \hat{A}_{(n)}^\mu &= \frac{N}{Rm_{(n)}} \left[\tilde{A}_{(0)}^\mu + \sum_{j=1}^{\infty} \frac{\sqrt{2}}{\epsilon} \frac{(-\tilde{r}_c)^{\delta_{n,0}}/j}{1/j^2 - 1/(R^2m_{(n)}^2)} \tilde{A}_{(j)}^\mu \right] \\ &= \frac{N}{Rm_{(n)}} \left[\epsilon A_{(0)}^\mu + \sum_{j=1}^{\infty} \frac{\sqrt{2}}{\epsilon} \frac{(-\tilde{r}_c)^{\delta_{n,0}}}{1/j^2 - 1/(R^2m_{(n)}^2)} A_{(j)}^\mu \right], \end{aligned} \quad (7.26)$$

where $N^{-2} = (E^\lambda)^2$. The overall factor $1/Rm_{(n)}$ stems from the final rescaling of the mass eigenstates. In the limit $\epsilon \rightarrow 0$, one finds for the massless mode $m_{(0)} \rightarrow \epsilon/(\sqrt{1 + \tilde{r}_c}R)$ and

$N \rightarrow 1$. For the massive modes we have $N \propto \epsilon$. Consequently, the mass eigenstates are given by

$$\begin{aligned}\hat{A}_{(0)}^\mu &= \sqrt{1 + \tilde{r}_c} A_{(0)}^\mu + \sum_{j=1}^{\infty} \frac{\sqrt{2}\tilde{r}_c}{\sqrt{1 + \tilde{r}_c}} A_{(j)}^\mu, \\ \hat{A}_{(n)}^\mu &= - \left[\frac{1}{4\tilde{r}_c} + \frac{\pi^2}{4} m_{(n)}^2 R^2 + \frac{1}{4\tilde{r}_c^2} \right]^{-1/2} \sum_{j=1}^{\infty} \frac{j^2}{m_{(n)}^2 R^2 - j^2} A_{(j)}^\mu,\end{aligned}\tag{7.27}$$

where we have included a global minus sign in the definition for the heavy mass eigenstates ($n \geq 1$) in order to recover $\hat{A}_{(n)}^\mu = A_{(n)}^\mu$ in the limit $\tilde{r}_c \rightarrow 0$. To express interactions in terms of the mass eigenstates the inverse transformation is needed. Due to the rescalings, the two basis sets are not related by an orthogonal basis transformation and we explicitly give the gauge eigenbasis

$$\begin{aligned}A_{(0)}^\mu &= \frac{1}{\sqrt{1 + \tilde{r}_c}} \hat{A}_{(0)}^\mu - \sum_{n=1}^{\infty} \frac{1}{\sqrt{2}} \left[\frac{1}{4\tilde{r}_c} + \frac{\pi^2}{4} m_{(n)}^2 R^2 + \frac{1}{4\tilde{r}_c^2} \right]^{-1/2} \hat{A}_{(n)}^\mu, \\ A_{(j)}^\mu &= - \sum_{n=1}^{\infty} \left[\frac{1}{4\tilde{r}_c} + \frac{\pi^2}{4} m_{(n)}^2 R^2 + \frac{1}{4\tilde{r}_c^2} \right]^{-1/2} \frac{m_{(n)}^2 R^2}{m_{(n)}^2 R^2 - j^2} \hat{A}_{(n)}^\mu\end{aligned}\tag{7.28}$$

in terms of the mass eigenstates. To compare (7.28) to our previous result for the mass-eigenstate wave function (7.17), one has to project the wave functions (7.17) onto the normalized Fourier modes, i.e.

$$\hat{T}_{mn} = \int_{-\pi R}^{\pi R} dy f_{(n)}(y) \frac{\sqrt{2}^{1-\delta_{m,0}}}{\sqrt{2\pi R}} \cos\left(\frac{m}{R}y\right).\tag{7.29}$$

A simple calculation shows that the coefficients \hat{T}_{mn} in (7.29) are indeed identical to those in $A_{(m)}^\mu = \hat{T}_{mn} \hat{A}_{(n)}^\mu$ to be read off from (7.28). Equivalently, one can check that the coefficients

$$T_{mn} = \int_{-\pi R}^{\pi R} dy (1 + r_c \delta(y)) f_{(m)}(y) \frac{\sqrt{2}^{1-\delta_{n,0}}}{\sqrt{2\pi R}} \cos\left(\frac{n}{R}y\right)\tag{7.30}$$

are the same as in $\hat{A}_{(m)}^\mu = T_{mn} A_{(n)}^\mu$ given by (7.27). Note that $T^T \neq \hat{T}$ due to the different scalar products to be used for the projections. As a final result, the two methods applied for calculating the spectrum and the mass eigenstates are compatible.

7.1.2 Gauge Fixing

Knowing the spectrum and the eigenstates of the vector bosons let us investigate the gauge fixing which is also affected by the brane kinetic terms in a non-trivial way. In terms of

Fourier modes, the mixing terms in (7.19) are given by

$$\mathcal{L} \supset \sum_{n=1}^{\infty} \frac{n}{R} A_{(n)}^{\mu} \partial_{\mu} A_{(n)5} \quad (7.31)$$

as in (2.8). To express the mixing in terms of the mass eigenstates it is convenient to make the rescalings explicit, i.e.

$$A_{(n)}^{\mu} = \sum_{m=0}^{\infty} \hat{T}_{nm} \hat{A}_{(m)}^{\mu} = \sum_{m=0}^{\infty} (S^{-1} D \hat{S})_{nm} \hat{A}_{(m)}^{\mu}, \quad (7.32)$$

where $S = \text{diag}(\epsilon, 1, 2, \dots)$, $\hat{S} = \text{diag}(Rm_{(n)})$, and D denotes the orthogonal transformation calculated from the eigenvectors (7.25). Thus, we find

$$\mathcal{L} \supset \sum_{m,n=1}^{\infty} m_{(m)} \hat{A}_{(m)}^{\mu} D_{nm} \partial_{\mu} A_{(n)5}, \quad (7.33)$$

where we have used that the $m = 0$ term in (7.32) does not contribute for $n \geq 1$ (see (7.28)). Hence, the gauge-fixing for KK mode m should have the form

$$\mathcal{L}_{\text{GF}}^{(m)} = -\frac{1}{2\xi} \left(\partial_{\mu} \hat{A}_{(m)}^{\mu} - \xi m_{(m)} \sum_{n=1}^{\infty} D_{mn}^T A_{(n)5} \right)^2, \quad (7.34)$$

in order to remove the mixing terms. Consequently, the Lagrangian \mathcal{L}_{GB} for the scalar would-be Goldstone modes is given by

$$\mathcal{L}_{\text{GB}} = \frac{1}{2} \sum_{n=1}^{\infty} (\partial_{\mu} A_{(n)5})^2 - \frac{\xi}{2} \sum_{k,m,n=1}^{\infty} A_{(k)5} D_{km} m_{(m)}^2 D_{mn}^T A_{(n)5}. \quad (7.35)$$

At this point, it is trivial to determine the Goldstone-boson mass eigenstates $\hat{G}_{(n)}$ with gauge dependent masses $\sqrt{\xi} m_{(n)}$, where $m_{(n)}$ is the corresponding vector-boson mass. The transformation matrix D is not only orthogonal but in the limit $\epsilon \rightarrow 0$ also block diagonal such that the submatrix of D acting on the higher KK modes ($n \geq 1$) is also orthogonal. Thus, we find

$$\mathcal{L}_{\text{GB}} = \frac{1}{2} \sum_{n=1}^{\infty} (\partial_{\mu} \hat{G}_{(n)})^2 - \frac{\xi}{2} \sum_{n=1}^{\infty} m_{(n)}^2 \hat{G}_{(n)}^2, \quad (7.36)$$

where $\hat{G}_{(n)} = \sum_{j=1}^{\infty} D_{nj}^T A_{5(j)}$, i.e.

$$\hat{G}_{(n)} = - \sum_{j=1}^{\infty} \left[\frac{1}{4\tilde{r}_c} + \frac{\pi^2}{4} m_{(n)}^2 R^2 + \frac{1}{4\tilde{r}_c^2} \right]^{-1/2} \frac{j m_{(n)} R}{m_{(n)}^2 R^2 - j^2} A_{5(j)}. \quad (7.37)$$

At this point the mass eigenstates and corresponding Goldstone modes are identified in the effective 4D theory. Their interactions (e.g. self-interactions in a non-Abelian model, or couplings to fermions) can be worked out by means of the basis transformations.

Additionally, we now show that the above gauge fixing can also be formulated in the 5D model before integrating out the extra dimension. Since the brane kinetic terms in the Lagrangian lead to a non-homogeneous weight function for the field strength of the vector bosons with respect to the extra dimension, this inhomogeneity forces us to choose a y -dependent gauge-fixing parameter

$$\frac{1}{\xi(y)} = \frac{1}{\xi'} (1 + r_c \delta(y)) , \quad (7.38)$$

where ξ' is y -independent. With the choice (7.38), in analogy to (2.10), the gauge-fixing Lagrangian reads

$$\begin{aligned} \mathcal{L}_{\text{GF}} &= - \int_0^{2\pi R} dy \frac{1}{2\xi(y)} (\partial_\mu A^\mu(y) - \xi(y) \partial_5 A_5(y))^2 \\ &= - \frac{1}{2\xi'} \int_0^{2\pi R} dy (1 + r_c \delta(y)) (\partial_\mu A^\mu(y))^2 \\ &\quad + \int_0^{2\pi R} dy (\partial_\mu A^\mu(y)) (\partial_5 A_5(y)) \\ &\quad - \frac{\xi'}{2} \int_0^{2\pi R} dy \frac{1}{1 + r_c \delta(y)} (\partial_5 A_5(y))^2 . \end{aligned} \quad (7.39)$$

Expanding the vector boson field according to (7.8), the first line in (7.39) simply adds the typical gauge-fixing terms for each gauge-boson mode to the first line in (7.9). Thus, the calculation of the spectrum is not modified by the above gauge fixing. In particular, unwanted gauge-dependent mixing between mass eigenstates is avoided. The second line is equivalent to the simple 5D-QED case in Chapter 2 and removes the mixing between the vector modes and the scalars. No new mixing terms are generated. The third line provides the correct mass term for the Goldstone modes. However, this is far from obvious because of the δ -function in the denominator.

As we have already seen in (7.37), the would-be Goldstone modes in 5D-QED with brane kinetic terms are no longer the simple Fourier modes of the scalar gauge-field component A_5 . Thus, in analogy to (7.8), we expand the scalar field according to

$$A_5 = \sum_{n=1}^{\infty} \hat{G}_{(n)}(x) g_{(n)}(y) , \quad (7.40)$$

where $g_{(n)}(y)$ denote the proper wave functions for the would-be Goldstone mass eigenstates $\hat{G}_{(n)}$. In terms of (7.40) the Goldstone Lagrangian reads

$$\begin{aligned} \mathcal{L} &= \frac{1}{2} (\partial_\mu \hat{G}_{(n)}) (\partial^\mu \hat{G}_{(m)}) \int_0^{2\pi R} dy g_{(n)} g_{(m)} \\ &\quad - \frac{\xi'}{2} \hat{G}_{(n)} \hat{G}_{(m)} \int_0^{2\pi R} dy \frac{1}{1 + r_c \delta(y)} (\partial_5 g_{(n)}) (\partial_5 g_{(m)}) . \end{aligned} \quad (7.41)$$

In analogy to (7.10), one would like to partially integrate the second line. However, the δ -function complicates the calculation. Hence, we instead partially integrate the first term in (7.41) and find

$$\begin{aligned} \mathcal{L} = & -\frac{1}{2} \left(\partial_\mu \hat{G}_{(n)} \right) \left(\partial^\mu \hat{G}_{(m)} \right) \int_0^{2\pi R} dy \left(\partial_5 g_{(n)} \right) \tilde{g}_{(m)} \\ & - \frac{\xi'}{2} \hat{G}_{(n)} \hat{G}_{(m)} \int_0^{2\pi R} dy \frac{1}{1 + r_c \delta(y)} \left(\partial_5 g_{(n)} \right) \left(\partial_5 g_{(m)} \right), \end{aligned} \quad (7.42)$$

where \tilde{g} is the primitive of g and the surface terms are again assumed to vanish. Thus, the wave functions should obey

$$\frac{\partial_5 g_{(m)}}{1 + r_c \delta(y)} = -m_{(m)}^2 \tilde{g}_{(m)} \quad (7.43)$$

or equivalently

$$\partial_5^2 \tilde{g}_{(m)} = -m_{(m)}^2 [1 + r_c \delta(y)] \tilde{g}_{(m)}. \quad (7.44)$$

Hence, the primitive of the wave function has to obey the same differential equation with the same boundary conditions as the wave function for the gauge modes (cf. (7.12) and (7.13)). In particular, \tilde{g} is even because g has to be odd due to the odd Z_2 parity of the scalar gauge field component. Also note that g is discontinuous at $y = 0$. The mass eigenvalues are of course given by (7.16). Using (7.44) in (7.42), we indeed find

$$\mathcal{L} = \left(\frac{1}{2} \left(\partial_\mu \hat{G}_{(n)} \right) \left(\partial^\mu \hat{G}_{(m)} \right) - \frac{\xi'}{2} m_{(m)}^2 \hat{G}_{(n)} \hat{G}_{(m)} \right) \int_0^{2\pi R} dy m_{(m)}^2 [1 + r_c \delta(y)] \tilde{g}_{(n)} \tilde{g}_{(m)}. \quad (7.45)$$

Hence, using the orthogonality of the functions $\tilde{g}_{(n)}$ and normalizing them such that the overall factor $m_{(m)}^2$ vanishes, i.e.

$$\tilde{g}_{(n)} = -\frac{1}{m_{(n)}} f_{(n)}, \quad (7.46)$$

we again arrive at the Lagrangian (7.36). As a consistency check, we have to show that the wave function $g_{(n)}$ coincide with the Fourier decomposition already found in (7.37). Hence, we project the wave function onto Fourier modes, i.e.

$$\begin{aligned} T_{mn} = & \int_0^{2\pi R} dy [1 + r_c \delta(y)] g_{(n)} \frac{\sin\left(\frac{m}{R}y\right)}{\sqrt{2\pi R}} = \int_0^{2\pi R} dy g_{(n)} \frac{\sin\left(\frac{m}{R}y\right)}{\sqrt{2\pi R}} \\ & = \frac{m/R}{m_{(n)}} \int_0^{2\pi R} dy f_{(n)} \frac{\cos\left(\frac{m}{R}y\right)}{\sqrt{2\pi R}}. \end{aligned} \quad (7.47)$$

The first equality is due to the antisymmetry of the wave functions and assures that there is an orthogonal transformation between the Goldstone and the Fourier modes. In contrast to the vector-boson sector, there are no rescalings involved, i.e. $T = \hat{T}^T$. In the second

step we have used partial integration and (7.46). Taking into account the factor in front of the integral, one finds exactly the result $T_{mn} = D_{mn}^T$ as in (7.34).

Finally, we show how to recover the Goldstone Lagrangian in the effective 4D theory using a Fourier decomposition of the scalar field. To deal with the δ -function in the denominator, it is convenient to rewrite the last line in (7.39) according to

$$\mathcal{L} \supset -\frac{\xi'}{2} \int_0^{2\pi R} dy \frac{1}{1+r_c \delta(y)} (\partial_5 A_5(y))^2 = -\frac{\xi'}{2} \int_0^{2\pi R} dy \left(1 - \frac{r_c \delta(y)}{1+r_c \delta(y)}\right) (\partial_5 A_5(y))^2. \quad (7.48)$$

Integrating out the extra dimension, the mass matrix reads

$$M_{5kl}^2 = \xi' \left(\frac{k^2}{R^2} \delta_{k,l} - \frac{r_c}{\pi R} \frac{1}{1+\delta(0)r_c} \frac{kl}{R^2} \right), \quad (7.49)$$

where k, l refer to the Fourier mode numbers. At this point, it is instructive to regularize the δ -function by using its representation (2.41) and analyzing a model which is truncated at a given mode number n . In the end, we consider the limit $n \rightarrow \infty$. The regularized mass matrix is given by

$$M_{5kl}^2 = \xi' \left(\frac{k^2}{R^2} \delta_{k,l} - \frac{r_c}{\pi R} \frac{1}{1 + \left(\frac{1}{2\pi R} + \sum_1^n \frac{1}{\pi R}\right) r_c} \frac{kl}{R^2} \right) = \xi' \left(\frac{k^2}{R^2} \delta_{k,l} - \frac{2\tilde{r}_c}{1 + (2n+1)\tilde{r}_c} \frac{kl}{R^2} \right) \quad (7.50)$$

and has to be compared to the Fourier-mode mass matrix in (7.35) for the truncated model. For a limited number of modes, it is hard to perform analytic calculations because we cannot use the techniques for calculating infinite sums. However, a truncated model is well suited for numerical computations. Such a computation shows that the two mass matrices indeed agree for any $n < 50$ where the matrices can be easily handled. Note that the underlying one-to-one correspondence between the masses of the gauge-boson modes and the Goldstone modes is still exact in the truncated model because the truncated Abelian model is still a gauge theory.

Taking the limit $n \rightarrow \infty$, the off-diagonal elements of the mass matrix (7.50) converge to zero for any k and l . Hence, in contrast to what we have found before, one could think that the Fourier modes are still mass eigenstates and the gauge-fixing procedure is inconsistent. However, there is no uniform convergence to a diagonal matrix because of the factors k and l in the numerator of (7.50). Thus, the basis rotation to the mass eigenstates does not have to converge to the unit matrix either. In Appendix A, we explicitly show how to perform the infinite sum over m in (7.35) [98]. We also show that the basis rotation D indeed transforms the diagonal matrix of KK masses $m_{(n)}^2$ into the diagonal matrix recovered from (7.50) in the naive limit $n \rightarrow \infty$ and vice versa. In a finite dimensional vector space, this is not possible. Here, as expected from our earlier calculations, the orthogonal basis

transformation D turns out to be the correct $n \rightarrow \infty$ limit of basis transformations from the Fourier basis to the mass basis. However, the same transformation in the vector-boson sector is completely unphysical. Hence, basis rotations in an infinitely dimensional vector space have to be handled with great care and should be questioned by a suitable limit from a truncated model, as introduced above.

7.1.3 Brane Kinetic Terms for Both S^1/Z_2 Branes

For simplicity, we have ignored brane kinetic terms on the second brane of the S^1/Z_2 orbifold, so far. In the general case, the Lagrangian of 5D-QED reads

$$\mathcal{L}(x, y) = -\frac{1}{4}F_{MN}(x, y)F^{MN}(x, y) - (r_0\delta(y) + r_\pi\delta(y - \pi R))\frac{1}{4}F_{MN}(x, y)F^{MN}(x, y), \quad (7.51)$$

Repeating the arguments from the beginning of Section 7.1.1, one obtains the differential equation

$$\partial_5^2 f_{(n)}(y) = -m_{(n)}^2 f_{(n)}(y) [1 + r_0\delta(y) + r_\pi\delta(y - \pi R)] \quad (7.52)$$

for the wave functions of the gauge-boson mass eigenstates. As already shown in [52], the corresponding transcendental equation for the KK masses is given by

$$\frac{m_{(n)}(r_0 + r_\pi)}{2} = \left(\frac{m_{(n)}^2 r_0 r_\pi}{4} - 1 \right) \tan(m_{(n)}\pi R), \quad (7.53)$$

while (7.17) still holds for the wave functions with the different normalization

$$N_{(n)} = \frac{1}{\sqrt{2}^{\delta_{n,0}}} \left[\pi R + r_0 + \frac{\pi}{4} R m_{(n)}^2 r_0^2 + r_\pi \cos^2(m_{(n)}\pi R) + \left(r_\pi \frac{m_{(n)}^2 r_0^2}{4} - r_0 \right) \sin^2(m_{(n)}\pi R) + \left(\frac{1}{m_{(n)}} - \frac{1}{4} m_{(n)} r_0^2 + m_{(n)} r_0 r_\pi \right) \cos(m_{(n)}\pi R) \sin(m_{(n)}\pi R) \right]^{-1/2}. \quad (7.54)$$

In (7.54), the transcendental eigenvalue equation (7.53) cannot be used to substantially simplify N as it is possible for $r_\pi = 0$. The same is true if the mass eigenstates are expressed in terms of Fourier modes and vice versa in analogy to (7.27) and (7.28). Thus, we do not state them explicitly although they can be easily computed using (7.29) and (7.30). Expanding in Fourier modes and diagonalizing the kinetic matrix is even more tedious. For kinetic terms on both branes, a detailed analysis on non-Abelian models without spontaneous symmetry breaking in unitary gauge can be found in [52]. To put forward the necessary generalizations of 5D-QED to the standard model case, we return to the simpler setup $r_\pi = 0$.

7.2 Spontaneous Symmetry Breaking

We now turn our attention to spontaneous symmetry breaking in the presence of brane kinetic terms at $y = 0$. Breaking the symmetry by a VEV of a Higgs field localized on the same brane introduces an additional mass term for the gauge field. The gauge part of the corresponding Lagrangian is then given by

$$\mathcal{L}(x, y) = -\frac{1}{4}F_{MN}F^{MN} - r_c \delta(y) \frac{1}{4}F_{MN}F^{MN} + \frac{(ve_5)^2}{2} \delta(y) A^\mu A_\mu. \quad (7.55)$$

In analogy to (7.12), the differential equation for the gauge-boson wave functions reads

$$\partial_5^2 f_{(n)}(y) - 2\pi R \delta(y) e^2 v^2 f_{(n)}(y) = -m_{(n)}^2 f_{(n)}(y) [1 + r_c \delta(y)], \quad (7.56)$$

where again $e = e_5/\sqrt{2\pi R}$ has been used. It can be solved along the lines presented in Section 7.1.1 and leads to the eigenvalue equation

$$\frac{m_{(n)} r_c}{2} \left(1 - \frac{e^2 v^2}{\tilde{r}_c m_{(n)}^2} \right) = -\tan(m_{(n)} \pi R) \quad (7.57)$$

and the wave functions

$$f_{(n)}(y) = \frac{N_{(n)}}{\sqrt{2\pi R}} \left[\cos(m_{(n)} y) \pm \frac{m_{(n)} r_c}{2} \left(1 - \frac{e^2 v^2}{\tilde{r}_c m_{(n)}^2} \right) \sin(m_{(n)} y) \right], \quad (7.58)$$

where

$$N_{(n)} = \sqrt{2} \left[1 + \pi^2 R^2 \tilde{r}_c^2 m_{(n)}^2 \left(1 - \frac{e^2 v^2}{\tilde{r}_c m_{(n)}^2} \right)^2 + \tilde{r}_c + \frac{e^2 v^2}{m_{(n)}^2} \right]^{-1/2}. \quad (7.59)$$

Since we need the Fourier modes in terms of the mass eigenstates for the investigation of the Goldstone-boson sector, we state explicitly

$$\begin{aligned} A_{(0)}^\mu &= \hat{T}_{0n} \hat{A}_{(n)}^\mu = - \sum_{n=0}^{\infty} N_{(n)} \frac{\tilde{r}_c m_{(n)}^2 - e^2 v^2}{m_{(n)}^2} \hat{A}_{(n)}^\mu, \\ A_{(j)}^\mu &= \hat{T}_{jn} \hat{A}_{(n)}^\mu = - \sum_{n=0}^{\infty} \sqrt{2} N_{(n)} \frac{\tilde{r}_c m_{(n)}^2 - e^2 v^2}{m_{(n)}^2 - j^2/R^2} \hat{A}_{(n)}^\mu, \end{aligned} \quad (7.60)$$

where (7.29) has been used. Calculating the mass eigenstates from a Fourier-mode expansion is difficult because there are mixing effects in the kinetic as well as in the mass matrix. There is no simple rescaling that transforms the mass matrix into a multiple of the unit matrix. Consequently, two successive diagonalizations would have to be performed.

Let us identify the Goldstone modes of this model. As in Chapter 2, there are additional mixing terms because the scalar brane mode also mixes with the gauge fields, i.e.

$$\mathcal{L} \supset \sum_{n=0}^{\infty} \sqrt{2}^{1-\delta_{n,0}} ev A_{(n)}^{\mu} \partial_{\mu} \chi + \sum_{n=1}^{\infty} \frac{n}{R} A_{(n)}^{\mu} \partial_{\mu} A_{(n)5}. \quad (7.61)$$

With the help of (7.60), the Goldstone modes $\hat{G}_{(n)}$ can be identified by their mixing with the mass eigenstates, that is

$$\mathcal{L} \supset \sum_{m=0}^{\infty} \hat{A}_{(m)}^{\mu} \partial_{\mu} \left[\left(\hat{T}_{0m} + \sum_{n=1}^{\infty} \sqrt{2} \hat{T}_{nm} \right) ev \chi + \sum_{n=1}^{\infty} \frac{n}{R} \hat{T}_{nm} A_{(n)5} \right]. \quad (7.62)$$

Calculating the infinite sum in the coefficient of χ , the Goldstone modes are given by

$$\hat{G}_{(m)} = \frac{1}{m_{(n)}} \left[ev N_{(m)} \chi + \sum_{n=1}^{\infty} \frac{n}{R} \hat{T}_{nm} A_{(n)5} \right]. \quad (7.63)$$

Following the steps of Section 7.1.2, the orthonormality of the transformation (7.63) can be shown in a quite tedious calculation. Consequently, gauge fixing mode by mode in the effective 4D model leads to the usual one-to-one correspondence between the Goldstone KK masses and the masses of the KK gauge bosons.

If brane kinetic terms of a bulk Higgs field $\Phi(x, y)$ are ignored spontaneous symmetry breaking in the bulk does not induce any additional mixing effects in the gauge sector. However, this is an arbitrary assumption and one should also allow BKTs for the scalar field. The corresponding Lagrangian is then given by

$$\mathcal{L}(x, y) = (D_M \Phi)^* (D^M \Phi) + r_{\Phi} \delta(y) (D_M \Phi)^* (D^M \Phi) - V(\Phi). \quad (7.64)$$

For a non-mode VEV v_5 of the scalar, there is not only a bulk mass term for the gauge boson but also a brane mass term due to the brane kinetic term. Thus, the gauge sector reads

$$\mathcal{L}(x, y) = -\frac{1}{4} F_{MN} F^{MN} - r_c \delta(y) \frac{1}{4} F_{MN} F^{MN} + \frac{(v_5 e_5)^2}{2} (1 + r_{\Phi} \delta(y)) A^{\mu} A_{\mu}, \quad (7.65)$$

and the corresponding differential equation for the wave functions of the mass eigenstates is given by

$$\partial_5^2 f_{(n)}(y) - r_{\Phi} \delta(y) e^2 v^2 f_{(n)}(y) - e^2 v^2 f_{(n)}(y) = -m_{(n)}^2 f_{(n)}(y) [1 + r_c \delta(y)], \quad (7.66)$$

where we have used $e_5 v_5 = ev$. Consequently, we find the eigenvalue equation

$$\frac{m_{(n)}^2 r_c}{2(m_{(n)}^2 - e^2 v^2)^{1/2}} \left(1 - \frac{\tilde{r}_{\Phi} e^2 v^2}{\tilde{r}_c m_{(n)}^2} \right) = -\tan((m_{(n)}^2 - e^2 v^2)^{1/2} \pi R), \quad (7.67)$$

and the wave functions

$$f_{(n)}(y) = \frac{N_{(n)}}{\sqrt{2\pi R}} \left[\cos((m_{(n)}^2 - e^2 v^2)^{1/2} y) \pm \frac{m_{(n)}^2 r_c}{2(m_{(n)}^2 - e^2 v^2)^{1/2}} \left(1 - \frac{\tilde{r}_\Phi e^2 v^2}{\tilde{r}_c m_{(n)}^2} \right) \sin((m_{(n)}^2 - e^2 v^2)^{1/2} y) \right], \quad (7.68)$$

where

$$N_{(n)} = \sqrt{2} \left[1 + 2\tilde{r}_c + \pi^2 R^2 \tilde{r}_c^2 \frac{m_{(n)}^4}{m_{(n)}^2 - e^2 v^2} \left(1 - \frac{\tilde{r}_\Phi e^2 v^2}{\tilde{r}_c m_{(n)}^2} \right)^2 - \tilde{r}_c \frac{m_{(n)}^2}{m_{(n)}^2 - e^2 v^2} \left(1 - \frac{\tilde{r}_\Phi e^2 v^2}{\tilde{r}_c m_{(n)}^2} \right) \right]^{-1/2}. \quad (7.69)$$

Let us now turn to the scalar sector of the model. In addition to the would-be Goldstone modes, there are massive physical CP-odd scalars. It is essential for the interpretation of the model to prove that the scalar sector can still be divided into its physical part with massive scalars and the would-be Goldstone modes being massless before gauge fixing. To show this, notice that the CP-odd part of the Higgs field $\chi(x, y)$ is affected by its brane kinetic term in complete analogy to the gauge fields. In terms of the Fourier modes, the states diagonalizing the kinetic matrix are given by

$$\hat{\chi}_{(n)} = T_{nm}^\Phi \chi_{(m)}, \quad (7.70)$$

where T_{nm}^Φ is given by (7.27) or (7.30) with r_c replaced by r_Φ . Thus, the bilinear terms of the scalar sector can be given in the following compact notation:

$$\mathcal{L}^{(n)} = \frac{1}{2} (\partial_\mu \hat{\chi}_{(n)})^2 + \frac{1}{2} (\partial_\mu A_{5(n)})^2 + \frac{1}{2} \begin{pmatrix} A_{5(n)} \\ \chi_{(n)} \end{pmatrix} \begin{pmatrix} e^2 v^2 & -ev \frac{n}{R} \\ -ev \frac{n}{R} & (\frac{n}{R})^2 \end{pmatrix} \begin{pmatrix} A_{5(n)} \\ \chi_{(n)} \end{pmatrix}. \quad (7.71)$$

Using $\chi_{(n)} = T_{nm}^{\Phi^{-1}} \hat{\chi}_{(m)} = \hat{T}_{nm}^\Phi \hat{\chi}_{(m)}$ and $\hat{T}_{nm}^\Phi = (S^{-1} D^\Phi \hat{S})_{nm}$ as given in (7.32), one finds

$$\mathcal{L}^{(n)} = \frac{1}{2} (\partial_\mu \hat{\chi}_{(n)})^2 + \frac{1}{2} (\partial_\mu \hat{A}_{5(n)})^2 + \frac{1}{2} \begin{pmatrix} \hat{A}_{5(n)} \\ \hat{\chi}_{(n)} \end{pmatrix} \begin{pmatrix} e^2 v^2 & -ev m_{\Phi(n)} \\ -ev m_{\Phi(n)} & m_{\Phi(n)}^2 \end{pmatrix} \begin{pmatrix} \hat{A}_{5(n)} \\ \hat{\chi}_{(n)} \end{pmatrix}, \quad (7.72)$$

where we have defined $\hat{A}_{5(n)} = D_{nm}^{\Phi T} A_{5(m)}$. The masses $m_{\Phi(n)}$ are given by the transcendental equation (7.16) with r_c replaced by r_Φ . By construction, also for the hatted modes only those with the same KK number mix. Thus, in analogy to (2.24), we can now define

$$G_{(n)} = \left(m_{\Phi(n)}^2 + e^2 v^2 \right)^{-1/2} \left(m_{\Phi(n)} \hat{A}_{(n)5} + ev \hat{\chi}_{(n)} \right), \quad (7.73)$$

$$a_{(n)} = \left(m_{\Phi(n)}^2 + e^2 v^2 \right)^{-1/2} \left(ev \hat{A}_{(n)5} - m_{\Phi(n)} \hat{\chi}_{(n)} \right).$$

The modes $G_{(n)}$ ($n \geq 0$) are massless before gauge fixing and the would-be Goldstone mass eigenstates have to be linear combinations of these modes. The modes $a_{(n)}$ ($n \geq 1$) have physical mass terms and have to be interpreted as physical massive scalar particles. The mixing terms between the scalar and the gauge boson sector are given by

$$\mathcal{L} \supset \sum_{n=0}^{\infty} ev A_{(n)}^{\mu} \partial_{\mu} \chi_{(n)} + \tilde{r}_{\Phi} \sum_{m,n=0}^{\infty} \sqrt{2}^{2-\delta_{n,0}-\delta_{m,0}} ev A_{(n)}^{\mu} \partial_{\mu} \chi_{(m)} + \sum_{n=1}^{\infty} \frac{n}{R} A_{(n)}^{\mu} \partial_{\mu} A_{(n)5}. \quad (7.74)$$

Expressing $\chi_{(n)}$ and $A_{5(n)}$ by the hatted modes and using (7.73), one can show that there is indeed no mixing of the gauge bosons with the physical modes $a_{(n)}$, as expected. The modes $G_{(n)}$ mix to form the would-be Goldstone mass eigenstates $\hat{G}_{(n)}$. It is straight-forward to calculate T_{nm}^G in $\hat{G}_{(n)} = T_{nm}^G G_{(m)}$. In a final step, one should again proof that T_{nm}^G is an orthonormal transformation. However, this is not an easy task because T_{nm}^G is a function of $m_{\Phi(m)}$ and $m_{(n)}$, i.e. of the masses of the physical scalars and the gauge bosons, respectively. We set this calculation aside and turn again to more phenomenological aspects.

7.3 Phenomenology

As a toy model, we first investigate the spontaneously broken Abelian U(1) model (7.55) coupled to a fermion on the brane $y = 0$. For simplicity, we again concentrate on a single BKT. The mass of the vector-boson zero mode, given by the transcendental equation (7.57), can be approximately calculated to first order in $X_e = \frac{\pi^2}{3} \frac{e^2 v^2}{M^2}$ by expanding the right hand side to third order in $m_{(0)}R$. One finds

$$m_{(0)}^2 = \frac{e^2 v^2}{1 + \tilde{r}_c} \left(1 - \frac{1}{(1 + \tilde{r}_c)^2} X_e \right). \quad (7.75)$$

Note that, in addition to the shift of order X_e , the brane kinetic term suppresses the zero mode mass. In the limit $\tilde{r}_c = 0$, we recover (2.33). It is, of course, a generic feature of the following calculations that we recover the results of the preceding chapters for vanishing brane kinetic terms. Spontaneous symmetry breaking by the Higgs field on the brane only leads to minor corrections for the masses of the heavy KK modes. Up to $\mathcal{O}(X_e)$ corrections, the masses are still given by Figure 7.3. Using the mode expansion (7.8), the coupling of a KK mode to the brane fermion is directly determined by its wave function at $y = 0$, i.e.

$$e_{(n)} = e N_{(n)}, \quad (7.76)$$

where $N_{(n)}$ is given in (7.59). Working to first order in X_e and using (7.75), one finds for the zero mode coupling

$$e_{(0)} = \frac{e}{\sqrt{1 + \tilde{r}_c}} \left(1 - \frac{1}{(1 + \tilde{r}_c)^2} X_e \right). \quad (7.77)$$

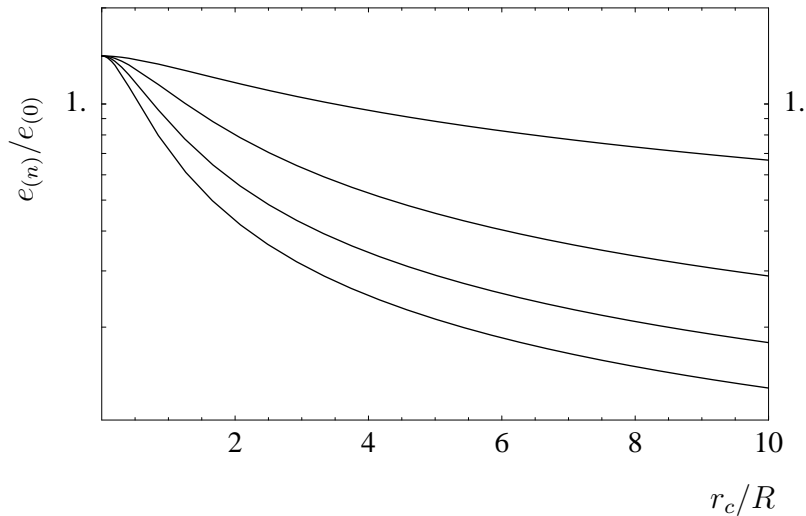


Figure 7.4: Coupling strength (normalized to the zero mode coupling) to a brane fermion for the first 4 heavy KK modes as a function of r_c/R .

In the low-energy limit of the model, the shifts in the mass and the coupling are unobservable. Measuring $m_{(0)}$ and $e_{(0)}$, there is no way to infer the basic parameters e and v . Nevertheless, the above results will be valuable in the following investigation of the SM. As can be seen from (7.76) in combination with (7.59), the brane kinetic terms lead to a suppression of the couplings of the heavy KK modes as displayed in Figure 7.4. At energy scales, where one is sensitive to the higher KK modes, this suppression as well as the reduced KK masses according to Figure 7.3 distinguishes this model from the special case with vanishing brane kinetic terms. Let us finally turn to the phenomenology of the SM extensions of Chapter 3 including brane kinetic terms.

7.3.1 Bulk-Bulk Model with a Brane Higgs

As a direct extension of (3.10), the bulk-bulk model with a brane Higgs is given by the Lagrangian

$$\begin{aligned}
 \mathcal{L}(x, y) = & -\frac{1}{4} B_{MN} B^{MN} - r_1 \delta(y) \frac{1}{4} B_{MN} B^{MN} \\
 & -\frac{1}{4} F_{MN}^a F^{aMN} - r_2 \delta(y) \frac{1}{4} F_{MN}^a F^{aMN} \\
 & + \delta(y) (D_\mu \Phi)^\dagger (D^\mu \Phi) + \mathcal{L}_{\text{GF}}(x, y) + \mathcal{L}_{\text{FP}}(x, y),
 \end{aligned} \tag{7.78}$$

where r_1 and r_2 are the BKTs for the two gauge groups.

As outlined in Section 3.2, the charged and the neutral gauge boson sector can be investigated separately. Concerning the W -boson zero modes, their masses and couplings to

left-handed fermion doublets on the brane are only affected by r_2 . They can be approximately calculated in complete analogy to the Abelian model and read

$$m_{W(0)}^2 = \frac{1}{1 + \tilde{r}_2} \frac{g^2 v^2}{4} \left(1 - \frac{1}{(1 + \tilde{r}_2)^2} \frac{\pi^2 g^2 v^2}{3 \cdot 4M^2} \right) = \frac{\tilde{g}^2 v^2}{4} \left(1 - \frac{1}{1 + \tilde{r}_2} X_{\tilde{g}} \right), \quad (7.79)$$

$$g_{W(0)} = \frac{g}{\sqrt{1 + \tilde{r}_2}} \left(1 - \frac{1}{(1 + \tilde{r}_2)^2} \frac{\pi^2 g^2 v^2}{3 \cdot 4M^2} \right) = \tilde{g} \left(1 - \frac{1}{1 + \tilde{r}_2} X_{\tilde{g}} \right), \quad (7.80)$$

where $\tilde{r}_2 = r_2/(2\pi R)$ and $\tilde{g} = g/\sqrt{1 + \tilde{r}_2}$. Moreover, we have defined

$$X_{\tilde{g}} = \frac{\pi^2 \tilde{g}^2 v^2}{3 \cdot 4M^2}. \quad (7.81)$$

We will see below in (7.98), how $X_{\tilde{g}}$ is related to X as defined in (4.3). In terms of the coupling \tilde{g} , it is quite striking that the shifts of order X for $\tilde{r}_2 = 0$ are suppressed. Such a suppression is a generic feature of brane kinetic terms in models with a Higgs boson on the brane.

Let us now consider the photon and Z -boson sector of the standard model. For $r_1 = r_2$, it is convenient to change basis according to (3.13). In this case, considering only the bilinear terms, the photon sector looks like 5D-QED with a BKT as discussed in Section 7.1. The Z -boson sector looks like the spontaneously broken model in Section 7.2. For $r_1 \neq r_2$, the model is complicated by the fact that the usual basis rotation (3.13) leads to mixing of the gauge fields within the brane kinetic terms. Thus, there is no field combination in 5D which can be associated with the Z boson or the photon. Hence, there is no obvious way to directly derive the mass eigenstates by an expansion like (7.8). Here, we have to combine the calculational tools introduced before.

In the weak A_μ^3, B_μ basis, before integration over the extra dimension the mass matrix is given by

$$M_{A^3 B}^2 = \delta(y) \frac{v^2}{4} \begin{pmatrix} g_5^2 & -g_5 g_5' \\ -g_5 g_5' & g_5'^2 \end{pmatrix}, \quad (7.82)$$

in analogy to the SM. To determine the masses and mass eigenstates we first make use of the results for the Abelian model. For the moment, we ignore the off-diagonal terms in the mass matrix and expand the fields using the wave functions (7.58), where r_c and e are replaced by r_2 and g for the field A_μ^3 and by r_1 and g' for the field B_μ , respectively. Thus, after integration over the extra dimension the mass matrix for the KK modes $(\hat{A}_{(0)\mu}^3, \hat{A}_{(1)\mu}^3, \dots, \hat{B}_{(0)\mu}, \hat{B}_{(1)\mu}, \dots)$ is given by

$$M_{A^3 B}^2 = \begin{pmatrix} \text{Diag}(m_{SU(2)(n)}^2) & M_{kl}^2 \\ M_{lk}^2 & \text{Diag}(m_{U(1)(n)}^2) \end{pmatrix}, \quad (7.83)$$

where $\text{Diag}(m_{SU(2)(n)}^2)$ and $\text{Diag}(m_{U(1)(n)}^2)$ denote the diagonal matrices of the mass eigenvalues given by (7.57), again with the corresponding replacements for the SU(2) and U(1) couplings and BKTs. Using (7.59), the off-diagonal block matrices can be written as

$$M_{kl}^2 = -\frac{gg'v^2}{4} N_{(k)}^{SU(2)} N_{(l)}^{U(1)}. \quad (7.84)$$

At this point of the calculation, the kinetic matrix of the modes is equal to the unit matrix such that we can start to diagonalize the mass matrix. Neglecting any corrections of order m_Z^2/M^2 , the mass matrix of the zero modes $\hat{A}_{(0)\mu}^3$ and $\hat{B}_{(0)\mu}$ reads

$$M_{A^3 B}^2 = \frac{v^2}{4} \begin{pmatrix} \tilde{g}_5^2 & -\tilde{g}_5 \tilde{g}'_5 \\ -\tilde{g}_5 \tilde{g}'_5 & \tilde{g}'_5{}^2 \end{pmatrix}, \quad (7.85)$$

where $\tilde{g} = g/\sqrt{1+\tilde{r}_2}$ and $\tilde{g}' = g'/\sqrt{1+\tilde{r}_2}$. This mass matrix is diagonalized by a basis rotation with the mixing angle

$$\tilde{c}_W^2 = c_W^2 \frac{1+\tilde{r}_1}{1+c_W^2 \tilde{r}_1 + s_W^2 \tilde{r}_2}, \quad (7.86)$$

where c_W is defined in (3.45). Using the mixing angle (7.86) to rotate the $\hat{A}_{(0)\mu}^3$ and $\hat{B}_{(0)\mu}$ modes into the new basis denoted by $\tilde{Z}_{(0)\mu}$ and $\tilde{A}_{(0)\mu}$, we find from (7.83) to first order in

$$\tilde{X} = \frac{\pi^2}{3} \frac{(\tilde{g}^2 + \tilde{g}'^2)v^2}{4M^2} = \frac{\pi^2}{3} \frac{\tilde{m}_Z^2}{M^2} \quad (7.87)$$

the mass matrix elements

$$\begin{aligned} M_{\tilde{Z}_{(0)}\tilde{Z}_{(0)}}^2 &= \tilde{m}_Z^2 \left[1 - \left(\frac{\tilde{c}_W^6}{1+\tilde{r}_2} + 2\frac{\tilde{c}_W^4 \tilde{s}_W^2}{1+\tilde{r}_2} + 2\frac{\tilde{c}_W^2 \tilde{s}_W^4}{1+\tilde{r}_1} + \frac{\tilde{s}_W^6}{1+\tilde{r}_1} \right) \tilde{X} \right], \\ M_{\tilde{Z}_{(0)}\tilde{A}_{(0)}}^2 &= -\tilde{m}_Z^2 \left(\frac{\tilde{c}_W^3 \tilde{s}_W^3}{1+\tilde{r}_2} - \frac{\tilde{c}_W^3 \tilde{s}_W^3}{1+\tilde{r}_1} \right) \tilde{X}, \\ M_{\tilde{A}_{(0)}\tilde{A}_{(0)}}^2 &= \tilde{m}_Z^2 \left(\frac{\tilde{c}_W^4 \tilde{s}_W^2}{1+\tilde{r}_2} + \frac{\tilde{c}_W^2 \tilde{s}_W^4}{1+\tilde{r}_1} \right) \tilde{X}. \end{aligned} \quad (7.88)$$

In the $(\tilde{Z}_{(0)\mu}, \hat{A}_{(1)\mu}^3, \dots, \tilde{A}_{(0)\mu}, \hat{B}_{(1)\mu}, \dots)$ basis, the complete mass matrix is approximately

given by

$$M^2 = \begin{pmatrix} M_{\tilde{Z}(0)\tilde{Z}(0)}^2 & \cdots & \tilde{s}_W^2 \tilde{c}_W M_{\tilde{r}_2(n)}^2 & \cdots & M_{\tilde{Z}(0)\tilde{A}(0)}^2 & \cdots & -\tilde{s}_W \tilde{c}_W^2 M_{\tilde{r}_1(l)}^2 & \cdots \\ \vdots & & & & \vdots & & & \\ \tilde{s}_W^2 \tilde{c}_W M_{\tilde{r}_2(n)}^2 & \text{Diag}(m_{SU(2)(n \geq 1)}^2) & & & -\tilde{s}_W \tilde{c}_W^2 M_{\tilde{r}_2(k)}^2 & & & M_{kl}^2 \\ \vdots & & & & \vdots & & & \\ M_{\tilde{Z}(0)\tilde{A}(0)}^2 & & -\tilde{s}_W \tilde{c}_W^2 M_{\tilde{r}_2(k)}^2 & & M_{\tilde{A}(0)\tilde{A}(0)}^2 & & & -\tilde{s}_W^2 \tilde{c}_W M_{\tilde{r}_1(n)}^2 \\ \vdots & & & & \vdots & & & \\ -\tilde{s}_W \tilde{c}_W^2 M_{\tilde{r}_1(l)}^2 & & M_{lk}^2 & & -\tilde{s}_W^2 \tilde{c}_W M_{\tilde{r}_1(n)}^2 & & \text{Diag}(m_{U(1)(n \geq 1)}^2) & \\ \vdots & & & & \vdots & & & \end{pmatrix}, \quad (7.89)$$

where

$$M_{\tilde{r}_2(n)}^2 = \sqrt{2} \tilde{m}_Z^2 \left(1 + \pi^2 R^2 \left(m_{(n)}^{SU(2)} \right)^2 \frac{\tilde{r}_2^2}{1 + \tilde{r}_2} \right)^{-1/2}, \quad (7.90)$$

$$M_{\tilde{r}_1(n)}^2 = \sqrt{2} \tilde{m}_Z^2 \left(1 + \pi^2 R^2 \left(m_{(n)}^{U(1)} \right)^2 \frac{\tilde{r}_1^2}{1 + \tilde{r}_1} \right)^{-1/2}.$$

In (7.89), only the terms which are important to determine the zero-mode masses and eigenstates to first order in \tilde{X} are kept. The exact diagonalization of (7.89) is more tedious and complicated. Instead, using the hierarchy of the matrix elements, we approximately determine the eigenvector of the Z -boson mass eigenstate to first order in \tilde{X} and find

$$\begin{aligned} \hat{Z}_{(0)\mu} &= \tilde{Z}_{(0)\mu} \\ &- \sum_{n=1}^{\infty} \sqrt{2} \tilde{s}_W^2 \tilde{c}_W \left(1 + \pi^2 R^2 \left(m_{(n)}^{SU(2)} \right)^2 \frac{\tilde{r}_2^2}{1 + \tilde{r}_2} \right)^{-1/2} \frac{\tilde{m}_Z^2}{\left(m_{(n)}^{SU(2)} \right)^2} \hat{A}_{(n)}^3 \\ &+ \sum_{n=1}^{\infty} \sqrt{2} \tilde{s}_W \tilde{c}_W^2 \left(1 + \pi^2 R^2 \left(m_{(n)}^{U(1)} \right)^2 \frac{\tilde{r}_1^2}{1 + \tilde{r}_1} \right)^{-1/2} \frac{\tilde{m}_Z^2}{\left(m_{(n)}^{U(1)} \right)^2} \hat{B}_{(n)}. \end{aligned} \quad (7.91)$$

Here, an order \tilde{X} admixture of the $\tilde{A}_{(0)\mu}$ state cannot be excluded but does not affect the calculation of the Z -boson mass. The admixture is found to be zero below. The mass is calculated by multiplying the first row of the mass matrix (7.89) with the eigenstate (7.91).

As an intermediate result, we state

$$\begin{aligned}
m_{Z(0)}^2 = & \frac{(\tilde{g}^2 + \tilde{g}'^2)v^2}{4} \left[1 - \left(\frac{\tilde{c}_W^6}{1 + \tilde{r}_2} + 2 \frac{\tilde{c}_W^4 \tilde{s}_W^2}{1 + \tilde{r}_2} + 2 \frac{\tilde{c}_W^2 \tilde{s}_W^4}{1 + \tilde{r}_1} + \frac{\tilde{s}_W^6}{1 + \tilde{r}_1} \right) \tilde{X} \right. \\
& - 2 \sum_{n=1}^{\infty} \tilde{s}_W^4 \tilde{c}_W^2 \frac{\tilde{m}_Z^2}{\left(m_{(n)}^{\text{SU}(2)}\right)^2} \left(1 + \pi^2 R^2 \left(m_{(n)}^{\text{SU}(2)}\right)^2 \frac{\tilde{r}_2^2}{1 + \tilde{r}_2} \right)^{-1} \\
& \left. - 2 \sum_{n=1}^{\infty} \tilde{s}_W^2 \tilde{c}_W^4 \frac{\tilde{m}_Z^2}{\left(m_{(n)}^{\text{U}(1)}\right)^2} \left(1 + \pi^2 R^2 \left(m_{(n)}^{\text{U}(1)}\right)^2 \frac{\tilde{r}_1^2}{1 + \tilde{r}_1} \right)^{-1} \right]. \tag{7.92}
\end{aligned}$$

If $\tilde{r}_1 = \tilde{r}_2$, (7.92) has to simplify to (7.79) known from the W -boson sector. By comparison, this observation implies

$$2 \sum_{n=1}^{\infty} \frac{1}{\left(m_{(n)}^{\text{SU}(2)}\right)^2} \left(1 + \pi^2 R^2 \left(m_{(n)}^{\text{SU}(2)}\right)^2 \frac{\tilde{r}_2^2}{1 + \tilde{r}_2} \right)^{-1} = \frac{\pi^2}{3} \frac{R^2}{1 + \tilde{r}_2} \tag{7.93}$$

and the analogous result for the sum over the $U(1)$ masses. The simple result (7.93) can also be proven directly by the summation technique introduced in Appendix A. Thus, we finally find

$$m_{Z(0)}^2 = \tilde{m}_Z^2 \left[1 - \left(\frac{\tilde{c}_W^2}{1 + \tilde{r}_2} + \frac{\tilde{s}_W^2}{1 + \tilde{r}_1} \right) \tilde{X} \right]. \tag{7.94}$$

Again, the shift due to the extra dimension is suppressed if one allows for the presence of brane kinetic terms. In analogy, one finds the eigenstate of the physical photon

$$\begin{aligned}
\hat{A}_{(0)\mu} = & \tilde{A}_{(0)\mu} \\
& + \sum_{n=1}^{\infty} \sqrt{2} \tilde{s}_W \tilde{c}_W^2 \left(1 + \pi^2 R^2 \left(m_{(n)}^{\text{SU}(2)}\right)^2 \frac{\tilde{r}_2^2}{1 + \tilde{r}_2} \right)^{-1/2} \frac{\tilde{m}_Z^2}{\left(m_{(n)}^{\text{SU}(2)}\right)^2} \hat{A}_{(n)}^3 \\
& + \sum_{n=1}^{\infty} \sqrt{2} \tilde{s}_W^2 \tilde{c}_W \left(1 + \pi^2 R^2 \left(m_{(n)}^{\text{U}(1)}\right)^2 \frac{\tilde{r}_1^2}{1 + \tilde{r}_1} \right)^{-1/2} \frac{\tilde{m}_Z^2}{\left(m_{(n)}^{\text{U}(1)}\right)^2} \hat{B}_{(n)}, \tag{7.95}
\end{aligned}$$

which is massless as it has to be. The masslessness implies that there is no admixture of $\tilde{Z}_{(0)\mu}$. In turn, orthogonality between the photon and the Z boson demands the absence of an admixture of $\tilde{A}_{(0)\mu}$ to the physical Z -boson state as stated above. Concerning the couplings to fermions on the brane $y = 0$, for the Z boson one finds

$$\begin{aligned}
T_{3(0)} = & T_3 \left(1 - \left[\frac{\tilde{c}_W^2}{1 + \tilde{r}_2} + \frac{\tilde{s}_W^2}{1 + \tilde{r}_1} \right] \tilde{X} \right), \\
Q_{(0)} = & Q \left(1 - \frac{1}{1 + \tilde{r}_1} \tilde{X} \right), \tag{7.96}
\end{aligned}$$

where the notation of Section 4.1 is used. In addition to this shift, one has to replace s_W by \tilde{s}_W and g by \tilde{g} in the usual Feynman rules (see Appendix B). Note that for $\tilde{r}_1 = \tilde{r}_2$ the shifts in (7.96) are equal and the Z coupling can equally well be parameterized by a shift for \tilde{g} only. The photon gauge coupling is shifted from e to \tilde{e} with no order \tilde{X} correction.

The quantities \tilde{e} , \tilde{g} , and \tilde{s}_W turn out to play the role of the usual SM parameters. They also obey the usual SM tree-level relations. For large BKTs, they substantially differ from the initial parameters in the Lagrangian e , g and s_W which are only bookkeeping devices. To quantify this statement, we derive the input parameters in terms of \tilde{e} , \tilde{g} , and \tilde{s}_W . One obtains

$$\alpha = \frac{\tilde{e}^2}{4\pi}, \quad (7.97)$$

and $m_{Z(0)}$ is already given in (7.94). At this point, we can identify

$$\tilde{X} = X = \frac{\pi^2 m_{Z(0)}^2}{3 M^2} \quad \text{and} \quad X_{\tilde{g}} = \tilde{c}_W^2 X \quad (7.98)$$

because one can use $m_{Z(0)}^2 = \tilde{m}_Z^2$ in terms which are already of order X . The Fermi constant G_F has to be again calculated from muon decay including the exchange of the heavy KK modes. Using (7.79), (7.80), (7.94), and (7.76) to find the leading order couplings of the heavy KK modes, the Fermi constant reads

$$G_F = \frac{\pi\alpha}{\sqrt{2}\tilde{s}_W^2\tilde{c}_W^2 m_{Z(0)}^2} \left(1 - \frac{2\tilde{c}_W^2}{1+\tilde{r}_2} X - \frac{\tilde{s}_W^2}{1+\tilde{r}_1} X + 2 \sum_{n=1}^{\infty} \frac{\tilde{m}_W^2}{m_{W(n)}^2} \left(1 + \pi^2 R^2 m_{W(n)}^2 \frac{\tilde{r}_2^2}{1+\tilde{r}_2} \right) \right). \quad (7.99)$$

The infinite sum is performed according to (7.93) and we finally find

$$G_F = \frac{\pi\alpha}{\sqrt{2}\tilde{s}_W^2\tilde{c}_W^2 m_{Z(0)}^2} \left(1 - \left[\frac{\tilde{c}_W^2}{1+\tilde{r}_2} + \frac{\tilde{s}_W^2}{1+\tilde{r}_1} \right] X \right). \quad (7.100)$$

With the help of (7.100), one defines an effective mixing angle \hat{s}_W which is shifted to first order in X with respect to \tilde{s}_W as in Chapter 4. All shifts in masses and couplings are suppressed if both \tilde{r}_1 and \tilde{r}_2 become large. This is extremely important for the investigation of precision observables at the Z pole. The bounds on the compactification scale are substantially reduced, if all brane kinetic terms are large.

In addition, the masses of the heavy KK modes are reduced by brane kinetic terms. Their couplings to brane fermions also decrease. As discussed at the beginning of Section 4.4, at energies above the Z pole 4-fermion contact interactions begin to dominate the deviations from SM predictions. In the presence of brane kinetic terms, they scale like $s/(1+\tilde{r}_{1,2})M^2$ as can be found in analogy to the above calculation of the Fermi constant. Hence, the strength of the contact interactions is also reduced.

In combination, brane kinetic terms effectively decouple the extra dimension from observation, as long as the energy is still small compared to the compactification scale. The model becomes more and more four-dimensional. If only \tilde{r}_1 or \tilde{r}_2 become large, only the shifts due to the gauge group with small brane kinetic term survive. The model tends to the brane-bulk or the bulk-brane model (cf. Section 7.3.2).

To check the correctness of the analytically calculated shifts, it has been valuable to numerically investigate a truncated model. For a finite number of Fourier modes, the kinetic and the mass matrix can be diagonalized numerically to find the spectrum and the couplings. Already for a model with 20 modes, the masses and couplings for the zero mode are in good agreement with the analytical results.

7.3.2 Other Models with a Brane Higgs

The results for the W sector are either trivial (for $SU(2)$ on the brane) or can be directly obtained from the last section. The neutral boson sector can also be handled in analogy to the calculations already presented. It is even simpler because there are no KK modes for the gauge group confined to the brane. Consequently, the mass matrices M_{kl}^2 in (7.83) degenerate to a single row or column. Following the steps of the calculation, one finds for $m_{Z(0)}$, $Q_{(0)}$, $T_{(0)}$ and G_F the results of the previous section in the limit $\tilde{r}_1 \rightarrow \infty$, $\tilde{r}_2 \rightarrow \infty$ for the bulk-brane, brane-bulk model, respectively. If the remaining brane kinetic term becomes larger, the extra-dimensional effects are suppressed and the model becomes more and more SM-like at energies below the compactification scale.

7.3.3 Bulk-Bulk Model with a Bulk Higgs

The investigation of the bulk-bulk model with a bulk Higgs is more involved. First of all, there is the additional brane kinetic term r_Φ of the scalar Higgs field in the bulk, as introduced in (7.65). Using the transcendental eigenvalue equation (7.67), we find for the mass and the coupling of the light W boson

$$\begin{aligned} m_{W(0)}^2 &= \frac{1 + \tilde{r}_\Phi}{1 + \tilde{r}_2} \frac{g^2 v^2}{4} \left(1 - \frac{(\tilde{r}_\Phi - \tilde{r}_2)^2}{(1 + \tilde{r}_2)^2 (1 + \tilde{r}_\Phi)} \frac{\pi^2}{3} \frac{g^2 v^2}{4M^2} \right) \\ &= \frac{\tilde{g}^2 \tilde{v}^2}{4} \left(1 - \frac{(\tilde{r}_\Phi - \tilde{r}_2)^2}{(1 + \tilde{r}_2)(1 + \tilde{r}_\Phi)^2} \tilde{c}_{WX}^2 \right), \end{aligned} \quad (7.101)$$

$$\begin{aligned} g_{W(0)} &= \frac{g}{\sqrt{1 + \tilde{r}_2}} \left(1 - \frac{(\tilde{r}_\Phi - \tilde{r}_2)}{(1 + \tilde{r}_2)^2} \frac{\pi^2}{3} \frac{g^2 v^2}{4M^2} \right) \\ &= \tilde{g} \left(1 - \frac{(\tilde{r}_\Phi - \tilde{r}_2)}{(1 + \tilde{r}_2)(1 + \tilde{r}_\Phi)} \tilde{c}_{WX}^2 \right), \end{aligned} \quad (7.102)$$

where, as before, $\tilde{g} = g/\sqrt{1+\tilde{r}_2}$ and, additionally, we define $\tilde{v} = v\sqrt{1+\tilde{r}_\Phi}$. Moreover, we have anticipated (7.98) for this model in which we find $\tilde{m}_Z^2 = (\tilde{g}^2 + \tilde{g}'^2)\tilde{v}^2/4$. The weak mixing angle \tilde{c}_W is still given by (7.86). Compared to the models with a brane Higgs boson, we find a qualitatively new behavior. With growing \tilde{r}_2 , the order X correction for the W -boson mass increase. Thus, these models are in conflict with the data if the brane kinetic term of the gauge field is large at a given compactification scale. On the other hand, for $\tilde{r}_\Phi = \tilde{r}_2$ the corrections vanish, no matter how large each brane kinetic term is. If only \tilde{r}_Φ is large, the model essentially looks as if the symmetry is broken by a brane Higgs. For $\tilde{r}_\Phi \sim \tilde{r}_1 \sim \tilde{r}_2$, the shift scales as in models with a brane Higgs. These results are quite generic for the order X corrections in this model.

Concerning the neutral gauge bosons, $\text{Diag}(m_{SU(2)(n)}^2)$ and $\text{Diag}(m_{U(1)(n)}^2)$ in the mass matrix (7.83) can be calculated using the eigenvalue equation (7.67). The off-diagonal blocks are less simple than (7.84) because there is no overall δ -function simplifying the integration over the wave functions of the mass eigenstates. As a result, we find

$$M_{kl}^2 = -\frac{gg'v^2}{4}N_{(k)}^{SU(2)}N_{(l)}^{U(1)}\left(\tilde{r}_\Phi - \frac{\left(m_{(k)}^{SU(2)}\right)^2\tilde{r}_2 - \left(m_{(l)}^{U(1)}\right)^2\tilde{r}_1 + \frac{(g'^2-g^2)v^2}{4}\tilde{r}_\Phi}{\left(m_{(k)}^{SU(2)}\right)^2 - \left(m_{(l)}^{U(1)}\right)^2 + \frac{(g'^2-g^2)v^2}{4}}\right). \quad (7.103)$$

To approximately diagonalize the mass matrix as in Section 7.3.1 we have to calculate M_{k0}^2 , M_{0l}^2 to leading order. This is easily done because the factor in brackets reduces to $(\tilde{r}_\Phi - \tilde{r}_2)$ or $(\tilde{r}_\Phi - \tilde{r}_1)$, respectively. No corrections of order X are needed. However, M_{00}^2 has to be analyzed to first order in X leading to a more lengthy calculation. After the determination of the shift, the remaining calculation proceeds as in the previous section. Again, one has to use (7.93) to calculate the infinite sums. We finally find

$$m_{Z(0)}^2 = \tilde{m}_Z^2\left(1 - \left[\frac{\tilde{c}_W^2}{1+\tilde{r}_2}\frac{(\tilde{r}_\Phi - \tilde{r}_2)^2}{(1+\tilde{r}_\Phi)^2} + \frac{\tilde{s}_W^2}{1+\tilde{r}_1}\frac{(\tilde{r}_\Phi - \tilde{r}_1)^2}{(1+\tilde{r}_\Phi)^2}\right]\tilde{X}\right) \quad (7.104)$$

for the mass of the Z boson. Concerning its coupling to brane fermions, \tilde{g} and \tilde{s}_W again replace g and s_W in the Feynman rules in Appendix B. The order X corrections are given by

$$T_{3f(0)} = T_{3f}\left(1 - \left[\tilde{c}_W^2\frac{\tilde{r}_\Phi - \tilde{r}_2}{(1+\tilde{r}_\Phi)(1+\tilde{r}_2)} + \tilde{s}_W^2\frac{\tilde{r}_\Phi - \tilde{r}_1}{(1+\tilde{r}_\Phi)(1+\tilde{r}_1)}\right]\tilde{X}\right), \quad (7.105)$$

$$Q_{f(0)} = Q_f\left(1 - \frac{\tilde{r}_\Phi - \tilde{r}_1}{(1+\tilde{r}_\Phi)(1+\tilde{r}_1)}\tilde{X}\right), \quad (7.106)$$

while the photon coupling $Q_f\tilde{e}$ is not shifted. Without brane kinetic terms, corrections of the Fermi constant arise only from heavy KK exchange in muon decay. With brane kinetic

terms, the additional shifts in couplings and masses yield

$$G_F = \frac{\pi\alpha}{\sqrt{2}\tilde{s}_W^2\tilde{c}_W^2 m_{Z(0)}^2} \left(1 - \frac{1 + \tilde{c}_W^2\tilde{r}_1 + \tilde{s}_W^2\tilde{r}_2}{(1 + \tilde{r}_1)(1 + \tilde{r}_2)} X + \frac{2}{1 + \tilde{r}_\Phi} X - \tilde{s}_W^2 \frac{1 + \tilde{r}_1}{(1 + \tilde{r}_\Phi)^2} X \right), \quad (7.107)$$

where the KK exchange has been summed as in (7.99). Together with (7.104) and the unaltered fine-structure constant α , (7.107) completes the list of input parameters.

The afore mentioned generic behavior of the corrections is reproduced. In certain limits of the brane kinetic terms, the model is in conflict with experimental precision data from the Z pole because the order X corrections grow. This contrasts the results for models with a brane Higgs bosons which become more SM-like for large brane kinetic terms. However, if all brane kinetic terms for the gauge and the scalar fields are of the same order, the camouflage of the extra dimension by brane kinetic terms is recovered. In particular, the contact interactions, being dominant for the discovery of extra dimensions at high energies, are as diminished by brane kinetic terms as in the other models investigated before.

Chapter 8

Conclusions

We have studied a specific class of 5-dimensional standard model extensions. In this class, some or all of the $SU(2)_L$ and $U(1)_Y$ gauge fields and Higgs bosons propagate in the fifth dimension, compactified on an S^1/Z_2 orbifold. The other degrees of freedom, including the fermions, are confined to one of the two boundaries of the S^1/Z_2 orbifold. Starting from the 5D Lagrangian, we have worked out the corresponding 4D effective theory for the towers of KK modes which reflect the higher-dimensional origin of the model. In particular, we have paid special attention to a consistent gauge-fixing procedure for the higher-dimensional models leading to the generalized R_ξ gauges. Applying the appropriate higher-dimensional gauge-fixing conditions, the known R_ξ gauge is recovered for each KK mass eigenstate after the fifth dimension has been integrated out. We do not only explicitly identify the physical particle spectrum as in the widely used unitary gauge but also the would-be Goldstone modes which are eaten up by the massive gauge bosons. This enables us to establish a close analogy between the traditional Higgs mechanism in the SM and the geometric mass generation for the KK modes by compactification. To further elaborate the analogy, we have proven the Goldstone boson equivalence theorem for W -pair production at tree-level, no matter if a vector boson acquires its mass by the Higgs mechanism, by compactification, or by a combination of both mechanisms. By proving the Ward identities underlying the Goldstone theorem in the W -pair channel we have also checked the consistency of the higher-dimensional models as gauge theories.

Based on the effective Lagrangians, we have derived analytic expressions for the KK mass spectrum of the gauge bosons and for their interactions to the fermionic matter. All the relevant Feynman rules are given. The afore mentioned proof of Ward identities provides an excellent tool for their verification.

We have also calculated a large number of precision observables, cross sections and asymmetries. Using these results, we have confronted the higher-dimensional SM extensions

with an extensive set of high precision data from measurements at and above the Z pole. In addition to simple one-parameter fits for the compactification scale M , we performed multi-parameter fits for M along with the SM input parameters to take possible correlations into account. No indication for extra-dimensional physics has been found up to LEP2 energies. From that, we derived bounds on the compactification scale in the different models in the range of 4-6 TeV at the 2σ confidence level. Depending on the model the correlations reduce the bounds up to 1 TeV with respect to the one-parameter fit. Furthermore, we have shown that the presence of an extra compact dimension relaxes the 2σ upper bound on the Higgs mass from 280 GeV in the SM to 400 GeV and 330 GeV in the brane-bulk and the bulk-bulk model with a brane Higgs, respectively. Note that the data set used in Section 4.3 is not identical to the one for the blue-band plot [70] and that the latest results for the top mass [99] have not been taken into account, yet.

In addition, we have estimated the sensitivity to the compactification scale M at a future e^+e^- collider such as TESLA. The GigaZ option should allow to increase the sensitivity to M by a factor two in almost all 5D models. At $\sqrt{s} = 800$ GeV and for an integrated luminosity of 1000 fb^{-1} the discovery potential depends crucially on the control of systematic errors. For a systematic uncertainty of 1% in each search channel, one will be able to explore compactification scales up to 15-20 TeV. If systematic uncertainties were smaller than the statistical uncertainties the sensitivity limit would be estimated to be in the range $M = 35\text{-}50$ TeV. For a sufficiently low compactification scale, $M \lesssim 10$ TeV, Higgsstrahlung and angular distributions of 2-fermion final states can be used to discriminate between different 5D models. In particular, Higgsstrahlung can be used to distinguish a brane from a bulk Higgs boson.

Furthermore, we have investigated models with brane kinetic terms which are required at the one-loop level for each bulk field. Including brane kinetic terms with their strength as a free parameter in the 5D Lagrangian, the gauge-fixing procedure has been identified beyond unitary gauge. Special attention has again been paid to the interplay of compactification and spontaneous symmetry breaking. In the corresponding effective 4D models the spectrum of KK modes as well as their couplings to fermions are calculated either exactly or at least approximately to first order in m_Z^2/M^2 .

We have shown that the appearance of brane kinetic terms tends to hide the extra dimension from observation. In particular, not only the heavy KK modes decouple for large brane kinetic terms [52] but also the shifts in masses and couplings are diminished. The aforementioned bounds on M roughly reduce by a factor $\sqrt{1 + \tilde{r}_c}$ if the dimensionless constant \tilde{r}_c sets the typical size of all brane kinetic terms. Only for a bulk-bulk model with a bulk Higgs in which \tilde{r}_c for the gauge bosons is much larger than \tilde{r}_c for the Higgs boson, the bounds can become more stringent. From an effective field theory point of view,

dimensionful parameters usually scale with the cut-off Λ of the theory. Here, we have $\tilde{r}_c = r_c/(2\pi R) = M/(2\pi\Lambda)$. Consequently, brane kinetic terms are expected to be small if the cut-off is a few times the compactification scale M as usually assumed. Regardless, recently large brane kinetic terms have been invoked for model building, e.g. for Higgsless SM extensions [53]. The consistency and predictivity of the non-renormalizable higher-dimensional models will be subject of further investigation. For example, questions of tree-level unitarity can be analyzed in the extended setup including brane kinetic terms [96]. Moreover, it is interesting to study the models in more detail as quantum theories at the loop-level.

On the experimental side, the LHC will explore a new energy regime. Resonant production of heavy KK states with a mass of 6-7 TeV [17, 38, 39] may be in reach at the LHC. Thus, the lower limits on the compactification scale indicate that the first KK excitation can be produced. However, direct production of the second or third heavy state differentiating higher-dimensional physics from alternatives is excluded within the presented setup, unless the brane kinetic terms are large. Hence, other methods to distinguish higher-dimensional models from other models with extra gauge bosons are essential [100]. If only gravity lives in extra dimensions or in case of universal extra dimensions the LHC phenomenology is of course rather different. At any rate, with the advent of the next generation of high-energy colliders, the question if more than four dimensions are visible in the TeV region will become even more exciting.

Appendix A

Infinite Sums

It is a special feature of higher-dimensional models, that the corresponding 4D theory includes an infinite number of degrees of freedom. Hence, we often have to calculate infinite sums to find amplitudes or basis rotations. Complex analysis provides an extremely helpful tool in this context. To be precise, we make use of the residue theorem

$$\frac{1}{2\pi i} \int_C f(z) dz = \sum_n \text{Res} f(z)|_{z=z_n}. \quad (\text{A.1})$$

On the left hand side, one integrates counter clockwise along a closed contour C enclosing a simply connected region of the complex plane. On the right hand side, the sum is taken over the residues $\text{Res} f(z)|_{z=z_n}$ at the poles of $f(z)$ inside the contour C . The residue theorem holds as long as $f(z)$ is analytic everywhere inside C except for the isolated singularities at $z = z_n$.

Let us first concentrate on infinite sums over simple functions of integers $g(n)$ [101]. Given a function $f(z)$ with a pole at each integer n , (A.1) tells us how to express the infinite sum by an integral in the complex plane. The function of choice is $f(z) = \pi \cot(\pi z)g(z)$, where $\text{Res} \pi \cot(\pi z)|_{z=n} = 1$. Consequently, as long as $g(z)$ is analytic at all integers, we can write

$$\frac{1}{2\pi i} \int_{C_N} \pi \cot(\pi z) g(z) dz = \sum_{n=-N}^N g(n) + S, \quad (\text{A.2})$$

where the contour C_N encloses the poles at $z = n$ on the real axis for $|n| \leq N$ and S is given by the sum of the residues of $\pi \cot(\pi z)g(z)$ at the poles of $g(z)$ inside C_N . A good choice for the contour C_n is a circle centered at the origin with radius $N + 1/2$. With this definition, we can easily take the limit $N \rightarrow \infty$. It can be shown [101] that $|\cot(\pi n)|$ is bounded along this contour such that the complex integral vanishes in the limit $N \rightarrow \infty$ as long as $|g(z)| \leq c/|z|^k$ with $k > 1$ and $c, k = \text{const}$. Hence, in the limit $N \rightarrow \infty$, (A.2)

implies

$$\sum_{n=-\infty}^{\infty} g(n) = - \{ \text{sum of the residues of } \pi \cot(\pi z) g(z) \text{ at the poles of } g(z) \}. \quad (\text{A.3})$$

The calculation of the infinite sum is reduced to the evaluation of a few residues. The above assumptions ($|g(z)| \leq c/|z|^k$ with $k > 1$; $g(z)$ has no poles at integers) are not very restrictive because the sum usually does not converge if they do not hold. As an example, let us calculate the sum over s -channel propagators in 5D-QED, i.e.

$$\sum_{n=1}^{\infty} \frac{1}{s - n^2/R^2} = -\frac{1}{2s} + \frac{1}{2} \sum_{n=-\infty}^{\infty} \frac{1}{s - n^2/R^2} = -\frac{1}{2s} + \frac{\pi R}{2\sqrt{s}} \cot(\pi R\sqrt{s}). \quad (\text{A.4})$$

In the second step, we have used that $g(z) = 1/(s - z^2/R^2)$ has two simple poles at $z = \pm\sqrt{s}R$. If s approaches n/R , the s -channel poles are recovered.

We now generalize the above analysis to sums over functions $g(m_{(n)})$ of KK masses $m_{(n)}$, given by transcendental equations like (7.16) [102]. While it is impossible to analytically calculate a single mass eigenvalue, it turns out that one can indeed calculate certain infinite sums. As a consequence of the transcendental equation (7.16), $1/(z + \frac{2}{r_c} \tan(\pi Rz))$ has poles at each mass eigenvalue and

$$\text{Res} \left. \frac{1}{z + \frac{2}{r_c} \tan(\pi Rz)} \right|_{z=m_{(n)}} = \left(1 + \frac{2\pi R}{r_c \cos^2(\pi Rz)} \right)^{-1} = \tilde{r}_c (1 + \tilde{r}_c + \tilde{r}_c^2 \pi^2 m_{(n)}^2 R^2)^{-1}, \quad (\text{A.5})$$

where we have used $\tilde{r}_c = r_c/(2\pi R)$. Thus, we immediately find

$$\sum_{n=-\infty}^{\infty} g(m_{(n)}) = \frac{1}{2\pi i} \int_C \frac{1}{\tilde{r}_c} \frac{1 + \tilde{r}_c + \tilde{r}_c^2 \pi^2 m_{(n)}^2 R^2}{z + \frac{2}{r_c} \tan(\pi Rz)} g(z) dz - S, \quad (\text{A.6})$$

where

$$S = \text{sum of the residues of the integrand in (A.6) at the poles of } g(z). \quad (\text{A.7})$$

In many cases, the integral again vanishes. However, this is not necessarily the case, as we can see in the following explicit example.

To demonstrate the full power of the complex integration method, let us calculate the sum

$$\sum_{n=1}^{\infty} D_{kn} m_{(n)}^2 D_{ln} = \sum_{n=1}^{\infty} (1 + \tilde{r}_c + \tilde{r}_c^2 \pi^2 m_{(n)}^2 R^2)^{-1} \frac{4\tilde{r}_c^2 R^2 k l m_{(n)}^4}{(k^2 - m_{(n)}^2 R^2)(l^2 - m_{(n)}^2 R^2)} \quad (\text{A.8})$$

in (7.35) which is important in the context of gauge fixing. We straightforwardly find

$$\begin{aligned} \sum_{n=1}^{\infty} D_{kn} m_{(n)}^2 D_{ln} &= \frac{1}{2} \sum_{n=-\infty}^{\infty} D_{kn} m_{(n)}^2 D_{ln} \\ &= \frac{1}{2\pi i} \int_C \frac{1}{z + \frac{2}{r_c} \tan(\pi Rz)} \frac{2\tilde{r}_c R^2 k l z^4}{(k^2 - z^2 R^2)(l^2 - z^2 R^2)} dz - S, \end{aligned} \quad (\text{A.9})$$

where, for $k \neq l$, S is given by the residues of the 4 simple poles at $z = \pm k/R$ and $z = \pm l/R$ which add up to $S = 2\tilde{r}_c kl/R^2$. For $k = l$, we have two double poles at $z = \pm k/R$ and their residues yield $S = (2\tilde{r}_c - 1)k^2/R^2$. For the contour C in (A.9), we take the limit $N \rightarrow \infty$ of C_N , which is a circle around the origin with radius $N + 1/4$. The constant $1/4$ is chosen to avoid any poles from the mass eigenvalues on the contour C_N . In the limit $N \rightarrow \infty$, we only have to keep terms in the integrand which are not suppressed by more than one power of z , i.e.

$$\sum_{n=1}^{\infty} D_{kn} m_{(n)}^2 D_{ln} = -(2\tilde{r}_c - \delta_{k,l}) \frac{kl}{R^2} + \lim_{N \rightarrow \infty} \frac{1}{2\pi i} \int_{C_N} \frac{1}{z + \frac{2}{r_c} \tan(\pi R z)} \frac{2\tilde{r}_c kl}{R^2} dz. \quad (\text{A.10})$$

Along the circle C_N , $|\tan(\pi R z)|$ is bounded by a constant independent of N . Thus, defining $z_N = (N + 1/4) \exp(i\theta)$, we have

$$\begin{aligned} \lim_{N \rightarrow \infty} \int_{C_N} \frac{1}{z + \frac{2}{r_c} \tan(\pi R z)} dz &= \lim_{N \rightarrow \infty} \int_0^{2\pi} \frac{iz_N}{z_N + \frac{2}{r_c} \tan(\pi R z_N)} d\theta \\ &= 2\pi i + \lim_{N \rightarrow \infty} \int_0^{2\pi} \frac{-i \frac{2}{r_c} \tan(\pi R z_N)}{z_N + \frac{2}{r_c} \tan(\pi R z_N)} d\theta \\ &= 2\pi i, \end{aligned} \quad (\text{A.11})$$

and we finally find

$$\sum_{n=1}^{\infty} D_{kn} m_{(n)}^2 D_{ln} = -(2\tilde{r}_c - \delta_{k,l}) \frac{kl}{R^2} + 2\tilde{r}_c \frac{kl}{R^2} = \delta_{k,l} \frac{k^2}{R^2}. \quad (\text{A.12})$$

Many similar sums can be calculated in close analogy to this explicit example.

Appendix B

KK Masses and Couplings to Fermions on the Brane

Here, we present exact analytic results for the masses and the couplings of the KK gauge modes to fermions in the minimal 5-dimensional extensions of the SM discussed in Chapter 3. No brane kinetic terms are considered.

In Fig. B.1, we display the propagators for the KK gauge and Goldstone modes in the R_ξ gauge. In addition, the masses of the KK gauge bosons can be determined as follows:

SU(2)_L⊗U(1)_Y-Bulk Model:

$$m_{\gamma(n)} = \frac{n}{R}, \quad (\text{B.1})$$

$$\sqrt{m_{W(n)}^2 - m_W^2 \cos^2 \beta} = \pi m_W^2 \sin^2 \beta R \cot \left(\pi R \sqrt{m_{W(n)}^2 - m_W^2 \cos^2 \beta} \right), \quad (\text{B.2})$$

$$\sqrt{m_{Z(n)}^2 - m_Z^2 \cos^2 \beta} = \pi m_Z^2 \sin^2 \beta R \cot \left(\pi R \sqrt{m_{Z(n)}^2 - m_Z^2 \cos^2 \beta} \right), \quad (\text{B.3})$$

where $n = 0, 1, 2, \dots$, $m_W = gv/2$ and $m_Z = \sqrt{g^2 + g'^2} v/2$.

SU(2)_L-Brane, U(1)_Y-Bulk Model:

$$m_{Z(n)} = \pi m_Z^2 \sin^2 \theta_W R \cot \left(\pi R m_{Z(n)} \right) + \frac{m_Z^2}{m_{Z(n)}} \cos^2 \theta_W. \quad (\text{B.4})$$

Note that there are no heavy KK excitations for the photon and W boson in this model.

SU(2)_L-Bulk, U(1)_Y-Brane Model:

$$m_{W(n)} = \pi m_W^2 R \cot \left(\pi R m_{W(n)} \right), \quad (\text{B.5})$$

$$m_{Z(n)} = \pi m_Z^2 \cos^2 \theta_W R \cot \left(\pi R m_{Z(n)} \right) + \frac{m_Z^2}{m_{Z(n)}} \sin^2 \theta_W. \quad (\text{B.6})$$

$$\begin{aligned}
\gamma_{(n)} \text{ propagator:} & \quad \mu \text{---}\overset{(n)}{\text{~~~~~}}\text{---}\nu & = \frac{i}{k^2 - m_{\gamma(n)}^2} \left(-g^{\mu\nu} + \frac{(1-\xi)k^\mu k^\nu}{k^2 - \xi m_{\gamma(n)}^2} \right) \\
\hat{W}_{(n)}^\pm \text{-boson propagator:} & \quad \mu \text{---}\overset{(n)}{\text{~~~~~}}\text{---}\nu & = \frac{i}{k^2 - m_{W(n)}^2} \left(-g^{\mu\nu} + \frac{(1-\xi)k^\mu k^\nu}{k^2 - \xi m_{W(n)}^2} \right) \\
\hat{Z}_{(n)} \text{-boson propagator:} & \quad \mu \text{---}\overset{(n)}{\text{~~~~~}}\text{---}\nu & = \frac{i}{k^2 - m_{Z(n)}^2} \left(-g^{\mu\nu} + \frac{(1-\xi)k^\mu k^\nu}{k^2 - \xi m_{Z(n)}^2} \right) \\
A_{(n)5} \text{ propagator:} & \quad \mu \text{---}\overset{(n)}{\text{-----}}\text{---}\nu & = \frac{i}{k^2 - \xi m_{\gamma(n)}^2} \\
\hat{G}_{(n)}^0 \text{ propagator:} & \quad \mu \text{---}\overset{(n)}{\text{-----}}\text{---}\nu & = \frac{i}{k^2 - \xi m_{Z(n)}^2} \\
\hat{G}_{(n)}^\pm \text{ propagator:} & \quad \mu \text{---}\overset{(n)}{\text{-----}}\text{---}\nu & = \frac{i}{k^2 - \xi m_{W(n)}^2}
\end{aligned}$$

Figure B.1: KK gauge- and Goldstone-boson propagators in the 5-dimensional extensions of the SM in the generalized R_ξ -gauge.

There are no heavy KK excitations for the photon field in this model.

In the following, we give the exact analytic expressions for the couplings of KK gauge bosons to fermions. In order to do so, we first introduce the following interaction Lagrangian:

$$\mathcal{L}_{\text{int}} = \sum_n g_{W(n)} \left(\hat{W}_{(n)\mu}^+ J_W^{+\mu} + \hat{W}_{(n)\mu}^- J_W^{-\mu} \right) + \sum_n g_{Z(n)} \hat{Z}_{(n)\mu} J_Z^\mu + \sum_n e_{(n)} \hat{A}_{(n)\mu} J_{\text{EM}}^\mu, \quad (\text{B.7})$$

with

$$\begin{aligned}
J_W^{+\mu} &= \frac{1}{2\sqrt{2}} \left[\bar{\nu}_i \gamma^\mu (1 - \gamma^5) e_i + \bar{u}_i \gamma^\mu (1 - \gamma^5) d_j V_{ij} \right], \\
J_Z^\mu &= \frac{1}{4 \cos \theta_W} \bar{f} \gamma^\mu \left[(2 T_{3f(n)} - 4 Q_{f(n)} \sin^2 \theta_W) - 2 T_{3f(n)} \gamma^5 \right] f, \\
J_{EM}^\mu &= \bar{f} Q_f \gamma^\mu f,
\end{aligned} \quad (\text{B.8})$$

and $\nu_i = (\nu_e, \nu_\mu, \nu_\tau)$, $e_i = (e, \mu, \tau)$, $u_i = (u, c, t)$ and $d_i = (d, s, b)$. In addition, f denotes the 12 SM fermions. After a basis transformation from the weak to the mass eigenstates, we obtain the following effective gauge couplings and quantum numbers for the three different higher-dimensional models ($n = 0, 1, 2, \dots$):

SU(2)_L⊗U(1)_Y-Bulk Model:

$$\begin{aligned}
e_{(0)} &= e, & e_{(n \geq 1)} &= \sqrt{2} e, \\
g_{Z(n)} &= \sqrt{2} g \left(1 + \frac{m_Z^2 \sin^2 \beta}{m_{Z(n)}^2 - m_Z^2 \cos^2 \beta} + \frac{\pi^2 m_Z^4 \sin^4 \beta}{M^2 (m_{Z(n)}^2 - m_Z^2 \cos^2 \beta)} \right)^{-1/2}, \\
g_{W(n)} &= \sqrt{2} g \left(1 + \frac{m_W^2 \sin^2 \beta}{m_{W(n)}^2 - m_W^2 \cos^2 \beta} + \frac{\pi^2 m_W^4 \sin^4 \beta}{M^2 (m_{W(n)}^2 - m_W^2 \cos^2 \beta)} \right)^{-1/2}, \\
T_{3f(n)} &= T_{3f}, & Q_{f(n)} &= Q_f,
\end{aligned} \tag{B.9}$$

with $M = 1/R$.

SU(2)_L-Brane, U(1)_Y-Bulk Model:

$$\begin{aligned}
g_{Z(n)} &= g, \\
T_{3f(n)} &= \frac{T_{3f} m_{Z(n)}^2}{c_W m_Z^2} \left[\frac{1}{s_W^2} \left(\frac{1}{2} - \frac{m_{Z(n)}^2}{m_Z^2} \right) + \frac{s_W^2}{2c_W^2} \left(\pi^2 \frac{m_{Z(n)}^2}{M^2} + \frac{m_{Z(n)}^2}{m_Z^2 s_W^2} + \frac{m_{Z(n)}^4}{m_Z^4 s_W^4} \right) \right]^{-1/2}, \\
Q_{f(n)} &= \frac{Q_f}{c_W} \left(\frac{m_{Z(n)}^2}{m_Z^2 s_W^2} - \frac{c_W^2}{s_W^2} \right) \left[\frac{1}{s_W^2} \left(\frac{1}{2} - \frac{m_{Z(n)}^2}{m_Z^2} \right) + \frac{s_W^2}{2c_W^2} \left(\pi^2 \frac{m_{Z(n)}^2}{M^2} + \frac{m_{Z(n)}^2}{m_Z^2 s_W^2} + \frac{m_{Z(n)}^4}{m_Z^4 s_W^4} \right) \right]^{-1/2}.
\end{aligned} \tag{B.10}$$

SU(2)_L-Bulk, U(1)_Y-Brane Model:

$$\begin{aligned}
g_{Z(n)} &= g, & g_{W(n)} &= \sqrt{2} g \left(1 + \frac{m_W^2}{m_{W(n)}^2} + \frac{\pi^2 m_W^4}{M^2 m_{W(n)}^2} \right)^{-1/2}, \\
T_{3f(n)} &= \frac{T_{3f} m_{Z(n)}^2}{s_W m_Z^2} \left[\frac{1}{c_W^2} \left(\frac{1}{2} - \frac{m_{Z(n)}^2}{m_Z^2} \right) + \frac{c_W^2}{2s_W^2} \left(\pi^2 \frac{m_{Z(n)}^2}{M^2} + \frac{m_{Z(n)}^2}{m_Z^2 c_W^2} + \frac{m_{Z(n)}^4}{m_Z^4 c_W^4} \right) \right]^{-1/2}, \\
Q_{f(n)} &= \frac{Q_f}{s_W} \left[\frac{1}{c_W^2} \left(\frac{1}{2} - \frac{m_{Z(n)}^2}{m_Z^2} \right) + \frac{c_W^2}{2s_W^2} \left(\pi^2 \frac{m_{Z(n)}^2}{M^2} + \frac{m_{Z(n)}^2}{m_Z^2 c_W^2} + \frac{m_{Z(n)}^4}{m_Z^4 c_W^4} \right) \right]^{-1/2}.
\end{aligned} \tag{B.11}$$

In Fig. B.2 we display the Feynman rules for the couplings of the KK gauge bosons to fermions that pertain to the above minimal 5-dimensional extensions of the SM.

$$\begin{array}{l}
 \begin{array}{c} f \\ \searrow \\ \text{---} \\ \nearrow \\ f \end{array} \text{---} \hat{A}_{(n)}^\mu = i e_{(n)} Q_f \gamma^\mu \\
 \begin{array}{c} \nu_i \\ \searrow \\ \text{---} \\ \nearrow \\ e_i \end{array} \text{---} \hat{W}_{(n)}^{-\mu} = \frac{i}{2\sqrt{2}} g_{W(n)} \gamma^\mu (1 - \gamma^5) \\
 \begin{array}{c} u_j \\ \searrow \\ \text{---} \\ \nearrow \\ d_i \end{array} \text{---} \hat{W}_{(n)}^{-\mu} = \frac{i}{2\sqrt{2}} g_{W(n)} \gamma^\mu (1 - \gamma^5) V_{ji}^* \\
 \begin{array}{c} f \\ \searrow \\ \text{---} \\ \nearrow \\ f \end{array} \text{---} \hat{Z}_{(n)}^\mu = \frac{i}{4 \cos \theta_W} g_{Z(n)} \gamma^\mu [(2T_{3f(n)} - 4Q_{f(n)} \sin^2 \theta_W) - 2T_{3f(n)} \gamma^5]
 \end{array}$$

Figure B.2: Feynman rules for couplings of the KK gauge bosons to fermions in the minimal 5-dimensional extensions of the SM.

Appendix C

Observables, SM Predictions, and Input Parameters

This Appendix specifies the data and the SM predictions for the one-parameter fits in Chapter 4. Moreover, we state the input variables for the multi-parameter fits.

In Figure C.1 we list the numerical values of the electroweak observables along with their SM predictions, used for the one-parameter fits in Section 4.3. Their correlations are taken from [70]. The data for fermion-pair production can be found in Table 8.2, the correlations for hadron production in Table 8.3 of [70]. The heavy flavor data is given in Table 8.7 and the W -pair production data in Table 9.1 of the same reference. For Bhabha scattering, combined data for the different experiments has not been available. The data of the different experiments is collected from [72–85]. The theoretical SM predictions are obtained by assuming a light SM Higgs boson.

For the multi-parameter fits using ZFITTER, one has to specify the input parameters of the SM. All input parameters are already restricted by independent experiments, e.g. the Fermi constant from muon decay, the Z mass from the direct LEP measurement, etc. This information has to be included in the fits (see Appendix D). We use the same input parameters as used for the Higgs-mass blue-band plot in the year 2002 [70, 103]. To be specific, we have

$$\begin{aligned} G_F &= 1.16637(1) \times 10^{-5} \text{ GeV}^{-2}, \\ \alpha(m_Z) &= 1/128.936(49), \\ m_Z &= 91.1875(21) \text{ GeV}, \\ m_t &= 174.3(5.1) \text{ GeV}, \\ \alpha_s(m_Z) &= 0.118(2), \end{aligned} \tag{C.1}$$

where the numbers in parentheses indicate the 1σ uncertainties. A Higgs mass $m_H < 114$ GeV is excluded by the direct search results from LEP. The fine-structure constant at the Z pole $\alpha(m_Z)$, the Z mass m_Z , and the Fermi constant G_F are already needed at tree-level. The top mass m_t , the strong coupling constant at the Z pole $\alpha_s(m_Z)$, and the Higgs mass m_H enter in the SM loop corrections calculated by ZFITTER (see Appendix D).

As discussed in Section 4.1, we introduce an effective weak mixing angle $\hat{\theta}_W$ by enforcing the tree-level SM relation

$$G_F = \frac{\pi\alpha(m_Z)}{\sqrt{2}\sin^2\hat{\theta}_W\cos^2\hat{\theta}_W m_Z^2}. \quad (\text{C.2})$$

Consequently, we use

$$\sin^2\hat{\theta}_W = 0.231, \quad (\text{C.3})$$

for the weak mixing angle which appears in $\Delta_{\mathcal{O}}^{5\text{DSM}}$ for many observables.

Observable	Exp. Value (\mathcal{O}^{EXP})	SM Prediction (\mathcal{O}^{SM})
M_W	80.451(61) GeV	80.391(19) GeV
$\Gamma_Z(\text{had})$	1.7444(20) GeV	1.7429(15) GeV
$\Gamma_Z(l^+l^-)$	83.984(86) MeV	84.019(27) MeV
$\Gamma_Z(\nu\bar{\nu})$	499.0(1.5) MeV	501.76(14) MeV
$Q_W(\text{Cs})$	- 72.65(44)	-73.10(3)
R_e	20.804(50)	20.744(18)
R_μ	20.785(33)	20.744(18)
R_τ	20.764(45)	20.790(18)
R_b	0.21664(68)	0.21569(16)
R_c	0.1729(32)	0.17230(7)
A_e	0.15138(216)	0.1478(12)
A_μ	0.142(15)	0.1478(12)
A_τ	0.1439(41)	0.1478(12)
A_b	0.921(20)	0.9347(1)
A_c	0.667(26)	0.6681(5)
A_s	0.895(91)	0.9357(1)
$A_{\text{FB}}^{(0,e)}$	0.0145(25)	0.01637(26)
$A_{\text{FB}}^{(0,\mu)}$	0.0169(13)	0.01637(26)
$A_{\text{FB}}^{(0,\tau)}$	0.0188(17)	0.01637(26)
$A_{\text{FB}}^{(0,b)}$	0.0982(17)	0.1036(8)
$A_{\text{FB}}^{(0,c)}$	0.0689(35)	0.0740(6)
$A_{\text{FB}}^{(0,s)}$	0.0976(114)	0.1037(8)

Table C.1: Precision measurements and the corresponding SM predictions for the observables under study [62].

Appendix D

Multi-Parameter Fits in the 5DSM

Here, we give a brief outline how to perform multi-parameter fits in the context of the 5DSM. The predictions for any observable are still calculated according to (4.1). However, in the context of a multi-parameter fit, it is necessary to find the radiatively corrected SM prediction \mathcal{O}^{SM} for any set of values for the SM input parameters $\alpha_{\text{em}}(m_Z)$, G_F , m_Z , $\alpha_s(m_Z)$, m_t , and m_H . Given the precision of the considered measurements, a tree-level analysis within the SM is far from adequate.

The Fortran program ZFITTER [63–66] is designed to provide the SM predictions except for Bhabha scattering and W -pair production. These channels are not analyzed in our multi-parameter fits. For the other observables, we have used ZFITTER version ZF6_36. After ZFITTER is appropriately initialized, the radiatively corrected SM predictions are accessible by calls to various ZFITTER routines. For cross sections and asymmetries cuts can be implemented according to the experimental data. As input parameters, the ZFITTER routines expect m_Z , $\alpha_s(m_Z)$, m_t , and m_H . Additionally, the electromagnetic coupling constant has to be parameterized by hadronic contributions to the running from low energies to the Z pole. Our fits are directly performed with respect to $\alpha_{\text{em}}(m_Z)$ using routines which translate between $\alpha_{\text{em}}(m_Z)$ and the corresponding hadronic contributions. The Fermi constant G_F cannot be fitted within ZFITTER because it is not a variable but fixed at its SM best fit value. It is so precisely known from muon decay that a fit would not make much sense anyway.

ZFITTER is well tested and works reliably. However, performing our fits we noted a bug in ZFITTER version ZF6_36. Calculating the total hadronic cross section at center-of-mass energies \sqrt{s} around the top mass, we found a discontinuity at $\sqrt{s} = m_t$. The discontinuity is roughly a 0.3% effect. It turned out, that this is due to a discontinuity in the parameterization of the strong coupling constant $\alpha_s(s)$ (a solution of the corresponding renormalization group equation). This bug will be fixed in future ZFITTER versions [104].

The discontinuity itself is not harmful for any of the presented results in Chapter 4 because it can only affect a single hadronic cross-section measurement at an energy near the top mass. However, the discontinuity is recovered in the χ^2 -function and leads to problems for the MINUIT routines to be discussed below. The slight distortions in Figure 4.4 arise from the discontinuity if the best fit value of m_t crosses one of the LEP2 energies. The small size of these distortions shows that the overall effect on the calculation of bounds is tiny.

To find the higher-dimensional predictions $\mathcal{O}^{5\text{DSM}}$ as a function of X from Fortran routines, we have implemented the correction factors $\Delta_{\mathcal{O}}^{5\text{DSM}}$ within a Fortran code. The minimization of χ^2 , needed in (4.26), is performed by the Fortran program MINUIT [67] which is specifically designed for the minimization of functions depending on many parameters. Calling the appropriate MINUIT routine, one has to specify the initial values for the fit parameters and another Fortran routine calculating the χ^2 -function. The χ^2 -function is called from the internal MINUIT routines for specific sets of fit parameters and has to return a value for χ^2 . If the minimization converges, MINUIT provides the minimal value of χ^2 along with the corresponding input parameters. To plot the χ^2 curves or contours as in Figs. 4.2 and 4.4, one can fix some of the parameters on an appropriate grid and fit the remaining parameters for each grid point. Either these plots or internal MINUIT routines can be used to determine the bounds according to (4.26).

The afore mentioned discontinuity in the χ^2 -function leads to a second artificial minimum where the MINUIT routines can be trapped. Thus, one has to carefully check the results provided by MINUIT. If the routines got trapped, it is easiest to rerun MINUIT choosing a different set of initial values for the parameters to avoid the artificial minimum.

Of course, the χ^2 -function depends on the observables and their correlations that are considered in a specific fit. It is important that the experimental information on the input parameters as stated in Appendix C is taken into account. A measurement of an input parameter, being independent of the other observables in the fit, is simply included as one of the observables. For deriving bounds, we moreover require $m_H > 114$ GeV.

The Fortran interface between ZFITTER and MINUIT, as used for SM fits, has been kindly provided by Prof. G. Quast. We have added the necessary extensions for fits in the 5DSM. This is also the case for the convenient user interface reading fit parameters and observables from an input file and providing the fit information in output files.

Appendix E

The Unified Approach in Statistics

In Section 4.2, we have introduced different statistical methods to derive bounds on parameters which can have unphysical values. We briefly explain the unified approach [69] and how it compares to (4.25) and (4.26).

To introduce the notation, we first consider a set of observables, in our case the precision observables or the LEP2 cross sections and asymmetries, which are assumed to be measured (at least approximately) with a Gaussian distribution around their true values. These true values are assumed to be (at least approximately) a linear function of a model parameter Θ , in our case X . The model parameter Θ is not a priori known but has to be estimated from the data set. The estimator $\bar{\Theta}$ is usually found by minimizing the appropriate χ^2 -function (4.24). It can be shown [68] that the estimator $\bar{\Theta}$ also obeys a Gaussian distribution around the true model parameter Θ , i.e. its likelihood is given by

$$P(\bar{\Theta}|\Theta) \sim \exp\left(-\frac{1}{2}\frac{(\bar{\Theta}-\Theta)^2}{\sigma^2}\right), \quad (\text{E.1})$$

where σ is a function of the uncertainties of the different observables and their sensitivities with respect to Θ .

If the parameter space for Θ is unrestricted confidence intervals are easily constructed. In the first step, for a given Θ , we can determine a lower and an upper bound $\bar{\Theta}_l$ and $\bar{\Theta}_u$ on the estimators such that

$$P(\bar{\Theta}_l < \bar{\Theta} < \bar{\Theta}_u|\Theta) = \int_{\bar{\Theta}_l}^{\bar{\Theta}_u} C \exp\left(-\frac{1}{2}\frac{(\bar{\Theta}-\Theta)^2}{\sigma^2}\right) d\bar{\Theta} = \alpha, \quad (\text{E.2})$$

where α is the confidence level, e.g. $\alpha = 0.95$, and C is an appropriate constant to normalize the probability distribution. By definition, only $(1 - \alpha)$ experiments yield an estimator outside the interval $[\bar{\Theta}_l, \bar{\Theta}_u]_{\Theta}$. However, $\bar{\Theta}_l$ and $\bar{\Theta}_u$ are not uniquely determined. The

remaining ambiguity can be removed by requiring an ordering principle for the inclusion of different values of $\bar{\Theta}$. The simplest ordering principle, i.e. including values of $\bar{\Theta}$ according to the size of their likelihood, leads to symmetric intervals with

$$\bar{\Theta}_l = \Theta - n\sigma \quad \text{and} \quad \bar{\Theta}_u = \Theta + n\sigma \quad (\text{E.3})$$

at the $n\sigma$ confidence level.

Finally, to estimate a confidence interval $[\Theta_l, \Theta_u]$ for the model parameter Θ , one includes Θ if $\bar{\Theta} \in [\bar{\Theta}_l, \bar{\Theta}_u]_{\Theta}$. Thus, in a fraction α of the experiments the true parameter Θ lies inside the estimated interval, as it should. This is Neyman's construction [69] for confidence intervals in the simple case where the observables are distributed according to a Gaussian and the parameter dependence is linear. Practically, the interval for Θ is most easily constructed by determining the χ^2 -function. For a given set of data, according to the assumptions, one finds

$$\chi^2(\Theta) = \chi_{\min}^2 + \Delta\chi^2(\Theta) = \chi^2(\bar{\Theta}) + \frac{(\bar{\Theta} - \Theta)^2}{\sigma^2}. \quad (\text{E.4})$$

Using (E.3), one recovers the well known fact that finding Θ_l and Θ_u amounts to finding the two roots of $\Delta\chi^2(\Theta) = n^2$, i.e. $\Theta_l = \bar{\Theta} - n\sigma$ and $\Theta_u = \bar{\Theta} + n\sigma$.

The problem becomes more complex if some part of the parameter space has no physical meaning, in our case $X < 0$. With the above construction, it is possible that the resulting confidence interval completely lies within the unphysical region. There are several possibilities to circumvent this problem. Here, we introduce the unified approach [69] which does not use Bayesian techniques and yields correct intervals in the sense of the frequentist's approach.

In the unified approach, only the afore mentioned ordering principle is altered. Here, one does not use the likelihood (E.1) as an ordering principle. Instead, one uses the likelihood ratio

$$R \sim P(\bar{\Theta}|\Theta)/P(\bar{\Theta}|\Theta_{\text{best}}), \quad (\text{E.5})$$

where Θ_{best} denotes the value of Θ in the physical region which leads to the largest likelihood $P(\bar{\Theta}|\Theta)$. As long as $\bar{\Theta}$ lies in the physical region, the denominator is simply a constant and R coincides with the simple likelihood if it is properly normalized. However, for an $\bar{\Theta}$ in the unphysical region R is larger than the simple likelihood. As a result, the confidence intervals for values of Θ close to the unphysical region become more and more asymmetric and are deformed into the unphysical region. An empty set for the confidence interval for Θ is thus avoided.

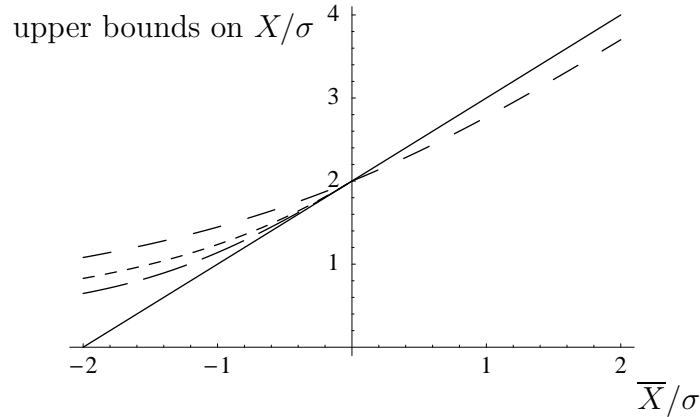


Figure E.1: 2σ upper bounds on X/σ as a function of \bar{X}/σ . Solid: $X < 0$ is also a physical value. Dashed: Bayesian approach according to (4.25). Short dashed: bounds according to (4.26). Long Dashed: unified approach. For $\bar{X} > 0$, only the Bayesian approach gives a different result.

To be specific, we concentrate on the case of the compactification scale parameterized by X which has a physical meaning only for $X \geq 0$. For $\bar{X} < 0$, we find

$$R(\bar{X} < 0|X) \sim \exp\left(-\frac{1}{2}\frac{(\bar{X} - X)^2}{\sigma^2}\right) / \exp\left(-\frac{1}{2}\frac{\bar{X}^2}{\sigma^2}\right). \quad (\text{E.6})$$

For $\bar{X} > 0$, we trivially have

$$R(\bar{X} > 0|X) \sim \exp\left(-\frac{1}{2}\frac{(\bar{X} - X)^2}{\sigma^2}\right). \quad (\text{E.7})$$

The problem of determining confidence intervals in the unified approach is now reduced to solving (E.2), where $\bar{\Theta}_l = \bar{X}_l$ and $\bar{\Theta}_u = \bar{X}_u$ are related by

$$R(\bar{X}_l|X) = R(\bar{X}_u|X). \quad (\text{E.8})$$

For the interesting case $\bar{X}_l < 0$, equation (E.8) leads to the relation

$$\bar{X}_u = X \left(1 + \sqrt{1 - 2\bar{X}_l/X}\right). \quad (\text{E.9})$$

Equation (E.2) can now be solved numerically for any given X and any confidence level. Finally, we search for a confidence interval for X given some experimentally determined \bar{X} . For $\bar{X} < 0$, the interval contains parts of the unphysical parameter space and one only states the largest X in the confidence interval as the bound on X . To calculate this bound, we search for the value of X which solves (E.2) with $\bar{X}_l = \bar{X}$ and \bar{X}_u given by (E.9).

Figure E.1 visualizes how the unified approach compares to (4.26) and the Bayesian approach (4.25). The 2σ bounds are shown as a function of \bar{X} , where both axes are normalized to σ . For $\bar{X}/\sigma < 0$, the Bayesian bound is least stringent. For $\bar{X}/\sigma < -2$, as expected the confidence interval is empty in the physical region if the simple likelihood is used as an ordering tool. Equation (4.26) yields a good approximation for the bounds from the unified approach unless \bar{X} lies far in the unphysical region.

The unified approach is well motivated and correct in the statistical sense. However, if the parameter dependence of the observables cannot be approximated as linear, bounds from (4.26) are still easily calculated while the unified approach becomes more and more complicated. Therefore, the bounds in Chapter (E.3) are calculated according to (4.26).

Appendix F

$\Delta_{\mathcal{O}}^{5\text{DSM}}$ for Precision Observables

In this appendix we explicitly state the shifts $\Delta_{\mathcal{O}}^{5\text{DSM}}$ in the predictions for electroweak precision observables in (4.1). The shifts are model dependent and we therefore present them one model at a time. For a few exemplary observables, explicit calculations for the shifts can be found in [18].

F.1 $\text{SU}(2)_L \otimes \text{U}(1)_Y$ -Bulk Model

In Table F.1, we present predictions for $\Delta_{\mathcal{O}}^{5\text{DSM}}/X$ in the bulk-bulk model, where $\Delta_{\mathcal{O}}^{5\text{DSM}}$ and X are defined by (4.1) and (4.3), respectively. The auxiliary parameters in Table F.1 are given by

$$\begin{aligned}
 \Delta_V &= \frac{4 Q_f \hat{s}_W^2}{2T_{3f} - 4Q_f \hat{s}_W^2} \Delta_\theta, \\
 \Delta_f &= \frac{8 \hat{s}_W^2 Q_f (2T_{3f} - 4Q_f \hat{s}_W^2)}{(2T_{3f} - 4Q_f \hat{s}_W^2)^2 + (2T_{3f})^2} \Delta_\theta, \\
 \Delta_h &= \frac{8 \hat{s}_W^2 \sum_q Q_q (2T_{3q} - 4Q_q \hat{s}_W^2)}{\sum_q [(2T_{3q} - 4Q_q \hat{s}_W^2)^2 + (2T_{3q})^2]} \Delta_\theta, \\
 Q_W^{\text{SM}} &= (Z - N) - 4Z \hat{s}_W^2,
 \end{aligned} \tag{F.1}$$

where Q_f and T_{3f} are the electric charge and the third component of the weak isospin of a fermion f , $q = u, d, c, s, b$, $N = 78$ is the number of neutrons, and $Z = 55$ the number of protons in the cesium nucleus. In (F.1), the parameters Δ_V , Δ_f and Δ_h are proportional to Δ_θ defined in (4.12), since they arise from substituting s_W^2 by \hat{s}_W^2 into the different electroweak observables. In detail, Δ_V parameterizes the higher-dimensional shift in the

Observable	$\Delta_{\mathcal{O}}^{5\text{DSM}}/X$
M_W	$\frac{1}{2} \left(s_\beta^4 \hat{s}_W^2 + \frac{\hat{s}_W^2}{c_W^2} \Delta_\theta \right)$
$\Gamma_Z(\nu\bar{\nu})$	$\hat{s}_W^2 (s_\beta^2 - 1)^2 - 1$
$\Gamma_Z(l^+l^-)$	$\hat{s}_W^2 (s_\beta^2 - 1)^2 - 1 + \Delta_l$
$\Gamma_Z(\text{had})$	$\hat{s}_W^2 (s_\beta^2 - 1)^2 - 1 + \Delta_h$
$Q_W(\text{Cs})$	$\left[(1 - s_\beta^2)^2 + 4Z (Q_W^{\text{SM}})^{-1} \Delta_\theta \right] \hat{s}_W^2$
R_l	$-\Delta_l + \Delta_h$
R_q	$\Delta_q - \Delta_h$
A_f	$\Delta_V - \Delta_f$
$A_{\text{FB}}^{(0,f)}$	$\Delta_V - \Delta_f + f \leftrightarrow e$

Table F.1: Predictions for $\Delta_{\mathcal{O}}^{5\text{DSM}}/X$ in the $\text{SU}(2)_L \otimes \text{U}(1)_Y$ -bulk model. The auxiliary parameters Δ_V , Δ_f and Δ_h are defined in (F.1).

vector coupling of the Z boson to fermions. Δ_f results from an analogous KK shift in the sum of the squared vector and axial vector couplings for a given fermion f . Similarly, Δ_h gives the corresponding KK shift in the total hadronic width of the Z boson.

F.2 $\text{SU}(2)_L$ -Brane, $\text{U}(1)_Y$ -Bulk Model

With the help of some new auxiliary parameters, we exhibit in Table F.2 the tree-level shifts $\Delta_{\mathcal{O}}^{5\text{DSM}}$ to the different electroweak observables for the brane-bulk model. The parameters δ_V and δ_A give the higher-dimensional modifications in the vector and axial-vector part of the $Z\bar{f}f$ coupling except of the modifications which are due to the difference between θ_W and $\hat{\theta}_W$. We have

$$\begin{aligned} \delta_V &= \frac{-2T_{3f}\hat{s}_W^2 + 4Q_f\hat{s}_W^2}{2T_{3f} - 4Q_f\hat{s}_W^2}, \\ \delta_A &= -\hat{s}_W^2. \end{aligned} \tag{F.2}$$

Observable	$\Delta_{\mathcal{O}}^{5\text{DSM}}/X$
M_W	$\frac{1}{2}(\hat{s}_W^2 \hat{c}_W^2 / \hat{c}_{2W})$
$\Gamma_Z(\nu\bar{\nu})$	$-\hat{s}_W^2$
$\Gamma_Z(l^+l^-)$	$\hat{s}_W^2 + \Delta_l + \delta_l$
$\Gamma_Z(\text{had})$	$\hat{s}_W^2 + \Delta_h + \delta_h$
$Q_W(\text{Cs})$	$4Z(Q_W^{\text{SM}})^{-1}\hat{s}_W^2\Delta_\theta$
R_l	$-\Delta_l + \Delta_h - \delta_l + \delta_h$
R_q	$\Delta_q - \Delta_h + \delta_q - \delta_h$
A_f	$\Delta_V - \Delta_f - \delta_f + \delta_V + \delta_A$
$A_{\text{FB}}^{(0,f)}$	$\Delta_V - \Delta_f - \delta_f + \delta_V + \delta_A + f \leftrightarrow e$

Table F.2: Predictions for $\Delta_{\mathcal{O}}^{5\text{DSM}}/X$ in the $SU(2)_L$ -brane, $U(1)_Y$ -bulk model. See text for the definition of the auxiliary parameters.

The parameter

$$\delta_f = \frac{(-16T_{3f}^2 + 16T_{3f}Q_f)\hat{s}_W^2 + (16T_{3f}Q_f - 32Q_f^2)\hat{s}_W^4}{(2T_{3f} - 4Q_f\hat{s}_W^2)^2 + (2T_{3f})^2} \quad (\text{F.3})$$

quantifies the shift in the sum of the squared vector and axial vector couplings of a given fermion f to the Z boson. In analogy to Δ_h , we finally define ($q = u, d, c, s, b$)

$$\delta_h = \frac{\sum_q [(-16T_{3f}^2 + 16T_{3f}Q_f)\hat{s}_W^2 + (16T_{3f}Q_f - 32Q_f^2)\hat{s}_W^4]}{\sum_q [(2T_{3f} - 4Q_f\hat{s}_W^2)^2 + (2T_{3f})^2]}. \quad (\text{F.4})$$

The parameters Δ_V , Δ_f and Δ_h , used in Table F.2, are defined in (F.1) with Δ_θ given by (4.18).

F.3 $SU(2)_L$ -Bulk, $U(1)_Y$ -Brane Model

As in the previous section, we introduce the auxiliary parameters Δ_V , Δ_f , Δ_h , δ_V , δ_A , δ_f , and δ_h to state the tree-level shifts $\Delta_{\mathcal{O}}^{5\text{DSM}}$ for the bulk-brane model in Table F.3.

Observable	$\Delta_{\mathcal{O}}^{5\text{DSM}}/X$
M_W	$\frac{1}{2}(\hat{s}_W^2 \hat{c}_W^2 / \hat{c}_{2W})$
$\Gamma_Z(\nu\bar{\nu})$	$-\hat{c}_W^2$
$\Gamma_Z(l^+l^-)$	$\hat{c}_W^2 + \Delta_l + \delta_l$
$\Gamma_Z(\text{had})$	$\hat{c}_W^2 + \Delta_h + \delta_h$
$Q_W(\text{Cs})$	$4Z(Q_W^{\text{SM}})^{-1}\hat{s}_W^2\Delta_\theta$
R_l	$-\Delta_l + \Delta_h - \delta_l + \delta_h$
R_q	$\Delta_q - \Delta_h + \delta_q - \delta_h$
A_f	$\Delta_V - \Delta_f - \delta_f + \delta_V + \delta_A$
$A_{\text{FB}}^{(0,f)}$	$\Delta_V - \Delta_f - \delta_f + \delta_V + \delta_A + f \leftrightarrow e$

Table F.3: Predictions for $\Delta_{\mathcal{O}}^{5\text{DSM}}/X$ in the $\text{SU}(2)_L$ -bulk, $\text{U}(1)_Y$ -brane model. See text for the definition of the auxiliary parameters.

Δ_V , Δ_f , Δ_h are given by (F.1), with Δ_θ defined in (4.23), while δ_V , δ_A , δ_f , and δ_h read ($q = u, d, c, s, b$)

$$\begin{aligned}
\delta_V &= -\frac{2T_{3f}\hat{c}_W^2}{2T_{3f} - 4Q_f\hat{s}_W^2}, \\
\delta_A &= -\hat{c}_W^2, \\
\delta_f &= \frac{(-16T_{3f}^2 + 16T_{3f}Q_f\hat{s}_W^2)\hat{c}_W^2}{(2T_{3f} - 4Q_f\hat{s}_W^2)^2 + (2T_{3f})^2}, \\
\delta_h &= \frac{\sum_q (-16T_{3f}^2 + 16T_{3f}Q_f\hat{s}_W^2)\hat{c}_W^2}{\sum_q [(2T_{3f} - 4Q_f\hat{s}_W^2)^2 + (2T_{3f})^2]}.
\end{aligned} \tag{F.5}$$

Appendix G

Kaluza-Klein $W_{(0)}W_{(0)}Z_{(n)}$ and $W_{(0)}W_{(0)}\gamma_{(n)}$ Couplings

For models with a brane Higgs boson, we present the Feynman rules for the triple gauge boson vertices shown in Fig. G.1. In the gauge basis, only the $W_{(0)}^+W_{(0)}^-Z_{(0)}$ and $W_{(0)}^+W_{(0)}^-\gamma_{(0)}$ vertices exist while the vertices $W_{(0)}^+W_{(0)}^-Z_{(n)}$ and $W_{(0)}^+W_{(0)}^-\gamma_{(n)}$ with $n \geq 1$ are forbidden by KK selection rules [42, 56]. However, in the mass eigenstate basis, couplings to heavy KK states are induced by the diagonalization of the gauge-boson mass matrix. Below, we give these couplings to first order in X . To this order the zero-mode couplings are unaffected, that is

$$g_{3(0)}^Z = g \cos \theta_W, \quad g_{3(0)}^\gamma = e \quad (\text{G.1})$$

with g from (3.45). For the higher modes ($n \geq 1$), one gets

$$g_{3(n)}^Z = \sqrt{2} e \frac{\hat{c}_W}{\hat{s}_W} (\hat{s}_W^2 - \hat{c}_W^2) s_\beta^2 \frac{3}{n^2 \pi^2} X, \quad (\text{G.2})$$

$$g_{3(n)}^\gamma = -\sqrt{2} e \hat{c}_W^2 s_\beta^2 \frac{6}{n^2 \pi^2} X \quad (\text{G.3})$$

in the bulk-bulk model with a brane Higgs,

$$g_{3(n)}^Z = \sqrt{2} e \hat{c}_W \frac{3}{n^2 \pi^2} X \quad (\text{G.4})$$

in the brane-bulk model, and

$$g_{3(n)}^Z = -\sqrt{2} e \frac{\hat{c}_W^2}{\hat{s}_W} \frac{3}{n^2 \pi^2} X \quad (\text{G.5})$$

in the bulk-brane model. In the latter two models, the $\gamma_{(n)}$ modes for $n \geq 1$ are absent.

Appendix H

Kaluza-Klein $H_{(0)}Z_{(0)}Z_{(n)}$ Couplings

In the bulk-bulk model with a bulk Higgs field, the KK selection rules forbid the couplings of two zero modes to higher modes. Moreover, the gauge eigenstates coincide with the mass eigenstates. Thus, for zero-mode final states, Higgsstrahlung is described by the same $H_{(0)}Z_{(0)}Z_{(0)}$ vertex as in the SM. In the bulk-bulk model with a brane Higgs only, the HZZ coupling can be derived in the gauge basis from

$$\begin{aligned}\mathcal{L}_{\text{HZZ}}(x) &= \frac{1}{4} \frac{g^2 v}{c_W^2} h \left(Z_{(0)}^\mu + \sum_{n=1}^{\infty} \sqrt{2} Z_{(n)}^\mu \right)^2 \\ &= \frac{g}{2} \frac{m_{Z(0)}}{c_W} \left(1 - \frac{\Delta_Z}{2} X \right) h \left(Z_{(0)}^\mu + \sum_{n=1}^{\infty} \sqrt{2} Z_{(n)}^\mu \right)^2,\end{aligned}\tag{H.1}$$

where h denotes the Higgs field on the brane and v its VEV. The second relation follows from (4.2). In the brane-bulk or bulk-brane model, the $Z_{(n)}^\mu$ tower coincides with the $U(1)_Y$ or $SU(2)_L$ KK modes for $n \geq 1$, respectively. Since a brane Higgs field breaks momentum conservation in the extra dimension, there are no selection rules.

In the mass eigenstate basis, the Lagrangian (H.1) leads to the vertex shown in Fig. H.1. In summary, the effective couplings are given by

$$g_{(0)}^{\text{ZH}} = g \quad \text{and} \quad g_{(n \geq 1)}^{\text{ZH}} = 0\tag{H.2}$$

in the bulk-bulk model with a bulk Higgs,

$$\begin{aligned}g_{(0)}^{\text{ZH}} &= g \left[1 - \left(2 + \frac{\Delta_Z}{2} \right) X \right], \\ g_{(n \geq 1)}^{\text{ZH}} &= \sqrt{2} g \left[1 - \left(1 + \frac{3}{2n^2\pi^2} + \frac{\Delta_Z}{2} \right) X \right]\end{aligned}\tag{H.3}$$

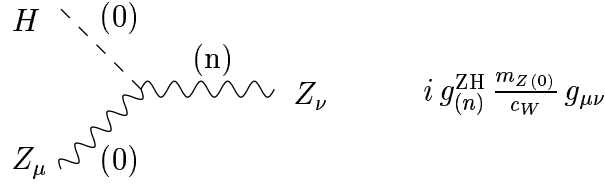


Figure H.1: The HZZ vertex. The numbers in parenthesis specify the KK modes.

in the bulk-bulk model with a brane Higgs,

$$g_{(0)}^{\text{ZH}} = g \left[1 - \left(2 \hat{s}_W^2 + \frac{\Delta_Z}{2} \right) X \right],$$

$$g_{(n \geq 1)}^{\text{ZH}} = \sqrt{2} s_W g \left[1 - \left(\hat{s}_W^2 + (3 \hat{s}_W^2 - 2) \frac{3}{2 n^2 \pi^2} + \frac{\Delta_Z}{2} \right) X \right]$$
(H.4)

in the brane-bulk model, and

$$g_{(0)}^{\text{ZH}} = g \left[1 - \left(2 \hat{c}_W^2 + \frac{\Delta_Z}{2} \right) X \right],$$

$$g_{(n \geq 1)}^{\text{ZH}} = \sqrt{2} c_W g \left[1 - \left(\hat{c}_W^2 + (3 \hat{c}_W^2 - 2) \frac{3}{2 n^2 \pi^2} + \frac{\Delta_Z}{2} \right) X \right]$$
(H.5)

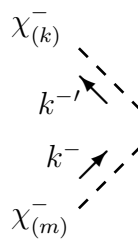
in the bulk-brane model. The factor $\sqrt{2}$ in $g_{(n \geq 1)}^{\text{ZH}}$ is the usual enhancement of couplings between higher KK modes and brane fields. The factors s_W and c_W reflect the fact that for $n \geq 1$ $Z_{(n)}^\mu$ is mainly $B_{(n)}^\mu$ or $A_{(n)}^{3\mu}$, respectively.

Appendix I

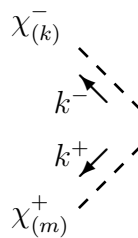
Feynman Rules for W Bosons and the Associated Goldstone Modes

Figures I.1, I.2, and I.3 list the relevant Feynman rules for W -pair production and the production of the associated Goldstone modes in the bulk-bulk model, as discussed in Chapter 6. The scalar modes χ^\pm are defined in (3.12). The Feynman rules are given in the weak basis, not in the basis of mass eigenstates. For the W -boson zero modes, the couplings to the Z -boson and photon KK modes in the mass eigenbasis are explicitly given in Appendix G.

Where it is important, arrows indicate if the particles are incoming or outgoing. One has to be aware of additional minus signs for complex fields, e.g. the second Feynman rule in Fig. I.2 can be also formulated as follows:



$$Z_{(l)\nu} = i e \frac{\frac{1}{2} - s_W^2}{c_W s_W} \left(\frac{1}{\sqrt{2}} \right)^{(\delta_{k,0} + \delta_{l,0} + \delta_{m,0} + 1)} \delta_{k,l,m} (-k^{-'} - k^-)^\mu ,$$



$$Z_{(l)\nu} = i e \frac{\frac{1}{2} - s_W^2}{c_W s_W} \left(\frac{1}{\sqrt{2}} \right)^{(\delta_{k,0} + \delta_{l,0} + \delta_{m,0} + 1)} \delta_{k,l,m} (k^+ - k^-)^\mu .$$

$W_{(m)\mu}^+$
 k^+
 k^-
 q
 $A_{(n)\lambda} = i e \left(\frac{1}{\sqrt{2}}\right)^{(\delta_{k,0} + \delta_{l,0} + \delta_{m,0} + 1)} \delta_{k,l,m} [g_{\mu\nu} (k^- - k^+)_{\lambda} + g_{\nu\lambda} (-q - k^-)_{\mu} + g_{\lambda\mu} (k^+ + q)_{\nu}]$
 $W_{(l)\nu}^-$

$W_{(k)5}^{\pm}$
 $A_{(l)\nu} = \pm e g_{\mu\nu} \left[\left(\frac{m}{R}\right) \left(\frac{1}{\sqrt{2}}\right)^{(\delta_{l,0} + 1)} \tilde{\delta}_{k,l,m} - \left(\frac{l}{R}\right) \left(\frac{1}{\sqrt{2}}\right)^{(\delta_{m,0} + 1)} \tilde{\delta}_{k,m,l} \right]$
 $W_{(m)\mu}^{\mp}$

$W_{(k)5}^+$
 k^+
 k^-
 $A_{(l)\nu} = i e \left(\frac{1}{\sqrt{2}}\right)^{(\delta_{l,0} + 1)} \tilde{\delta}_{k,l,m} (k^+ - k^-)^{\mu}$
 $W_{(m)5}^-$

$\chi_{(k)5}^{\pm}$
 $A_{(l)\nu} = \pm e \frac{qv}{2} g_{\mu\nu} \left(\frac{1}{\sqrt{2}}\right)^{(\delta_{k,0} + \delta_{l,0} + \delta_{m,0} + 1)} \delta_{k,l,m}$
 $W_{(m)\mu}^{\mp}$

$\chi_{(k)5}^+$
 k^+
 k^-
 $A_{(l)\nu} = i e \left(\frac{1}{\sqrt{2}}\right)^{(\delta_{k,0} + \delta_{l,0} + \delta_{m,0} + 1)} \delta_{k,l,m} (k^+ - k^-)^{\mu}$
 $\chi_{(m)5}^-$

Figure I.1: Vertices for the coupling of the photon KK modes to W -boson and scalar modes living in the bulk in the weak eigenbasis.

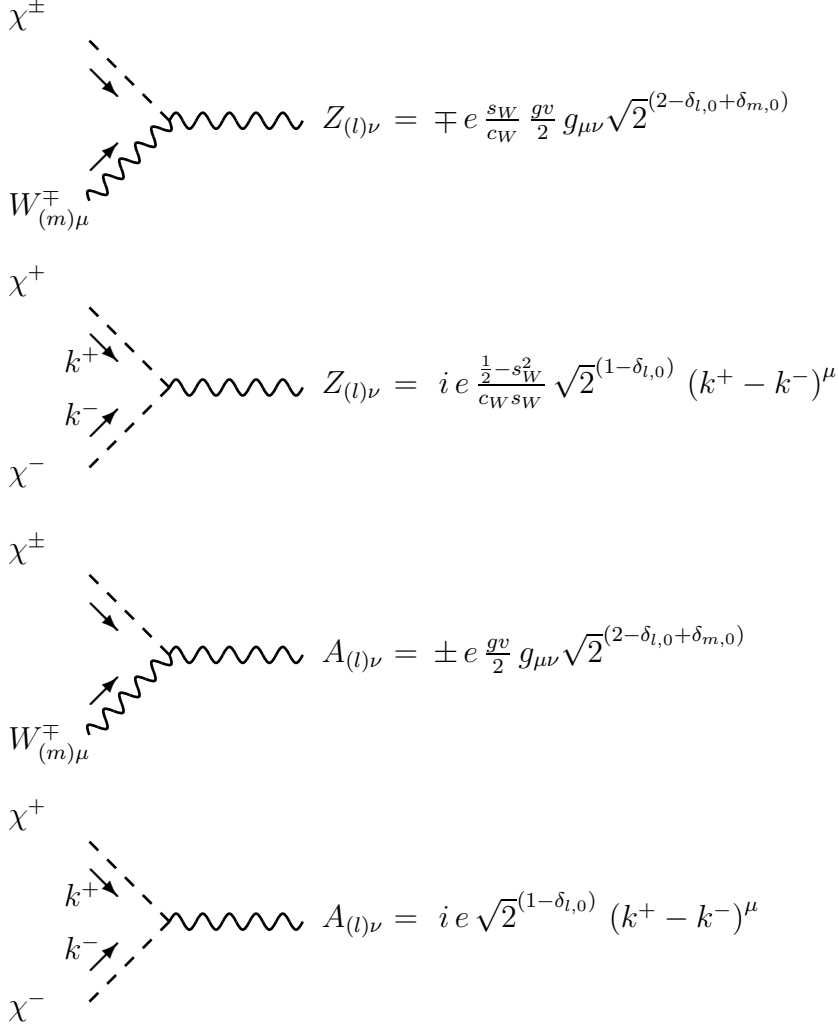


Figure I.3: Vertices for the coupling of the Z -boson and photon modes to charged scalar modes being restricted to the brane $y = 0$ in the weak eigenbasis.

Bibliography

- [1] T. Kaluza, “On the problem of unity in physics,” *Sitzungsber. Preuss. Akad. Wiss. Berlin (Math. Phys.)* **1921** (1921) 966.
- [2] O. Klein, “Quantum theory and five-dimensional theory of relativity,” *Z. Phys.* **37** (1926) 895.
- [3] F. Feruglio, “Extra dimensions in particle physics,” [hep-ph/0401033](#).
- [4] M. B. Green, J. H. Schwarz, and E. Witten, *Superstring theory VOL. 1: Introduction*. University Press (Cambridge Monographs On Mathematical Physics), Cambridge, Uk, 1987.
- [5] I. Antoniadis, “A possible new dimension at a few TeV,” *Phys. Lett.* **B246** (1990) 377.
- [6] J. D. Lykken, “Weak scale superstrings,” *Phys. Rev.* **D54** (1996) 3693, [hep-th/9603133](#).
- [7] E. Witten, “Strong coupling expansion of Calabi-Yau compactification,” *Nucl. Phys.* **B471** (1996) 135, [hep-th/9602070](#).
- [8] P. Horava and E. Witten, “Eleven-dimensional supergravity on a manifold with boundary,” *Nucl. Phys.* **B475** (1996) 94, [hep-th/9603142](#).
- [9] N. Arkani-Hamed, S. Dimopoulos, and G. R. Dvali, “The hierarchy problem and new dimensions at a millimeter,” *Phys. Lett.* **B429** (1998) 263, [hep-ph/9803315](#).
- [10] I. Antoniadis, N. Arkani-Hamed, S. Dimopoulos, and G. R. Dvali, “New dimensions at a millimeter to a Fermi and superstrings at a TeV,” *Phys. Lett.* **B436** (1998) 257, [hep-ph/9804398](#).
- [11] N. Arkani-Hamed, S. Dimopoulos, and G. R. Dvali, “Phenomenology, astrophysics and cosmology of theories with sub-millimeter dimensions and TeV scale quantum gravity,” *Phys. Rev.* **D59** (1999) 086004, [hep-ph/9807344](#).

- [12] K. R. Dienes, E. Dudas, and T. Gherghetta, “Extra spacetime dimensions and unification,” *Phys. Lett.* **B436** (1998) 55, [hep-ph/9803466](#).
- [13] C. Csaki, “TASI lectures on extra dimensions and branes,” [hep-ph/0404096](#).
- [14] C. D. Hoyle *et al.*, “Sub-millimeter tests of the gravitational inverse-square law,” [hep-ph/0405262](#).
- [15] L. Randall and R. Sundrum, “A large mass hierarchy from a small extra dimension,” *Phys. Rev. Lett.* **83** (1999) 3370, [hep-ph/9905221](#).
- [16] L. Randall and R. Sundrum, “An alternative to compactification,” *Phys. Rev. Lett.* **83** (1999) 4690, [hep-th/9906064](#).
- [17] I. Antoniadis and K. Benakli, “Large dimensions and string physics in future colliders,” *Int. J. Mod. Phys.* **A15** (2000) 4237, [hep-ph/0007226](#).
- [18] A. Mück, “Large Extra Dimensions: A 5D Standard Model,” 2004. Diploma thesis.
- [19] H. Georgi, A. K. Grant, and G. Hailu, “Chiral fermions, orbifolds, scalars and fat branes,” *Phys. Rev.* **D63** (2001) 064027, [hep-ph/0007350](#).
- [20] J. Papavassiliou and A. Santamaria, “Chiral fermions and gauge fixing in five-dimensional theories,” *Phys. Rev.* **D63** (2001) 125014, [hep-ph/0102019](#).
- [21] T. Appelquist, H.-C. Cheng, and B. A. Dobrescu, “Bounds on universal extra dimensions,” *Phys. Rev.* **D64** (2001) 035002, [hep-ph/0012100](#).
- [22] K. Agashe, N. G. Deshpande, and G. H. Wu, “Universal extra dimensions and $b \rightarrow s$ gamma,” *Phys. Lett.* **B514** (2001) 309, [hep-ph/0105084](#).
- [23] C. Macesanu, C. D. McMullen, and S. Nandi, “Collider implications of universal extra dimensions,” *Phys. Rev.* **D66** (2002) 015009, [hep-ph/0201300](#).
- [24] T. G. Rizzo, “Probes of universal extra dimensions at colliders,” *Phys. Rev.* **D64** (2001) 095010, [hep-ph/0106336](#).
- [25] F. J. Petriello, “Kaluza-Klein effects on Higgs physics in universal extra dimensions,” *JHEP* **05** (2002) 3, [hep-ph/0204067](#).
- [26] A. J. Buras, M. Spranger, and A. Weiler, “The impact of universal extra dimensions on the unitarity triangle and rare K and B decays.,” *Nucl. Phys.* **B660** (2003) 225, [hep-ph/0212143](#).

- [27] P. Bucci and B. Grzadkowski, “The effective potential and vacuum stability within universal extra dimensions,” *Phys. Rev.* **D68** (2003) 124002, [hep-ph/0304121](#).
- [28] J. F. Oliver, J. Papavassiliou, and A. Santamaria, “Universal extra dimensions and $Z \rightarrow b$ anti- b ,” *Phys. Rev.* **D67** (2003) 056002, [hep-ph/0212391](#).
- [29] J. F. Oliver, *Aspects of universal extra dimensional models and their latticized versions*. PhD thesis, University of Valencia, 2004. [hep-ph/0403095](#).
- [30] I. Antoniadis, E. Kiritsis, and T. N. Tomaras, “A D-brane alternative to unification,” *Phys. Lett.* **B486** (2000) 186, [hep-ph/0004214](#).
- [31] P. Nath and M. Yamaguchi, “Effects of Kaluza-Klein excitations on $(g - 2)_\mu$,” *Phys. Rev.* **D60** (1999) 116006, [hep-ph/9903298](#).
- [32] P. Nath, Y. Yamada, and M. Yamaguchi, “Probing the nature of compactification with Kaluza-Klein excitations at the Large Hadron Collider,” *Phys. Lett.* **B466** (1999) 100, [hep-ph/9905415](#).
- [33] W. J. Marciano, “Fermi constants and new physics,” *Phys. Rev.* **D60** (1999) 093006, [hep-ph/9903451](#).
- [34] M. Masip and A. Pomarol, “Effects of SM Kaluza-Klein excitations on electroweak observables,” *Phys. Rev.* **D60** (1999) 096005, [hep-ph/9902467](#).
- [35] R. Casalbuoni, S. De Curtis, D. Dominici, and R. Gatto, “SM Kaluza-Klein excitations and electroweak precision tests,” *Phys. Lett.* **B462** (1999) 48–54, [hep-ph/9907355](#).
- [36] C. D. Carone, “Electroweak constraints on extended models with extra dimensions,” *Phys. Rev.* **D61** (2000) 015008, [hep-ph/9907362](#).
- [37] A. Delgado, A. Pomarol, and M. Quiros, “Electroweak and flavor physics in extensions of the standard model with large extra dimensions,” *JHEP* **01** (2000) 30, [hep-ph/9911252](#).
- [38] T. G. Rizzo and J. D. Wells, “Electroweak precision measurements and collider probes of the standard model with large extra dimensions,” *Phys. Rev.* **D61** (2000) 016007, [hep-ph/9906234](#).
- [39] A. Strumia, “Bounds on Kaluza-Klein excitations of the SM vector bosons from electroweak tests,” *Phys. Lett.* **B466** (1999) 107, [hep-ph/9906266](#).

- [40] A. Delgado, A. Pomarol, and M. Quiros, “Supersymmetry and electroweak breaking from extra dimensions at the TeV-scale,” *Phys. Rev.* **D60** (1999) 095008, hep-ph/9812489.
- [41] K. Cheung and G. Landsberg, “Kaluza-Klein states of the standard model gauge bosons: Constraints from high-energy experiments,” *Phys. Rev.* **D65** (2002) 076003, hep-ph/0110346.
- [42] A. Mück, A. Pilaftsis, and R. Rückl, “Minimal higher-dimensional extensions of the standard model and electroweak observables,” *Phys. Rev.* **D65** (2002) 085037, hep-ph/0110391.
- [43] A. Mück, A. Pilaftsis, and R. Rückl, “Probing minimal 5D extensions of the standard model: From LEP to an e^+e^- linear collider,” *Nucl. Phys.* **B687** (2004) 55, hep-ph/0312186.
- [44] J. M. Cornwall, D. N. Levin, and G. Tiktopoulos, “Derivation of gauge invariance from high-energy unitarity bounds on the S-matrix,” *Phys. Rev.* **D10** (1974) 1145.
- [45] M. S. Chanowitz and M. K. Gaillard, “The TeV physics of strongly interacting W ’s and Z ’s,” *Nucl. Phys.* **B261** (1985) 379.
- [46] S. De Curtis, D. Dominici, and J. R. Pelaez, “The equivalence theorem for gauge boson scattering in a five-dimensional standard model,” *Phys. Lett.* **B554** (2003) 164, hep-ph/0211353.
- [47] T. Ohl and C. Schwinn, “Unitarity, BRST symmetry and Ward identities in orbifold gauge theories,” hep-ph/0312263.
- [48] R. S. Chivukula, D. A. Dicus, and H.-J. He, “Unitarity of compactified five-dimensional Yang-Mills theory,” *Phys. Lett.* **B525** (2002) 175, hep-ph/0111016.
- [49] R. S. Chivukula, D. A. Dicus, H.-J. He, and S. Nandi, “Unitarity of the higher-dimensional standard model,” *Phys. Lett.* **B562** (2003) 109, hep-ph/0302263.
- [50] S. De Curtis, D. Dominici, and J. R. Pelaez, “Strong tree-level unitarity violations in the extra-dimensional standard model with scalars in the bulk,” *Phys. Rev.* **D67** (2003) 076010, hep-ph/0301059.
- [51] H. Georgi, A. K. Grant, and G. Hailu, “Brane couplings from bulk loops,” *Phys. Lett.* **B506** (2001) 207, hep-ph/0012379.

- [52] M. Carena, T. M. P. Tait, and C. E. M. Wagner, “Branes and orbifolds are opaque,” *Acta Phys. Polon.* **B33** (2002) 2355, [hep-ph/0207056](#).
- [53] S. Gabriel, S. Nandi, and G. Seidl, “6D Higgsless standard model,” [hep-ph/0406020](#). And references therein.
- [54] D. M. Ghilencea, S. Groot Nibbelink, and H. P. Nilles, “Gauge corrections and FI-term in 5D KK theories,” *Nucl. Phys.* **B619** (2001) 385, [hep-th/0108184](#).
- [55] H.-C. Cheng, K. T. Matchev, and M. Schmaltz, “Radiative corrections to Kaluza-Klein masses,” *Phys. Rev.* **D66** (2002) 036005, [hep-ph/0204342](#).
- [56] D. A. Dicus, C. D. McMullen, and S. Nandi, “Collider implications of Kaluza-Klein excitations of the gluons,” *Phys. Rev.* **D65** (2002) 076007, [hep-ph/0012259](#).
- [57] M. Kubo, C. S. Lim, and H. Yamashita, “The Hosotani mechanism in bulk gauge theories with an orbifold extra space S^1/Z_2 ,” *Mod. Phys. Lett.* **A17** (2002) 2249, [hep-ph/0111327](#).
- [58] C. Csaki, C. Grojean, H. Murayama, L. Pilo, and J. Terning, “Gauge theories on an interval: Unitarity without a Higgs,” *Phys. Rev.* **D69** (2004) 055006, [hep-ph/0305237](#).
- [59] Bronstein, Semendjajew, Musiol, and Mühlig, *Taschenbuch der Mathematik*. Verlag Harri Deutsch, Frankfurt, 2. Aufl., 1995. Chapter 4.4.2.3.
- [60] N. Arkani-Hamed, A. G. Cohen, and H. Georgi, “(De)constructing dimensions,” *Phys. Rev. Lett.* **86** (2001) 4757, [hep-th/0104005](#).
- [61] C. T. Hill, S. Pokorski, and J. Wang, “Gauge invariant effective Lagrangian for Kaluza-Klein modes,” *Phys. Rev.* **D64** (2001) 105005, [hep-th/0104035](#).
- [62] **Particle Data Group** Collaboration, K. Hagiwara *et al.*, “Review of particle physics,” *Phys. Rev.* **D66** (2002) 010001.
- [63] D. Y. Bardin *et al.*, “ZFITTER v.6.21: A semi-analytical program for fermion-pair production in e^+e^- annihilation,” *Comput. Phys. Commun.* **133** (2001) 229, [hep-ph/9908433](#).
- [64] D. Y. Bardin, M. S. Bilenky, T. Riemann, M. Sachwitz, and H. Vogt, “DIZET: A program package for the calculation of electroweak one loop corrections for the process $e + e^- \rightarrow f^+ f^-$ around the Z0 peak,” *Comput. Phys. Commun.* **59** (1990) 303.

- [65] D. Y. Bardin *et al.*, “QED corrections with partial angular integration to fermion-pair production in e^+e^- annihilation,” *Phys. Lett.* **B255** (1991) 290, hep-ph/9801209.
- [66] D. Y. Bardin *et al.*, “Analytic approach to the complete set of QED corrections to fermion-pair production in e^+e^- annihilation,” *Nucl. Phys.* **B351** (1991) 1, hep-ph/9801208.
- [67] F. James and M. Roos, “MINUIT: A system for function minimization and analysis of the parameter errors and correlations,” *Comput. Phys. Commun.* **10** (1975) 343.
- [68] W. T. Eadie *et al.*, *Statistical Methods in Experimental Physics*. North-Holland, Amsterdam, 1971.
- [69] G. J. Feldman and R. D. Cousins, “A Unified approach to the classical statistical analysis of small signals,” *Phys. Rev.* **D57** (1998) 3873, physics/9711021.
- [70] **ALEPH** Collaboration, D. Abbaneo *et al.*, “A combination of preliminary electroweak measurements and constraints on the standard model,” hep-ex/0112021.
- [71] **Particle Data Group** Collaboration, D. E. Groom *et al.*, “Review of particle physics,” *Eur. Phys. J.* **C15** (2000) 1.
- [72] **ALEPH** Collaboration, R. Barate *et al.*, “Study of fermion-pair production in e^+e^- collisions at 130 GeV to 183 GeV,” *Eur. Phys. J.* **C12** (2000) 183, hep-ex/9904011.
- [73] **ALEPH** Collaboration, M. N. Minard and I. Tomalin, “Fermion-pair production in e^+e^- collisions at 189 GeV and limits on physics beyond the standard model,” Prepared for International Europhysics Conference on High-Energy Physics (EPS-HEP 99), Tampere, Finland, 15-21 Jul 1999.
- [74] **ALEPH** Collaboration, M. N. Minard, “Fermion-pair production in e^+e^- collisions from 192 to 202 GeV,” ALEPH-2000-025.
- [75] **ALEPH** Collaboration, M. N. Minard, “Fermion-pair production in e^+e^- collisions at high energy and limits on physics beyond the standard model,” ALEPH-2001-019.
- [76] **DELPHI** Collaboration, P. Abreu *et al.*, “Measurement and interpretation of fermion-pair production at LEP energies from 130 GeV to 172 GeV,” *Eur. Phys. J.* **C11** (1999) 383.

- [77] **DELPHI** Collaboration, P. Abreu *et al.*, “Measurement and interpretation of fermion-pair production at LEP energies of 183 and 189 GeV,” *Phys. Lett.* **B485** (2000) 45, [hep-ex/0103025](#).
- [78] **DELPHI** Collaboration, A. Behrmann, “Results on fermion-pair production at LEP running from 192 to 202 GeV,” DELPHI-2000-128.
- [79] **DELPHI** Collaboration, A. Behrmann, “Results on fermion-pair production at LEP running in 2000,” DELPHI-2001-094.
- [80] **L3** Collaboration, M. Acciarri *et al.*, “Measurement of hadron and lepton-pair production at $130 \text{ GeV} < \sqrt{s} < 189 \text{ GeV}$ at LEP,” *Phys. Lett.* **B479** (2000) 101, [hep-ex/0002034](#).
- [81] **OPAL** Collaboration, K. Ackerstaff *et al.*, “Tests of the standard model and constraints on new physics from measurements of fermion-pair production at 130 GeV to 172 GeV at LEP,” *Eur. Phys. J.* **C2** (1998) 441, [hep-ex/9708024](#).
- [82] **OPAL** Collaboration, G. Abbiendi *et al.*, “Tests of the standard model and constraints on new physics from measurements of fermion-pair production at 183 GeV at LEP,” *Eur. Phys. J.* **C6** (1999) 1, [hep-ex/9808023](#).
- [83] **OPAL** Collaboration, G. Abbiendi *et al.*, “Tests of the standard model and constraints on new physics from measurements of fermion-pair production at 189 GeV at LEP,” *Eur. Phys. J.* **C13** (2000) 553, [hep-ex/9908008](#).
- [84] **OPAL** Collaboration, “Tests of the standard model and constraints on new physics from measurements of fermion-pair production at 192-202 GeV at LEP,” 2000. OPAL PN 424.
- [85] **OPAL** Collaboration, “Measurement of standard model processes in e^+e^- collisions at $\sqrt{s} \sim 203 - 209 \text{ GeV}$,” 2001. OPAL PN 469.
- [86] W. Alles, C. Boyer, and A. J. Buras, “ W -boson production in e^+e^- collisions in the Weinberg-Salam model,” *Nucl. Phys.* **B119** (1977) 125.
- [87] **ECFA/DESY LC Physics Working Group** Collaboration, J. A. Aguilar-Saavedra *et al.*, “TESLA Technical Design Report Part III: Physics at an e^+e^- Linear Collider,” [hep-ph/0106315](#).
- [88] W. Kilian, M. Krämer, and P. M. Zerwas, “Higgsstrahlung and WW fusion in e^+e^- collisions,” *Phys. Lett.* **B373** (1996) 135, [hep-ph/9512355](#).

- [89] A. Aranda, C. Balazs, and J. L. Diaz-Cruz, “Where is the Higgs boson?,” *Nucl. Phys.* **B670** (2003) 90, [hep-ph/0212133](#).
- [90] S. Riemann, “Fermion-pair production at a linear collider: A sensitive tool for new physics searches,” LC-TH-2001-007.
- [91] D. Bourilkov, “Sensitivity to contact interactions and extra dimensions in di-lepton and di-photon channels at future colliders,” [hep-ph/0305125](#).
- [92] B. W. Lee, C. Quigg, and H. B. Thacker, “Weak interactions at very high energies: The role of the Higgs-boson mass,” *Phys. Rev.* **D16** (1977) 1519.
- [93] J. Horejsi, “Electroweak interactions and high-energy limit: An introduction to equivalence theorem,” *Czech. J. Phys.* **47** (1997) 951, [hep-ph/9603321](#).
- [94] C. Grosse-Knetter and I. Kuss, “The equivalence theorem and effective Lagrangians,” *Z. Phys.* **C66** (1995) 95, [hep-ph/9403291](#).
- [95] M. E. Peskin and D. V. Schroeder, “An Introduction to quantum field theory,” Reading, USA: Addison-Wesley (1995), Fig. 21.10.
- [96] A. Mück, L. Nilse, A. Pilaftsis, and R. Rückl. Work in preparation.
- [97] Bronstein, Semendjajew, Musiol, and Mühlig, *Taschenbuch der Mathematik*. Verlag Harri Deutsch, Frankfurt, 2. Aufl., 1995. Chapter 9.1.3.
- [98] L. Nilse. University of Manchester, private communications.
- [99] **D0** Collaboration, V. M. Abazov *et al.*, “A precision measurement of the mass of the top quark,” *Nature* **429** (2004) 638–642, [hep-ex/0406031](#).
- [100] T. G. Rizzo, “Kaluza-Klein / Z' differentiation at the LHC and linear collider,” *JHEP* **06** (2003) 021, [hep-ph/0305077](#).
- [101] M. R. Spiegel, *Schaum’s outline series: Complex Variables*. McGraw-Hill, New York, 1964.
- [102] G. Bhattacharyya, H. V. Klapdor-Kleingrothaus, H. Päs, and A. Pilaftsis, “Neutrinoless double beta decay from singlet neutrinos in extra dimensions.,” *Phys. Rev.* **D67** (2003) 113001, [hep-ph/0212169](#).
- [103] Private communication with G. Quast.
- [104] Private communication with D. Bardin.

Dank

An dieser Stelle möchte ich mich bei all jenen bedanken, die zum Gelingen dieser Arbeit beigetragen haben. Insbesondere gilt mein Dank:

- Prof. Dr. Rückl, der mir die Bearbeitung meines äusserst interessanten Promotions-themas ermöglicht, mich immer unterstützt und mir in zahlreichen Diskussionen immer wieder neue Denkanstöße gegeben hat.
- Dr. Apostolos Pilaftsis, der mich den zusätzlichen Dimensionen näherbrachte und mich auch in Manchester nicht vergessen hat.
- Lars Nilse für die Zusammenarbeit auf dem Gebiet der brane kinetic terms.
- Prof. Dr. Quast für seine Hilfe bei den Multiparameterfits.
- Thomas Binoth und Thorsten Ohl für unzählige Diskussionen und ihre Hilfe bei physikalischen Fragen aller Art.
- Ana Alboteanu und Thomas Binoth für das Korrekturlesen dieser Arbeit.
- meinen Zimmergenossen Frank Deppisch, Stefan Karg und Andreas Redelbach für die gute Nachbarschaft und die vielen Diskussionen.
- Brigitte Wehner und Alexander Wagner für ihre Unterstützung in Verwaltungs- und Computerangelegenheiten.
- allen Mitarbeitern des Lehrstuhls und des gesamten Instituts für das hervorragende Arbeitsklima und den ein oder anderen guten Tip in allen Lebenslagen.
- der Studienstiftung des Deutschen Volkes für die Unterstützung während meiner Promotion.
- all den lieb gewonnenen Freunden, die das Studium und die Promotion in Würzburg auch abseits der Uni so schön gemacht haben.
- meinen Eltern, die mich immer bedingungslos unterstützt haben.
- und vor allem natürlich Dir Nicole.

Lebenslauf

Angaben zur Person

Geburtsdatum und -ort	04.03.1975, Fulda
Familienstand	verheiratet, keine Kinder
Staatsangehörigkeit	deutsch

Ausbildung

August 1981 - Juli 1985	Grundschule Margretenhaun
August 1985 - Juni 1994	Freiherr-vom-Stein-Gymnasium, Fulda
Juni 1994	Allgemeine Hochschulreife
Okt. 1994 - Sept. 1995	Wehrdienst
November 1995	Beginn des Studiums der Physik an der Julius-Maximilians-Universität Würzburg
August 1997	Vordiplom im Fach Physik
August 1998 - August 1999	Studium der Physik an der University of Texas at Austin
August 1999	Master of Arts in Physik
Oktober 1999 - Juni 2001	Fortsetzung des Studiums der Physik an der Julius-Maximilians-Universität Würzburg
Juni 2001	Diplom im Fach Physik
seit Juli 2001	Promotionsstudium im Fach Physik an der Julius-Maximilians-Universität Würzburg